FEDERAL UNIVERSITY OF CEARÁ

CENTER OF TECHNOLOGY

DEPARTMENT OF HYDRAULIC AND ENVIRONMENTAL ENGINEERING

POST-GRADUATION PROGRAM IN GEOTECHNICS

ANA RAINA CARNEIRO VASCONCELOS

SELF-SENSING OF SOIL-CEMENT COMPOSITES BASED ON CARBON NANOTUBES FOR CIVIL ENGINEERING MONITORING

FORTALEZA

2024

ANA RAINA CARNEIRO VASCONCELOS

SELF-SENSING OF SOIL-CEMENT COMPOSITES BASED ON CARBON NANOTUBES FOR CIVIL ENGINEERING MONITORING

A Dissertation presented for the Graduate Program in Civil Engineering: Hydraulic and Environmental Engineering of the Federal University of Ceará, as a fulfillment of the requirements for the Degree of Master. Area within the Graduate Program: Geotechnics.

Advisor: Prof. Mariana Vella Silveira, Ph.D.
Co-advisior: Prof. Esequiel Fernandes Teixeira Mesquita, Ph.D.

FORTALEZA
2024

Dados Internacionais de Catalogação na Publicação
Universidade Federal do Ceará
Sistema de Bibliotecas
Gerada automaticamente pelo módulo Catalog, mediante os dados fornecidos pelo(a) autor(a)

V45s Vasconcelos, Ana Raina Carneiro.
Self-sensing of soil-cement composites based on carbon nanotubes for civil engineering monitoring / Ana Raina Carneiro Vasconcelos. – 2024.
111 f. : il. color.

Dissertação (mestrado) – Universidade Federal do Ceará, Centro de Tecnologia, Programa de Pós-Graduação em Engenharia Civil: Recursos Hídricos, Fortaleza, 2024.
Orientação: Profa. Dra. Mariana Vella Silveira.
Coorientação: Prof. Dr. Esequiel Fernandes Teixeira Mesquita.

1. Carbon Nanotubes. 2. Soil-cement composites. 3. Superplasticizer admixture. 4. Dispersion. 5. Structural Health Monitoring. I. Título.

CDD 627

ANA RAINA CARNEIRO VASCONCELOS

SELF-SENSING OF SOIL-CEMENT COMPOSITES BASED ON CARBON NANOTUBES FOR CIVIL ENGINEERING MONITORING

A Dissertation presented for the Graduate Program in Civil Engineering: Hydraulic and Environmental Engineering of the Federal University of Ceará, as a fulfillment of the requirements for the Degree of Master. Area within the Graduate Program: Geotechnics.

Approved in:_____/___/_____.

COMMITTEE MEMBERS

_____

Prof. Mariana Vella Silveira, Ph.D. (Advisor)
Federal University of Ceará

_____

Prof. Esequiel Fernandes Teixeira Mesquita, Ph.D. (Co-advisor)
Federal University of Ceará

_____

Prof. Luis Paulo Mourão dos Santos, Ph.D.
Federal University of Ceará

_____

Prof. Antonella D'Alessandro, Ph.D.
University of Perugia

To the Most Sacred Heart of Jesus and to the Immaculate Heart of Mary, for honor and glory forever and ever.

ACKNOWLEDGEMENTS

To God the Father, who designed this path in geotechnical. To Jesus Christ, who bears fruit from every little sacrifice in these years. To the Holy Spirit, who makes me persevere in the face of my limitations. To Our Lady, who is such a Mother, fortress, and intercessor on this journey.

To my parents, Ana Altina, and Carlos Carolino, to my sister, Ana Dêgyla, and to my grandmother, my Radinha, who have been so supportive in every way, with so many words of wisdom and so many actions of true love, making this stage a step for all of us.

To my grandmother Teresa Moreira, aunt Rosa and Carol Vasconcelos, and my cell sister, Maria Edilene Pereira, who made their houses available to be my home.

To Prof. Mariana Vella Silveira and Prof. Dr. Esequiel Fernandes Teixeira Mesquita, for his guidance and friendship, which were essential for this work.

To my 'cyrineus', Ryan Araújo de Matos, Me. Nádia Pitombeira, and Letícia Castro from the Federal University of Ceará, who helped with friendship and companionship in carrying out many works.

To the Advanced Materials Laboratory, mainly to Prof. Dr. Luis Paulo Mourão dos Santos, for their valuable contributions and suggestions.

To the Advanced Microscopy Laboratory and Raman Spectroscopy Laboratory, mainly to Prof Francisco Carlos Carneiro Soares Salomão, for having collaborated in the realization of this work.

To the Soil Mechanics and Pavement Laboratory (LMSP), Polymer and Materials Innovation Laboratory (LABPIM), Analytical Center, and X-ray Laboratory for the help in the experimental stage, which made this work possible.

To FUNCAP and CNPQ for the financial support with the funding of the research.

To the professor participating in the examining committee, Prof. Antonella D'Alessandro, for their time and valuable collaborations.

To the MC Bauchemie, MatChem and CTNano, for provided materials for the study.

To Shalom Catholic Community and my friends, for their help and commitment.

This present work was carried out with the support of the Coordination for the Improvement of Higher Education Personnel – Brazil (CAPES) – Funding Code 001.

Since I realized that it was impossible to accomplish anything by myself, the task you have imposed upon me ceased to seem difficult; I felt that the only thing necessary was to unite myself more and more to Jesus and that the rest would be given to me as an addition.
(Saint Therese of Lisieux, 1898)

ABSTRACT

Civil infrastructures are sometimes exposed to a dynamic and complex environment, accelerating their deterioration over time. Cracks, fissures, and reduction in structural integrity becomes inevitable. Early detection of the damage location and size is crucial to prevent catastrophic failures. As a result, different smart and self-sensing materials in civil structural monitoring have become the object of study in recent years, with carbon nanotubes emerging as particularly promising. The integration of carbon nanotubes into composite materials enhances self-sensing properties, which are already widely utilized for monitoring stress and strain through electrical responses. However, overcoming the challenges posed by the high aspect ratio and Van der Waals forces of the carbon nanotubes to achieve uniform distribution and stability for composites remains a significant hurdle. By ensuring dispersion and uniformity within composites, the potential arises to transform them into efficient smart materials for Structural Health Monitoring, through the analysis of electrical properties and detection of soil-cement composites. In this way, it is proposed in this dissertation the development of self-sensing soil-cement composites incorporating carbon nanotubes for monitoring. Physicochemical characterization techniques were employed to ensure the efficiency and stability of multi-walled carbon nanotubes dispersion in superplasticizer admixtures and soil-cement composites. Subsequently, the electrical properties were investigated using the two-probe method in soil-cement samples. The obtained results demonstrate promising outcomes regarding the effective role of superplasticizer admixture in enhancing dispersion and ensuring structural stability throughout the useful life of dispersions and composites containing carbon nanotubes. Furthermore, the dissertation highlights the electrical and sensing properties of these smart composites, noting increases in resistivity during the cure process. However, it's noted that the fixed quantity of carbon nanotubes did not reach the percolation threshold, thereby failing to achieve more significant electrical values. The findings establish a solid and positive indications for the development of self-sensing soil-cement composites based on carbon nanotubes for employment as strain-stress monitoring in civil engineering.

Keywords: carbon nanotubes; soil-cement composites; superplasticizer admixture; dispersion; structural health; resistivity monitoring.

RESUMO

Infraestruturas civis muitas vezes são expostas a um ambiente dinâmico e complexo, acelerando sua deterioração ao longo do tempo. Fendas, fissuras e redução na integridade estrutural tornam-se inevitáveis. A detecção precoce da localização e do tamanho dos danos é crucial para prevenir falhas catastróficas. Como resultado, diferentes materiais inteligentes e auto-sensíveis no monitoramento estrutural civil têm sido objeto de estudo nos últimos anos, com os nanotubos de carbono emergindo como particularmente promissores. A integração de nanotubos de carbono em materiais compostos melhora as propriedades de auto-sensibilidade, que já são amplamente utilizadas para monitorar estresse e deformação através de respostas elétricas. No entanto, superar os desafios apresentados pela alta superfície específica e forças de Van der Waals dos nanotubos de carbono para alcançar uma distribuição uniforme e estabilidade para os compósitos ainda é um obstáculo significativo. Ao garantir a dispersão e uniformidade dentro dos compósitos, surge o potencial de transformá-los em materiais inteligentes eficientes para Monitoramento de Saúde Estrutural, através da análise de propriedades elétricas e detecção de compósitos de solo-cimento. Desta forma, propõe-se nesta dissertação o desenvolvimento de compósitos de solo-cimento auto-sensíveis incorporando nanotubos de carbono para monitoramento. Técnicas de caracterização físico-química foram empregadas para garantir a eficiência e estabilidade da dispersão de nanotubos de carbono de parede múltipla em aditivos superplastificantes e compósitos de solo-cimento. Posteriormente, as propriedades elétricas foram investigadas utilizando o método de duas sondas em amostras de solo-cimento. Os resultados obtidos demonstram resultados promissores quanto ao papel efetivo do aditivo superplastificante em melhorar a dispersão e garantir estabilidade estrutural ao longo da vida útil de soluções e compósitos contendo nanotubos de carbono. Além disso, a dissertação destaca as propriedades elétricas e sensoriais destes compósitos inteligentes, observando aumentos na resistividade durante o processo de cura. No entanto, observa-se que a quantidade fixa de nanotubos de carbono não atingiu o limiar de percolação, não alcançando assim valores elétricos mais significativos. As descobertas estabelecem indicações sólidas e positivas para o desenvolvimento de compósitos de solo-cimento auto-sensíveis baseados em nanotubos de carbono para uso no monitoramento de tensões e deformações na engenharia civil.

Palavras-chave: nanotubos de carbono; compósitos de solo-cimento; aditivos superplastificantes; dispersão; saúde estrutural; monitoramento de resistividade.

LIST OF FIGURES

LIST OF TABLES

SUMMARY

1 INTRODUCTION

Engineering works are vital for regional development, relying on geotechnical materials like soil or rock for their foundation, earth structures or excavation. Soil, abundant near the earth's surface, originates from rock decomposition and is a particulate medium with void spaces between grains. Geotechnical engineering, though not an exact science due to nature's variability, plays a crucial role in ensuring the safety and performance of structures ((WU *et al.*, 2024; ZHANG, Wengang *et al.*, 2024)).

Understanding soil mechanics is essential for geotechnical projects, focusing on settlement and stability. Settlement, a downward displacement caused by soil deformation under external stresses, must be monitored to prevent structural damage (BANDARRA *et al.*, 2024; MD NUJID; THOLIBON; MUKHLISIN, 2024).

In geotechnical infrastructure systems, the incorporation of additives, especially cement, is essential for enhancing soil properties. Many infrastructures are constructed using soil or soil-cement composites. This deliberate addition aims to strengthen the soil's capacity and promote stability, ultimately maximizing its ability to withstand the demands imposed by the structures constructed (ALAO, 2024; QI; CUI; WANG, 2024; WYJADŁOWSKI *et al.*, 2024). The complex interaction among these materials, coupled with external factors such as environmental conditions and usage patterns, can lead to degradation and loss of structural integrity over time, demanding improvements (LOBIANCO; DEL ZOPPO; DI LUDOVICO, 2022; SAKR; SADHU, 2023; SIVASURIYAN; VIJAYAN, 2023; ZHOU, Jian *et al.*, 2023).

Monitoring during and after construction helps assess structure performance, ensuring safety and integrity (SINGH *et al.*, 2023; KIM, Sang Yeob *et al.*, 2024; ZHANG, Jiawen *et al.*, 2024). Structural health monitoring (SHM) involves assessing these structural conditions, typically through sensor systems linked to a central data repository. This allows for real-time detection and characterization of emerging damage, offering crucial insights into structural integrity throughout its service life (PRASAD *et al.*, 2024; ZHANG, Wei Heng *et al.*, 2024). SHM stands apart from traditional assessment approaches by employing non-destructive testing, encompassing a monitoring system comprising sensors and data processing capabilities, facilitating remote access, and enabling efficient management of data acquisition frequency and duration (BUI TIEN *et al.*, 2024; GLASHIER; KROMANIS; BUCHANAN, 2024). While the implementation of SHM systems carries a significant initial investment, the potential benefits in terms of maintenance optimization, early detection of structural failures, prevention of equipment and structure losses, and most importantly, the

avoidance of human injuries or fatalities, can far outweigh these costs (FERGUSON *et al.*, 2024; ROBERTS; AVENDAÑO-VALENCIA; GARCÍA CAVA, 2024).

Another noteworthy progress in SHM application, particularly in full-scale analysis, has been the development of methods to minimize the impact of environmental factors on collected data. Today, smart materials are revolutionizing the field of SHM, particularly with the advent of nano-modified composites. Recent advancements in nanotechnology have brought forth a new class of sensors termed self-sensing materials, set to revolutionize structural monitoring in civil infrastructure (DENG *et al.*, 2024; YU, Xiao *et al.*, 2024). This new maintenance paradigm relies on next-generation structures composed entirely or partially of self-sensing materials, effectively transforming the structure itself into a sensor (JAWED ROSHAN et al., 2023; DE IULIIS; CARDONI; PAOLO CIMELLARO, 2024).

Self-monitoring materials integrate functional fillers (e.g., micro carbon fibers, metal fibers, carbon nanotubes) into a composite or concrete. Incorporating conductive particles, like carbon nanotubes (CNT), in the soil-cement matrix establish a conductive network in the composite, which undergoes changes under external loads or environmental factors, impacting the material's electrical behavior (DEVI, Rekha; GILL, 2021; RODRÍGUEZ-TEMBLEQUE *et al.*, 2020; SEO *et al.*, 2022). These findings highlight the potential of self-sensing soil-cement composites in civil engineering, especially for SHM. They emphasize how these composites can provide real-time information about structural conditions, aiding in anomaly detection due to seismic events or other factors.

Self-sensing soil composites can find application in geotechnical structures like energy infrastructure, embankments, pavements, and earth dams. Smart materials with CNTs enhance a structure's ability to sense stresses, deformations, cracks, or damage, often improving mechanical properties and durability. Exploring nanotube-modified in soil-cement composites and their sensory properties holds promise for enabling self-monitoring of structures and early detection of damage, presenting an intriguing research area.

1.1 Motivation

Essentially, from the year 2014, the implementation of self-sensing materials based on nanomaterials showed a growing advance (BIRGIN et al., 2023; GULISANO et al., 2023; MEONI, A. et al., 2022; MESQUITA et al., 2023). This growth in the number of records is related to the technological development in self-sensing cement composites for

SHM in the world, while China, the United States and Italy command the largest number of records.

In the last decade, there has been a growing development of the CNT, especially applied to structural health monitoring, as is possible to observe below:

- Ubertini *et al*. (2014) proposed the application of CNT sensors for monitoring the structural health of concrete structures, such as reinforced concrete beams;
- Rao *et al*. (2020) developed sensor for dynamic sensing, investigating their utilization on a large reinforced concrete bridge girder, using three different types of multi-walled nanotubes.
- Castaneda-Saldarriaga *et al*. (2021) reported on the manufacturing and multipurpose experimental characterization of a cement-based matrix composite with carbon nanotube into a reinforced-concrete beam.
- Gupta *et al.* (2021) validated the large-scale application of self-sensing concrete in airport runway pavements and to use electrical resistance tomography for characterizing spatially distributed damage during accelerated pavement testing, with multi-walled carbon nanotube thin films.
- Siahkouhi *et al.* (2023) included carbon nanotubes as a functional filler to provide intrinsic self-sensing properties to railway sleepers for detect hanging sleeper defects.
- Su *et al*. (2024) introduced electric field-tunable self-sensing nanocomposites with aligned carbon nanotube networks in an epoxy matrix as a promising solution for precise pavement health assessment.

This suggests that self-sensing materials are becoming an effective tool for monitoring the structural integrity of critical infrastructures in real-time. Although there is a large amount of work regarding the use of SHM in civil engineering, the small amount stands out when related to monitoring in soil-cement. The complexity of interactions, such as environmental conditions, material properties, applied loads, and construction techniques, exposes civil infrastructures and geotechnical structures to degradation, damage, and loss of resistance over their useful life, makes it necessary to develop techniques to monitor for measuring responses and capturing structural behavior changes resulting from these microcracks.

A search of the “World Intellectual Property Organization – WIPO” in May 2024, using the expression “self-monitoring in cement” and “self-monitoring in soil-cement”

showed the existence of 53 and 3, respectively registered applications focused on self-monitoring. When searching in the “United States Patents Trademark Office - USPTO”, the expression “SHM” AND “cement”, 88 registered applications were found. When searching the expression "SHM" AND "soil-cement", there were 0 registered applications.

The originality of this work lies in its pioneering approach to integrating carbon nanotubes into soil-cement composites for structural monitoring applications in civil engineering. By harnessing the unique properties of carbon nanotubes, this research aims to create self-sensing materials capable of providing real-time data on structural integrity. Its main motivation is to ensure the safety and reliability of structures and infrastructures by detecting and quantifying any damage.

1.2 Objectives

The main aim of this work is to develop self-sensing soil-cement composites utilizing carbon nanotubes for structural monitoring applications, with a specific focus on civil engineering.

Additionally, to achieve the main goal, specific objectives were designed and concluded through the three papers that complete this Master’s Thesis. The specific objectives are:

- Elaborate a systematic review about the use of smart and self-sensing materials through nanomaterials in civil engineering SHM;
- Evaluate the efficiency and stability of the MWCNT dispersion in superplasticizer admixtures and in soil-cement composites;
- Characterize of chemical dispersion of the MWCNT dispersion in superplasticizer admixtures and in soil-cement composites;
- Investigate of the electrical properties of the soil-cement composites for different concentrations of superplasticizer admixture.
- Contribute to the technical-scientific development of Structural Health Monitoring, specifically in self-sensing materials in civil engineering.

1.3 Work organization

The present master's thesis is divided into 5 chapters. In short, the structure of this master's thesis is shown in Figure 1.

Figure 1 - Structure of the master's thesis

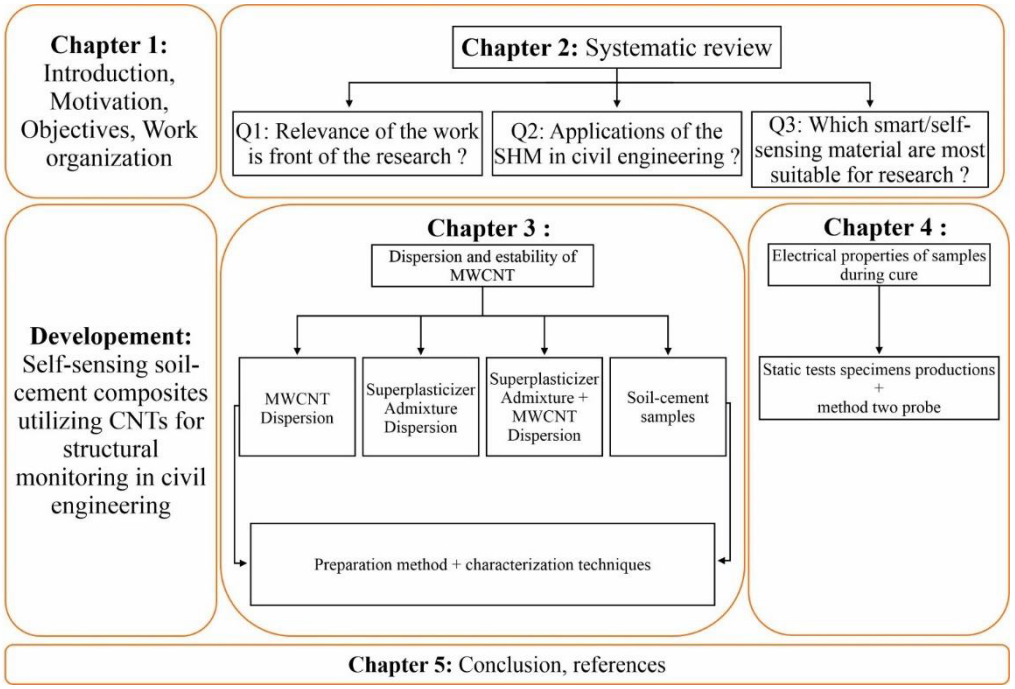

Source: The author.

Chapter 1 presents introductory concepts about self-monitoring structures, with introduction of the cement and soil-cement monitoring. This chapter also presents the motivation of the work, as well as the objectives defined for the realization of the work.

Chapter 2 presents a systematic review of the smart and self-sensing materials in SHM. This section provides detailed analyses of research findings, explores their applications in civil engineering, and highlights advanced technologies, notably emphasizing the significance of carbon nanotubes.

Chapter 3 presents a study conducted as part of the development a self-sensing soil-cement composite. It outlines the evaluation of MWCNT dispersion efficiency and stability in superplasticizer admixtures and soil-cement composites, alongside the characterization of MWCNT chemical dispersion.

Chapter 4 presents the findings of the study on the electrical properties of soil-cement composites across various concentrations of superplasticizer admixture. It provides a

comprehensive analysis and interpretation of the results, shedding light on the implications for structural monitoring applications.

Chapter 5 summarizes the main insights and conclusions drawn from the research. Additionally, it suggests avenues for further exploration and development in this field, aiming to advance knowledge and foster innovation in self-sensing materials for civil engineering applications.

2 APPLICATIONS OF SMART AND SELF-SENSING MATERIALS FOR STRUCTURAL HEALTH MONITORING IN CIVIL ENGINEERING: A SYSTEMATIC REVIEW

2.1 Introduction

Civil infrastructure, such as bridges, buildings, water supply lines, offshore platforms, and oil tanks, are sometimes exposed to a dynamic and complex environment, with extreme fluctuations in temperature and high levels of CO_2, accelerating their deterioration over time (MIN et al., 2012; KIM et al., 2021). Fractures, crevices, and an unavoidable decline in structural strength ensue. Early detection of the damage location and size is crucial to prevent catastrophic failures. Traditional methods of periodic visual inspections and manual evaluations are restricted in their capacity to detect early structural degradation or damage, emphasizing the necessity for improved monitoring approaches. Nevertheless, most destructive, and non-destructive techniques do not provide continuous health monitoring data requiring the use of smart materials to help to solve this problem (TAHERI, 2019; ZHANG, Ru *et al.*, 2023).

Significant research efforts to address these limitations have focused on the development of smart materials, which can detect damage through vibration-impedance and piezoresistivity, for example (ALAVI *et al.*, 2016). There has been interest in local health monitoring for critical members of a host structure by utilizing smart sensors such as fiber optic sensors and piezoelectric sensors during the last decades. All the commercially viable sensors for require an external power source, either battery or solar power. Additionally, many of these sensors have shown limitations of excessive cost and low durability, as well as limited detection capacity and area (ALEXAKIS; LIU; DEJONG, 2020).

Thus, the use of Structural Health Monitoring (SHM) systems is crucial for a rapid assessment of the health status of these structures, ensuring their safety and reliability (LEE; LE; KIM, 2019a; KIM et al., 2021). SHM systems, responsible for monitoring and recording data over time, are essential for understanding the health status of structures and identifying changes resulting from damage. It consists of three sequential stages: global damage detection, damage classification, and damage estimation. In Stage 1, a global occurrence of damage is detected through monitoring changes in structural systems. In Stage 2, types of damage are classified, recognizing patterns and behavioral characteristics. In Stage 3, the location and extent of the damage are estimated using a method based on experimental

or numerical shape (KIM et al., 2010; SOLEYMANI; JAHANGIR; NEHDI, 2023b). A good SHM should involve and integrate the following features: accurate, reliable, and distributed strain measurements; the possibility of assessing shape and displacements; detection of local damages; reliable protection of the sensors; no need for surface installations; high durability; measurements from the real zero state of the structural element (KULPA *et al.*, 2021).

In general, the utilization of smart structural materials solely as sensors, without the need for additional sensor components, is termed self-sensing. Self-sensing materials are formed by dispersing electrically conductive nanomaterials (i.e., conductive phase) into a mixture matrix to create a continuous conductive network and provide intrinsic sensing properties to the composite. The formation of an extensive conductive pathway is governed by various mechanisms, such as contacting conduction, tunnelling effect, field emission effect, and ionic conduction (SEVIM; JIANG; OZBULUT, 2022; GULISANO et al., 2023; SONG et al., 2023). In this context, composite sensors capable of self-monitoring their deformation state through piezoresistivity are developed, providing electrical variations when mechanically deformed (ZHANG, Ru *et al.*, 2023). These composites can be manufactured using diverse types of conductive additives, which reduce their electrical resistivity, such as carbon fiber, steel fiber, graphene, and carbon nanotubes (ALEXAKIS; LIU; DEJONG, 2020; PARIDA; MOHARANA, 2023b).

The present article utilizes the methodology of systematic review, following the Preferred Reporting Items for Systematic Reviews and Meta-Analyses approach. Through this rigorous review process, the aim is to track the progression of selected articles over time, offering a visual representation of studies conducted in different countries. The principal objective is to provide an in-depth understanding of SHM applications in civil infrastructure, with a specific emphasis on the potential of self-sensing materials. By highlighting of the chosen journal, the article aims to examine the significance of the study and pinpoint the most relevant self-sensing techniques for prospective research.

2.2 Research methods

To investigate the applications of SHM in civil engineering in terms of smart and self-sensing materials, a systematic literature review was conducted. From there, it will be possible to ascertain the relevance of the study, applications of SHM in civil engineering, as well as distinguish the main smart and self-sensing techniques more suitable for future

studies. For the development of this review, the PRISMA (Preferred Reporting Items for Systematic Review and Meta-Analysis) methodology was adopted, which guided the selection of studies for this systematic review. Thus, the methodological process involves three distinct phases (AZHARI; BANTHIA, 2012; CARDOSO *et al.*, 2023):

a) Accessing vast scientific and academic databases through keyword techniques and searching;
b) Screening for inclusion and exclusion criteria;
c) Implementing an eligibility process to assess relevant material and evaluate study data.

The bibliographic search took place in February 2024, covering the following databases: ScienceDirect, Scopus, and Springer. To search in the repositories, the descriptors used were: ("Civil engineering" AND "SHM") AND ("smart materials" AND "self-sensing"), aiming to identify and investigate articles exploring the application of self-sensing smart materials in the context of civil engineering, specifically concerning structural health monitoring. Review articles, encyclopedias, book chapters, conference abstracts, editorials, and other materials were excluded.

The articles were classified for relevance through a selection procedure. Initially, 764 researches articles were identified and exported from the databases, containing title, author, publication year, and abstract in .RIS format for the Mendeley Reference Manager software. The screening phase involved reading the title, abstract, and keywords of each record in the text file, resulting in the selection of 344 articles.

The eligibility criteria was chosen to include an article in the main dataset, after full reading. Three criteria were established for the inclusion of an article in this review:

a) The article must explicitly relate to the implementation of SHM in the field of civil engineering;
b) The article must focus on at least one analysis linked to SHM, whether experimental, methodological, numerical, or mathematics;
c) The article must include characterization of the smart and self-sensing materials used.

After the complete reading and advanced search based on the above criteria, 229 articles were disqualified for not meeting the research criteria. Finally, after checking for duplicate studies, a final number of documents included in the systematic review was obtained, totaling 33. A visual representation of the PRISMA search phases is available in Figure 2.

Figure 2 - PRISMA flowchart of the systematic review process

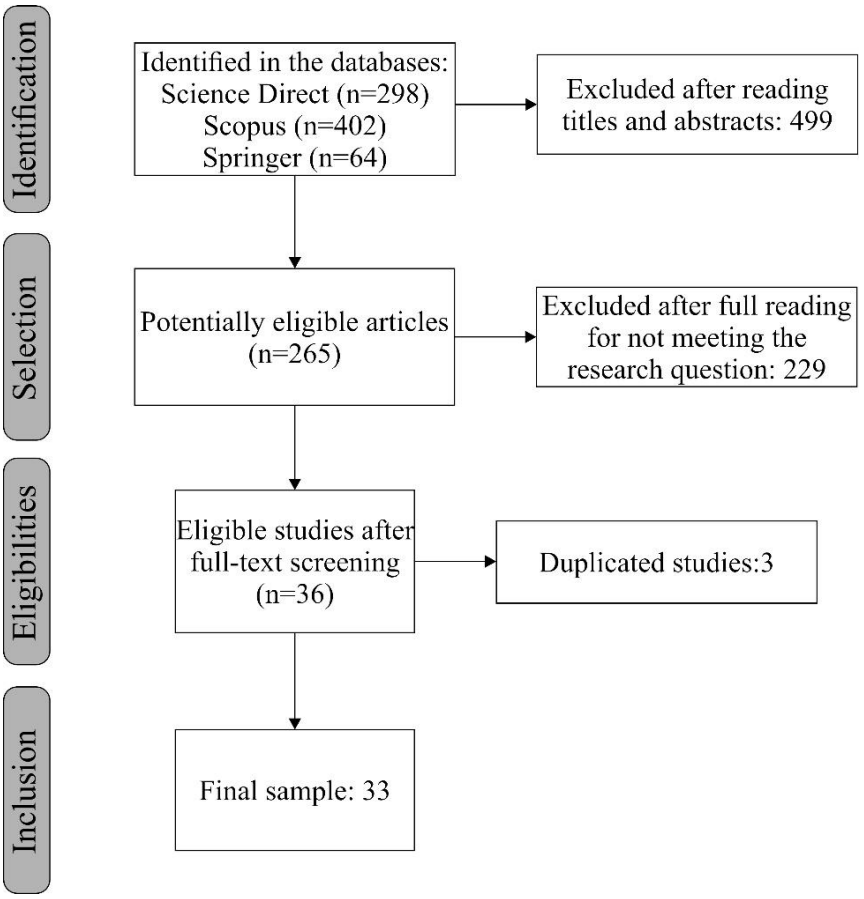

Source: The author.

2.3 Descriptive analysis results

In this section, a comprehensive analysis of the reviewed articles is presented, covering various dimensions, and utilizing tables and figures to illustrate the results. Figure 3 illustrates the chronological distribution of research papers over the specified period, following the application of the criteria adopted to define the articles. The data analysis reveals a growing trend in the use of self-sensing materials in civil engineering, beginning in 2014 and continuing to increase over the years, as indicated by the upward trend line. Additionally, the results reveal that approximately 78% of the publications were disseminated over the last five years. Moreover, the number of articles on the subject reached 9 in 2023, reinforcing the ongoing relevance of these materials. This suggests that self-sensing materials

are becoming an effective tool for monitoring the structural integrity of critical infrastructures in real-time.

Figure 3 - Distribution of research papers by year

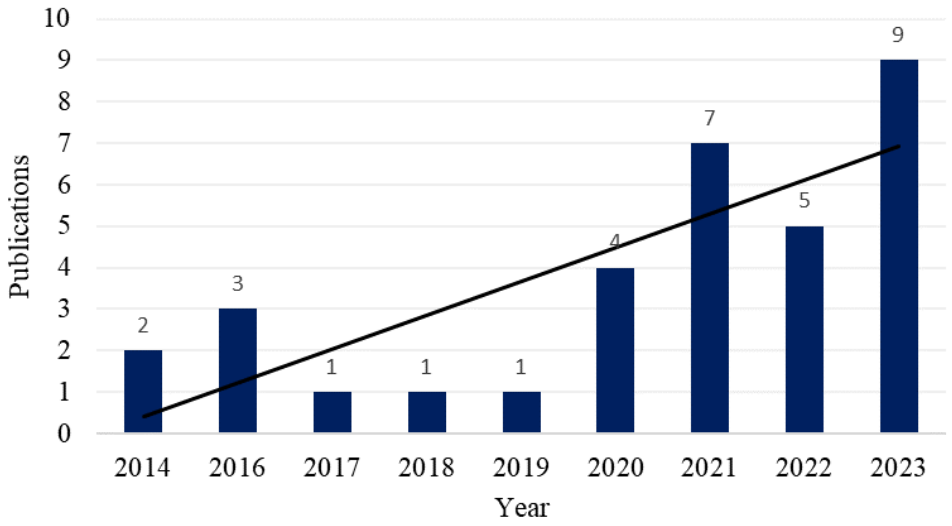

Source: The author.

The analysis of the geographical distribution of publications, as illustrated in Figure 4, highlights the universality of self-sensing materials in civil engineering, with representations in various countries. It is observed that the articles cover a diversity of countries, distributed across different continents, including South America, North America, and Europe. A massive portion of the studies on the subject in question comes from China, the United States, and Italy, which contributed, respectively, 15%, 13%, and 13% of the total published articles.

The broad geographical representation underscores the diverse perspectives and methodologies influencing advancements in civil engineering and self-sensing materials. This prevalence reflects the leadership of these countries in the field, characterized by significant investments in research and infrastructure, as well as a robust community of experts and academic institutions dedicated to this area of study.

Figure 4 - Publications by country of the authors

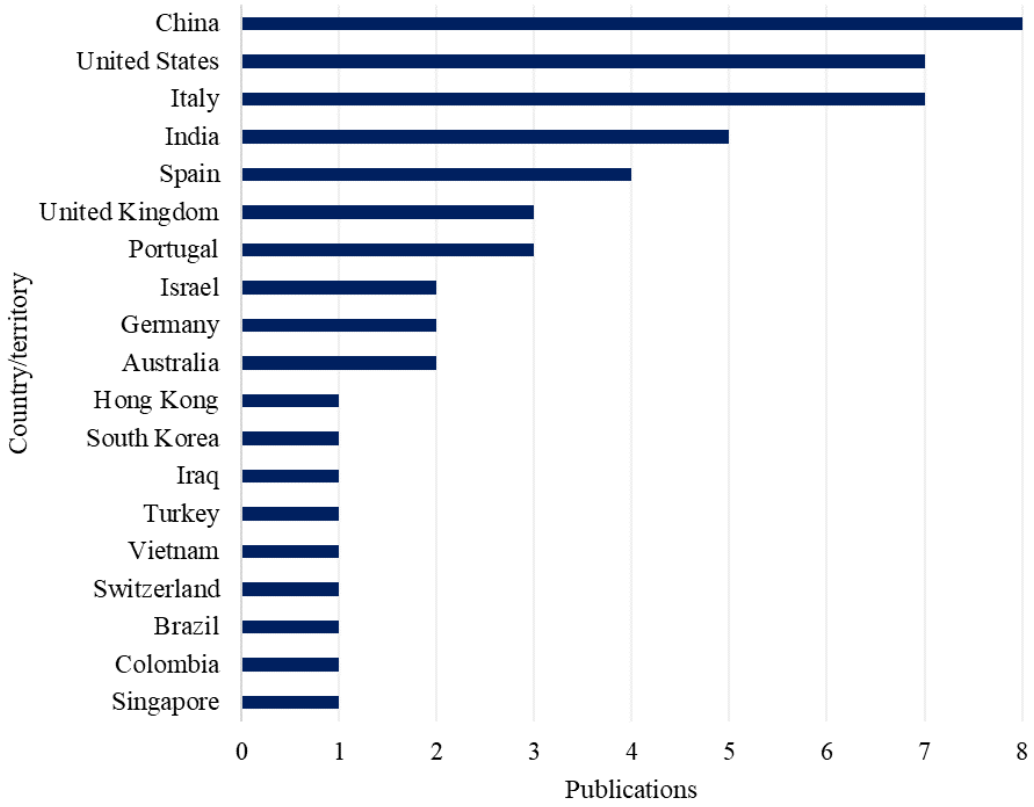

Source: The author.

Figure 5 highlights the particular emphasis of SHM applications in beams and columns, followed by transportation and geotechnics. This suggests a predominance of the use of smart materials in fundamental components of infrastructures, such as elements of safety and durability of these constructions, as well as functionality, safety, and operational efficiency in transportation. However, there are gaps in development of self-sensing in the areas of bridges and metal structures, building structures and historic buildings. This indicates an opportunity for researchers to further explore the potential of SHM in these specific areas and develop solutions more tailored to the demands and challenges associated with civil construction and the structural integrity of buildings.

Figure 5 - Publications by subject area

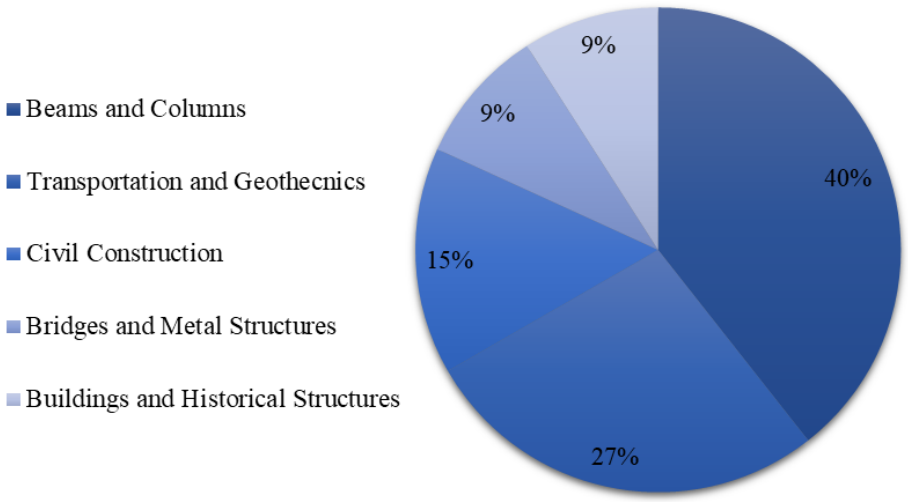

Source: The author.

Furthermore, in the analysis of bridges and metallic structures, the predominant presence of commercial sensors is highlighted, especially fiber optic sensors and fiber Bragg grating sensors. These local sensors are integrated into global SHM systems (HASNI et al., 2018; BRITTO; VASANTHANATHAN; NAGARAJ, 2018; HAQ; BHALLA; NAQVI, 2020). While there is a technology base for SHM in these components, there is still significant room for innovation and ongoing research aimed at enhancing these systems and adapting them to self-sensing materials for more precise and effective monitoring.

Finally, Figure 6 provides an overview of the distribution of publications across various engineering journals. The journal Construction and Building Materials stands out, accounting for approximately 30% of experimental and numerical studies, significantly serving as a platform for scientific dissemination in this field. Additionally, journals such as Sensors and Actuators A: Physical, with three publications, Composites Part B: Engineering, and Cement and Concrete Composites also notably contribute to the discourse, each representing a substantial portion of the analyzed publications.

This diversity of scientific communication vehicles reflects the breadth of the discourse and the importance attributed to advancing knowledge about self-sensing materials in civil engineering. Therefore, it is emphasized that the higher number of publications in certain journals not only indicates quantity but also the quality and prestige of these outlets in the specific field of self-sensing materials in civil engineering.

Figure 6 - Percentage distribution of reviewed articles according to journal name

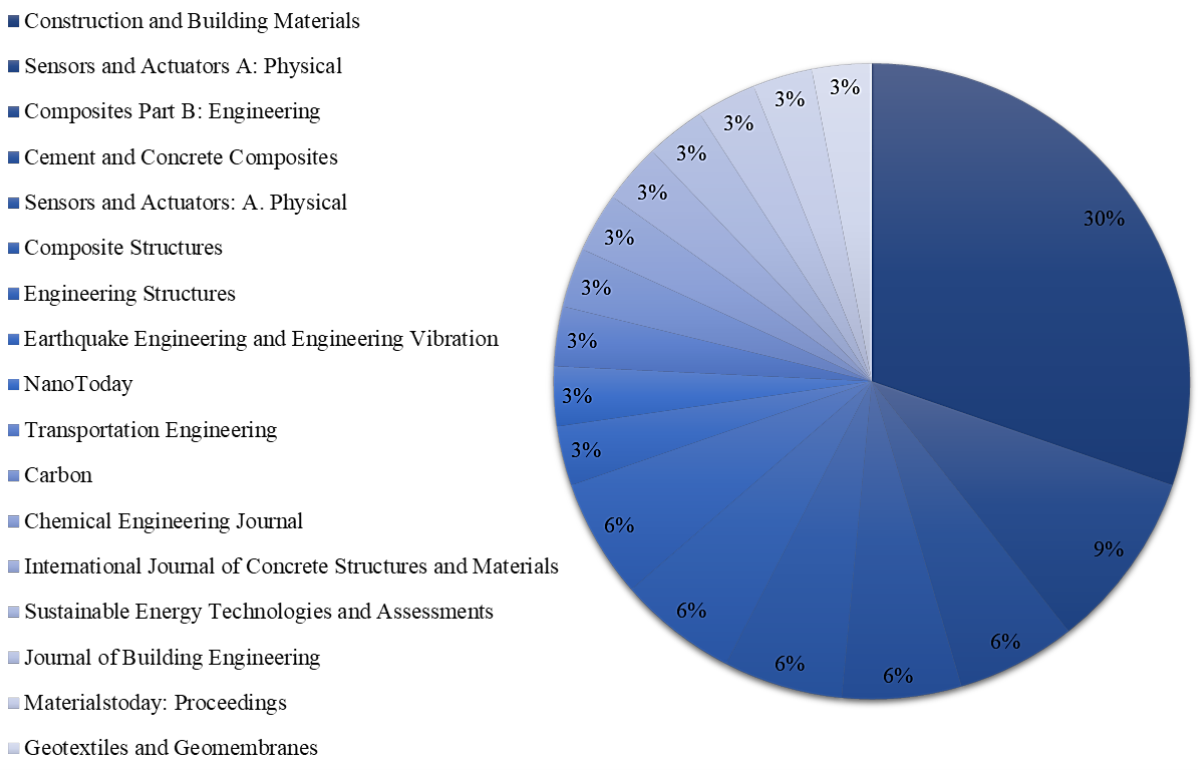

Source: The author.

2.4 SHM for Civil Infrastructures

Recently, many researchers have focused on the possibility of using variations in the properties of a structure as an indication of its structural damage and as an uncertain impact due to varying ambient conditions (KIM, Jeong Tae *et al.*, 2010). Hence, SHM of structures is widely used for the evaluation of the condition of the infrastructure based on measuring real-time strain values as a crucial parameter of the structure (ABEDI *et al.*, 2022). The applications extend to a large contribution to civil infrastructure, including civil construction, bridges and metal structures, buildings and historical structures, transportation and geotechnics, and beams and columns. Figure 7 illustrates the comprehensive fields of SHM in civil engineering.

Figure 7 - SHM application of smart material and self-sensing in civil engineering

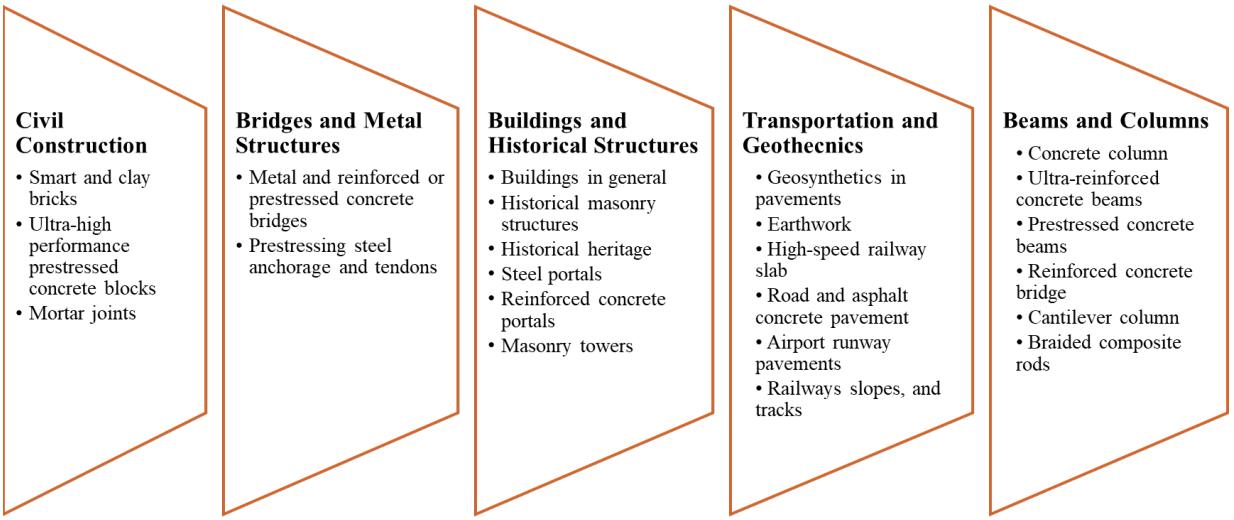

Source: The author.

The civil construction industry is susceptible to structural issues such as settlements, heavy loads, and material aging. Inadequate maintenance can result in dangerous collapses. Smart bricks, mortar joints, and ultra-high performance concrete blocks have been developed to monitor deformations and identify damages, assisting in preventive maintenance (MEONI; D'ALESSANDRO; UBERTINI, 2020; MEONI et al., 2021, 2022; NALON et al., 2024a). These intelligent materials have become more popular for detecting structural problems. However, integrating these technologies into existing infrastructures presents challenges, including compatibility with conventional construction practices, cost-effectiveness, and long-term durability.

Bridges and other civil infrastructures are designed to safely bear loads, but they face degradation from operational and environmental factors over time. Most failures involve steel member fractures, often due to fatigue cracking, a progressive process involving initiation, slow growth, and abrupt failure phases (ALAVI *et al.*, 2016; BHALLA; KAUR, 2018; CHAKRABORTY *et al.*, 2019). Early detection of damage is vital to prevent catastrophic failures. Prestressed concrete bridges, along with anchorage and tendons for prestressing steel, and structural bridges on pedestrian walkways, steel, enhanced with the incorporation of nanomaterials, serve as self-sensing components in SHM for evaluation and assessment purposes (KULPA *et al.*, 2021).

The monitoring of structures encompasses two phases: early construction and long-term post-construction. During early construction, factors like hydration temperature and moisture content influence about concrete properties and shrinkage. This phase is critical due to high energy consumption and emissions from raw materials extraction and transportation.

In the long term, structures face severe weather and environmental conditions, necessitating SHM to detect and prevent corrosion caused by water penetration and chloride ingress, serving as a key practice in conservation engineering (YIN et al., 2020; LIN; PUTRANTO; WANG, 2021). Preservation and rehabilitation of valuable historic heritage buildings require effective and efficient monitoring systems to ensure proper maintenance of durability and functionality of the building structures and materials. Moisture transportation and retention in building infrastructure are some of the most common problems, often inducing structural damage and resulting in harmful microbial growth that affects human health (ZHAO et al., 2012; DROUGKAS et al., 2023a).

In the fields of transportation geotechnics, the availability of reliable conditions and performance data is paramount, whether concerning pavement/railway/coastal engineering and directly affect the provision of accurate and precise information (NOSENZO et al., 2013; SENADHEERA et al., 2023; KELLY, 2024). Rail and road infrastructure deteriorates over time due to various factors, including material fatigue, overloading, ground movement, and environmental effects (HASNI et al., 2017; ALEXAKIS; LIU; DEJONG, 2020). Cemented stabilized sand or geosynthetics have found wide application in different infrastructure constructions but exhibit low ductility and susceptibility to cracking. Maintenance and renewal costs for typical railway, tracks and substructure represent 50–60% of the total costs of such infrastructure over its entire service life (FUGGINI *et al.*, 2016; SIAHKOUHI *et al.*, 2023a). Distresses such as nanocracks, which evolve into microcracks and eventually macrocracks, significantly contribute to the degradation of pavement structures over time. Factors like material aging, environmental conditions, heavy usage, and overloading accelerate this process (ABEDI; CORREIA; FANGUEIRO, 2021; SU et al., 2023). Amongst all SHM methods, self-sensing composites incorporating nanomaterials provide a more integrated, real-time, and practical solution for infrastructure damage detection, considering geomaterial properties and smart pavements (BIRGIN *et al.*, 2023).

In the case of structural components, such as beams, columns, and connections, which are typically subjected to different external and internal loads, deterioration may occur due to the exposure to severe conditions associated with the environment, loading, effects of aggressive actions, corrosion of embedded metal, frost, overload, concretes resistance to volume changes, abrasion/erosion, and chemical actions (TAN et al., 2021; GABEN; GOLDFELD, 2022). Ultra-reinforced, prestressed beams or columns like concrete filled steel tubular columns tended to undergo more intense deterioration processes. Additionally, it is well-founded that corrosion of steel reinforcement and fatigue damage lead to degradation of

concrete structural performance. Therefore, reduced durability and shortened service life are evident in these structural components (CASTAÑEDA-SALDARRIAGA *et al.*, 2021). However, it is challenging to assess during their service life through visual inspection and direct core sampling examination. Beams and columns doped with nanoparticles constitute robust materials capable of transducing strain into changes in electrical resistance (UBERTINI et al., 2014b).

2.5 Smart and self-sensing materials for advanced SHM

Sensor-based health diagnostic methods can be replaced with conventional nondestructive techniques due to their robustness, reliability, and ease of implementation. SHM sensors collect data from structures when subjected to external forces, either permanently or temporarily attached to the structure (MEONI; D'ALESSANDRO; UBERTINI, 2020; ABEDI et al., 2022). Multisensing, reusable, and non-bonded configurations of piezoelectric sensors, transductors piezoceramics, Fiber Bragg grating, fiber optic sensors, and lead zirconate titanate are gaining popularity (KIM, Jeong Tae *et al.*, 2010; MEONI, A. *et al.*, 2021; PARIDA; MOHARANA, 2023b).

Taheri (2019) classify four advanced sensor technologies currently used in SHM:

a) Fiber optic sensors detect changes in light signals transmitted along optical fibers. These sensors, primarily made of glass fibers, offer advantages such as high sensitivity and immunity to electromagnetic interference, with fiber optic Bragg grating (FBG) sensors being prominent (YIN et al., 2020; KULPA et al., 2021; DROUGKAS et al., 2023a; NALON et al., 2024a;).
b) Piezoelectric sensors detect parameters like acoustic emission, temperature, and strain by converting them into electrical charges. Piezoelectric materials, such as ceramics like Lead Zirconate Titanate (PZT), act as sensors, actuators, and transducers (NOSENZO et al., 2013; ALAVI et al., 2016; PARIDA; MOHARANA, 2023b; SENADHEERA et al., 2023). Piezoelectric patches and "smart patches" have been utilized for rehabilitation, and vibration damping (FUGGINI *et al.*, 2016; HASNI *et al.*, 2017; SIAHKOUHI *et al.*, 2023a).
c) Electrochemical sensors fall into three main categories: potentiometric, amperometric, and conductometric. In corrosion monitoring of reinforced concrete structures, electrochemical sensors such as those measuring open

circuit potential, surface potential, concrete resistivity, polarization resistance, noise analysis, and galvanic current are employed (LEE, Eunji; KIM, 2020; AHMED et al., 2021; GRABOWSKI et al., 2022).

d) Wireless sensors function as nodes and platforms for autonomous data acquisition rather than traditional sensors. They enable attachment of sensors like piezoelectric pads, leveraging mobile computing and wireless communication capabilities. Wireless technology reduces wiring needs, lowering installation costs, and allowing flexible system configurations (SU *et al.*, 2023).

In general, they enable early damage detection, vibration control, and distributed monitoring of stress, temperature, and deformation (MEONI, A. *et al.*, 2022; NALON *et al.*, 2024a). However, their intrinsic fragility limits its application and can be difficult to install due to their extremely small dimensions (ALEXAKIS; LIU; DEJONG, 2020; ABEDI; GOMES CORREIA; FANGUEIRO, 2021; LANDI et al., 2022a). Such sensors must be integrated into smart materials to create advanced structural global monitoring systems in a variety of applications (CHAKRABORTY *et al.*, 2019; MEONI, A. *et al.*, 2021). There are advanced nondestructive evaluation techniques, such as ground-penetrating radar, spectral analysis of surface waves, DIC and 3-D laser scanning. The system must interface and integrate the original practice principally based on traditional sensors and combine the response of several diffuse sensors, installed on the structure to monitor the progress of changes, damage with improved degradation (BHALLA; KAUR, 2018; LIN; PUTRANTO; WANG, 2021).

Given the existence of such complex and integrated systems, there is an effort to develop materials that can effectively be used as building materials while acting as sensors to monitor the health of structures (DANOGLIDIS *et al.*, 2016). Thus, a new generation of multifunctional building materials has emerged for SHM approaches: smart materials with self-monitoring and self-detection of damage. These self-sensing composites can be produced with various types of conductive fillers that reduce their electrical resistivity. Consequently, they demonstrate detectable changes in electrical resistivity in response to variations in voltage/deformation and crack propagation resulting from monotonic and cyclic loads, making them promising alternatives for SHM architectures (SENADHEERA et al., 2023; HENRIQUE NALON et al., 2024a;). One of the main benefits of these materials is the reduced cost. This is crucial because, while a SHM system improves safety and lowers

management/inspection costs, it becomes unfeasible for large-scale infrastructures if material production and integration costs are too high (NALON *et al.*, 2024b).

Conductive particles, both fibrous, powder, nanoplatelets offer a lot of conductive channels for the development of self-sensing materials (DINESH; SUJI; PICHUMANI, 2023c; SONG *et al.*, 2023). Figure 8 highlights the nanomaterials used as composite additives to produce smart and self-sensing materials. Carbon nanotubes have the most citations and consequently the most studies, followed by carbon fiber and steel fiber. There is a notoriety regarding graphite powder, graphene nanoplatelet and carbon black nanoparticle. In smaller quantities, there are rubber fiber, Ni nanofiber and fine steel slag aggregate. For reasons of relevance, those most applied in civil engineering SHM will be explained.

Figure 8 – Cloud of nanomaterials that constitute smart materials

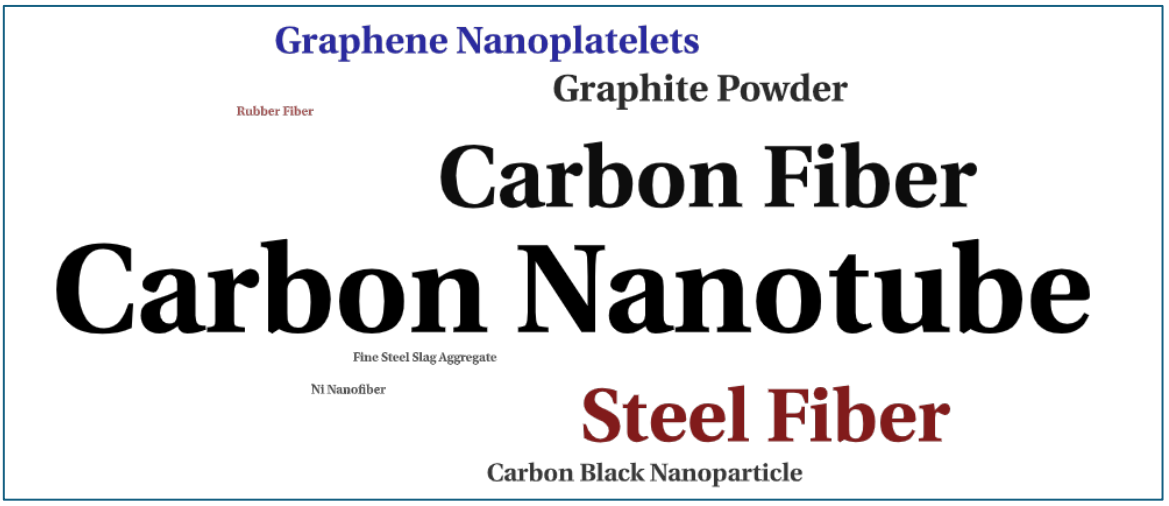

Source: The author.

2.5.1 Carbon nanotubes (CNT)

Carbon nanotubes have garnered significant interest as one of the most promising conductive nanoparticles for SHM applications over the past 15 years (RODRÍGUEZ-TEMBLEQUE *et al.*, 2020). Multi-wall carbon nanotubes (MWCNTs) consist of concentric cylinders of graphene sheets arranged around a hollow core (MATOS et al., 2023; MESQUITA et al., 2023a). They exhibit a high aspect ratio, low bulk density, and an extremely high specific surface area. MWCNTs exhibit exceptional mechanical, thermal, and electrical characteristics, with Young's modulus reaching up to 1 TPa and fracture deformations of approximately 6%. These nanoscale fibers with superior stiffness, strength,

and aspect ratio, making them reinforcements in composite materials (DANOGLIDIS et al., 2016; KONSTA-GDOUTOS et al., 2017; MATOS et al., 2023). One of the great challenges of this material is related to its dispersion, which directly affects the piezoresistive behavior (RAO; SINDU; SASMAL, 2020; LYNGDOH; DAS, 2021; RAO; SASMAL, 2022a; MESQUITA et al., 2023b).

Table 1 presents a review of studies using CNT and MWCNT (8 articles) and with combination Ni nanofiber (CNT_Ni, with 1 article).

The applications include in-situ pavement, concrete airport runway pavements, railway sleepers, building construction, high-speed rail infrastructure, and reinforced concrete beams, among others. The weight percentages of CNT relative to the binder vary according to the specific application, with an average around 0.5 to 2%. Experimental methods include monotonic compression tests and dynamic loads, as well as electrical measurements to assess properties such as compressive strength and electrical resistance. Additionally, numerical modeling has emerged as a valuable tool for understanding the behavior of structures enhanced with CNT. This diversity of applications reflects the growing interest in using CNT to enhance the properties of concrete structures and pavements. The remarkable mechanical and sensing properties of CNT suggest that they are ideal candidates for high-performance and self-sensing cementitious composites.

Table 1 – Review of studies using carbon nanotubes for civil engineering SHM

Filler type	Application	Content	Num.	Exp.	Method	Reference
CNT	In-situ pavement	0.2 wt% of the epoxy resin weight		X	Cyclic compressive, temperature, and roller compaction	(SU *et al.*, 2023)
CNT	Concrete airport runway pavements	2 wt% of the aqueous solution weight		X	Electrical impedance tomography in cycles of loading	(GUPTA, Sumit *et al.*, 2021)
CNT	Concrete railway sleeper	0.5 to 1 wt% of the cement weight	X	X	Static and dynamic loading with dynamic modeling	(SIAHKOUHI *et al.*, 2023a)
CNT_Ni	Building	0.1% and 0.5% to 1.9% (respectively) of the cement weight		X	Monotonic compression and cyclic compression	(YIN, Tianjiao *et al.*, 2020)
CNT	High-speed rail infrastructure	0 to 25 wt% of the cement weight		X	Compressive strength and electrical resistance	(NGUYEN *et al.*, 2020a)
CNT	Reinforced concrete beams	0.2 to 0.8 wt% of the cement weight		X	Compression test and electric measurement	(MEONI et al., 2022)
CNT	Reinforced concrete beams	0 to 2 wt% of the cement weight		X	Compressive strength and electrical resistance	(MESQUITA *et al.*, 2023a)
CNT	Large structures	0.1 to 0.75 wt% of the cement weight		X	Dynamic loads	(CHAKRABORTY *et al.*, 2019)
CNT	Reinforced concrete beams	2 wt% of the cement weight		X	Dynamic loads and electric measurement	(BHALLA; KAUR, 2018)
CNT	Reinforced plates	-	X		Stochastic uncertainties	(GARCÍA-MACÍAS *et al.*, 2016)

Source: The author.

2.5.2 Carbon fibers (CF)

Composites reinforced with carbon fibers, with a high aspect ratio, exhibit better self-sensitivity. In research, there is a notable improvement and durability in corrosive environments (METAXA; KONSTA-GDOUTOS; SHAH, 2013; BROWN; SANCHEZ, 2016). For piezoresistivity-based detection of composites, the fiber length is typically up to 10 mm, as longer fibers have a greater tendency to agglomerate, and it is more difficult to disperse (WANG et al., 2018; ZHOU et al., 2020; DONG et al., 2022a; CHU et al., 2023). Thus, CFs are considered a superior additive for improving the electrical conductivity and piezoresistive properties of cementitious composites compared to steel fibers (KANG; ASLANI; HAN, 2024).

Table 2 presents a review of studies using CF (7 articles) and a combination of CF with CNT (CF_CNT, with 2 articles). CF is deployed in weigh-in-motion systems for pavement, as well as in support structures and prestressed bridge tendons, displaying its versatility in enhancing structural performance. The weight or volume percentages of the fibers relative to the binding materials or the structure vary depending on the specific application, around 0.75 wt% of the cement weight to 25 vol% fiber fractions in CFRP (Carbon Fiber Reinforced Polymer). Experimental methods include compression tests, cyclic loading, tension, electrical resistance, and electromechanical models to evaluate properties such as compressive strength, long-term recovery capacity, and detection stability. Numerical method refers to the electromechanical model. Additionally, studies on the combination of CF with CNTs underscore ongoing efforts to explore synergistic effects in enhancing material properties, particularly under static flexural loading conditions.

Table 2 – Review of studies using carbon fibers for civil engineering SHM

Filler type	Application	Content	Num.	Exp.	Method	Reference
CF	Weigh-in-motion system in pavement	1 wt% of the binder weight	X	X	Compression load and electromechanical model	(BIRGIN *et al.*, 2023)
CF_CNT	Beams and columns	0 to 0.75 wt% of the cement weight		X	Compressive strength and electrical measurements	(ROOPA; HUNASHYAL, 2022)
CF	Support Structures	56 vol% of the fiber volume		X	Cycle loading test	(YANG, C. Q. *et al.*, 2016)
CF	Tendon of the prestressed bridge	15.9% and 23.8 vol% fiber fractions in CFRP		X	Tensile and electrical resistance tests	(YIN, Jie *et al.*, 2017)
CF	Reinforced concrete beams	1 wt% of the total mass weight		X	Tensile and compressive strains	(MEONI, A.; D'ALESSANDRO; UBERTINI, 2020)
CF	Reinforced concrete beams	Throughout the area		X	Compression test and electric measurements	(NALON *et al.*, 2024a)
CF_CNT	Reinforced concrete beams	0.55 wt% of the total mass weight		X	Static flexural loading	(LIN, Tzu Hsuan; PUTRANTO; WANG, 2021)

Source: The author.

2.5.3 Steel fibers (SF)

Steel fibers are gradually replacing traditional steel bars, providing significant reinforcement to structures. SFs are known for their high energy absorption capacity and durability, improving the mechanical properties of composite materials (NGUYEN et al.,

2020b; SUN; QIAO, 2023a; YANG et al., 2023a). Compared with other fibers, carbon steel fibers are more effective in improving the deformation and sensing ability of ultra-high performance. They have a good response regarding the effects of temperature, relative humidity, and storage age on the electrical properties of composites (KIM, Min Kyoung; KIM; AN, 2018; LE *et al.*, 2021; QIU *et al.*, 2021).

Table 3 presents a review of studies using SF (5 articles) and with combination of FSSA (SF_FSSA, with 1 article) in various structural contexts, primarily with smart bricks, in addition to prestressed concrete block, columns, and masonry buildings.

Table 3 – Review of studies using steel fibers for civil engineering SHM

Filler type	Application	Content	Num.	Exp.	Method	Reference
SF	Smart Bricks	0.5 wt% of the clay weight		X	Eccentric axial compression	(MEONI, A.; D'ALESSANDRO; UBERTINI, 2020)
SF_FSSA	Prestressed concrete block	0.5 wt% and 2 wt% of the cement weight		X	Eccentric axial compression	(KIM, Tae Uk *et al.*, 2021)
SF	Smart Bricks	0.5 wt% of the clay weight	X	X	Nonlinear model and eccentric compression	(MEONI, A. *et al.*, 2021)
SF	Smart bricks	0.25 wt% of the clay weight		X	Temperature and humidity variation	(MEONI et al., 2022)
SF	Columns tubular	0.5 wt% of the cement weight		X	Piezoresistive in monotonic loading	(SUN, Ming-qing *et al.*, 2014)
SF	Masonry buildings	0.25 w% of the total mass weight		X	Life cycle analysis	(LANDI et al., 2022a)

Source: The author.

The weight percentages of SF in relation to clay or cement highlight the adaptable nature of these materials, around 0.5%. Experimental methods encompass eccentric axial compression, temperature, and humidity variation studies, piezoresistive testing under

monotonic loading, and life cycle analysis. Numerical method refers to the nonlinear stress-strain model. These experiments reveal the multifaceted nature of SF applications, ranging from structural reinforcement in masonry buildings to innovative uses in smart brick technology. The incorporation of nonlinear modeling and rigorous testing underscores a comprehensive approach to understanding SF behavior under different conditions, indicative of ongoing research aimed at enhancing structural durability, efficiency, and sustainability.

2.5.4 Graphene nanoplatelets (GNPs)

Graphene nanoplatelets are a type of carbon nanomaterial composed of small stacks of graphene sheets. These sheets are obtained from graphite layers through a process involving the intercalation of small molecules followed by mechanical or thermal exfoliation (SENADHEERA *et al.*, 2023). GNPs offer cost efficiency and superior dispersibility, a significant advantage over other nanomaterials or pure graphene, simplifying their incorporation into various matrices (ABEDI; CORREIA; FANGUEIRO, 2021; SEVIM; JIANG; OZBULUT, 2022). They exhibit distinct geometric variations in their two-dimensional structure. Therefore, hybrid nanomaterials, such as GNP_CNT with different dimensions (2D/1D), can produce a synergistic enhancing effect and impart excellent properties to cementitious composites (LIU, Yi *et al.*, 2020; WANG, Yunyang; ZHANG, 2022). Through mechanisms such as crack bridging and deflection, they hinder crack propagation at the nanoscale (DONG, et al., 2021; ABEDI et al., 2022).

Table 4 provides a review of studies using GNP (2 articles) and their combinations with carbon CNT and CF (GNP_CNT and GNP_CNT_CF, adding 2 articles). GNP is utilized in asphalt mixtures for road pavements and geotextiles for pavements, with distribution ranging from volumetric proportions in asphalt mixtures to widespread use in geotextiles. Experimental methodologies include cyclic compressive stress testing, tensile loading, transverse strains, and electro-mechanical modeling, aimed at evaluating mechanical and electrical properties. Numerical method refers to the electromechanical model. The combination of CNT, GNP, and CF in concrete beams highlights the versatility of these materials in enhancing compressive strength and electrical conductivity.

Table 4 – Review of studies using graphene nanopleteles for civil engineering SHM

Filler type	Application	Content	Num.	Exp.	Method	Reference
GNP	Asphalt mixtures in road pavements	5 vol% of the binder volume		X	Cyclic compressive stress	(GULISANO *et al.*, 2023)
GNP_CNT_CF	Concrete beam reinforced	0.35 to 3 wt% of the cement weight		X	Compressive strength and electrical measurements	(ABEDI *et al.*, 2022)
GNP	Geotextiles in pavements	Throughout the area	X	X	Tensile loading, transverse strains, and electro-mechanical model	(YANG, Ziqian *et al.*, 2023b)
GNP_CNT	Geocomposites in pavements	0.17 wt% of the cement weight		X	Compressive strength and electrical measurements	(SUN, Jiongfeng; QIAO, 2023b)

Source: The author.

2.5.5 Graphite powder (GP)

Graphite finds various applications, whether in powder form, nanofibers, or reduced from oxides. Graphite powder is attractive due to its lightweight and high conductivity. Nevertheless, GP equips a smooth surface in the microstructural scale, which lessens the surface bonding strength and consequently reduces the mechanical properties (SUN et al., 2021; DONG et al., 2022b). Graphite was characterized by ease of application, capable of being dispersed in the mortar binder through mechanical mixing, allowing their application in large quantities without the use of specialized equipment (DROUGKAS *et al.*, 2023b). Due to poor adhesion and low interlocking with cement, GP exacerbated concrete defects, decreasing the elastic modulus, cyclo-hop effect, and compressive strength (DINESH; SUJI; PICHUMANI, 2023a). The best results could be obtained with optimized contents of self-sensing materials and graphite. So, GP is used to reduce the percolation threshold of the

other nanomaterials embedded cement (DINESH; SUJI; PICHUMANI, 2023d; LANDI et al., 2022b).

Table 5 provides a review of studies using GP, as well as a combination with SF (GP_SF), CF, and CNT (GP_CF_CNT) in beams, columns, and historical masonry buildings, totaling 3 articles. The weight or volume percentages of the materials relative to the binder demonstrate the variety of proportions used in different application contexts, around 0 to 20%. Experimental methods involve compression strength tests and electrical measurements, aiming to evaluate both the mechanical and electrical properties of the composite materials. Also noteworthy is the detailed mechanical and electrical characterization in historical masonry buildings, reflecting the preservation of cultural heritage while seeking innovative solutions to reinforce their structure.

Table 5 – Review of studies using graphite powder for civil engineering SHM

Filler type	Application	Content	Num.	Exp.	Method	Reference
GP	Beams and columns	5 wt% of the cement weight		X	Compressive strength and electrical measurements	(DINESH; SUJI; PICHUMANI, 2023b)
GP_SF	Beams and columns	0.75 vol% of the cement weight		X	Compressive strength and electrical measurements	(DINESH; SUJI; PICHUMANI, 2023c)
GP_CF_CNT	Historic masonry buildings	0 to 20%, 0.2% and 0.4 wt%, respectively, of the binder weight		X	Mechanical and electrical characterization	(DROUGKAS *et al.*, 2023a)

Source: The author.

2.5.6 Carbon black nanoparticles (CBN)

Carbon black nanoparticles are conductive additives commonly used in self-sensitive materials (NALON *et al.*, 2020). Formed during the thermal decomposition of hydrocarbons, CBNs have a diameter of less than 300 nm. They fuse to form aggregates during production, with their structure depending on factors such as fuel type and combustion

temperature (HENRIQUE et al., 2024; NALON et al., 2024). The incorporation of CBN offers high electrical conductivity and can act as a microencapsulation agent, together with lime, providing self-sensing and self-healing properties in composites (MONTEIRO; CACHIM; COSTA, 2017; DONG et al., 2022; HUSSAIN et al., 2022).

Table 6 highlights a review of studies using CBN (1 article) and a combination with CNT (1 article), in masonry structures and concrete columns. The weight percentages of the materials relative to the binder around 0% to 9% of the binder weight, demonstrating the flexibility of these composites in different structural contexts. Experimental methods include cyclic compression tests, eccentric axial compression, and monotonic compression, emphasizing the variety of loading conditions considered to evaluate the strength and performance of these materials in different scenarios.

Table 6 – Review of studies using carbon black nanoparticles for civil engineering SHM

Filler type	Application	Content	Num.	Exp.	Method	Reference
CBN	Concrete masonry	0% to 9 wt% of the binder weight		X	Eccentric axial compression	(NALON et al., 2024)
CBN_CNT	Concrete column	6 wt% of the cement weight		X	Cyclic and monotonic loading	(DING, Siqi *et al.*, 2019)

Source: The author.

2.6 Final comments

Methods for assessing damage and stress in structures often are expensive and limited-duration techniques. However, the emergence of self-sensing materials presents clear advantages with respect to traditional monitoring technologies, within the smart materials category. These innovative materials, when integrated into load-bearing structures, offer enhanced compatibility and similar durability to civil works.

An analysis of reviewed literature, by PRISMA methodology, reveals a growing relevance of self-sensing materials in civil engineering, as evidenced by their increasing adoption in SHM practices. Journals like Construction and Building Materials have become focal points for research in this domain, with a notable surge observed since 2014, indicating

their escalating effectiveness in continuous SHM. Geographically, global interest in self-sensing materials is evident, with China, the United States, and Italy leading in contributions.

Thus, smart, and self-sensing materials are indispensable in various engineering constructions of pavements, bridges, high-rise buildings, dams, and tunnels. Through quantitative studies, carbon-based materials have become more attractive as conductive additives due to their superior electrical conductivity and operational stability. Particularly, CNTs have raised interest in the last few years, due to their high specific mechanical and transport properties, and suggest that they are ideal candidates for high performance and self-sensing composites. Most of them are mainly made of cementitious composites and suffer from frequent service loads and harsh environmental conditions. In this regard, intrinsic self-sensing materials would be an appropriate supplement to the existing sensing technologies, allowing for long-term, wide distribution, and low-cost monitoring of infrastructures.

3. EFFICIENT DISPERSION FOR UNIFORMITY OF CARBON NANOTUBES DISTRIBUTION AND STABILITY IN AQUEOUS SOLUTIONS FOR SOIL-CEMENT COMPOSITES

3.1 Introduction

In nanotechnology, the use of nanoparticles to monitor the structural integrity of civil construction and enhance mechanical properties has emerged as a prominent application (HUANG; WANG, 2016; GAO et al., 2019; YOO; OH; BANTHIA, 2022; LUO et al., 2023). Chemical admixtures containing a low content of nanoparticles improve the physical properties, electrical conductivity, and mechanical properties of cement-based composites, indicating their potential for reinforcement and intelligent self-sensing. So, integrating nanomaterials into soil-cement mixtures represents a promising avenue for enhancing mechanical strength, durability, and overall performance, showcasing potential advancements in sustainable and resilient construction practices. In this comprehensive field, carbon nanotubes stand out (METAXA; KONSTA-GDOUTOS; SHAH, 2013; TAHA et al., 2018; SUH et al., 2023).

Carbon nanotubes (CNTs) are carbon atoms arranged in concentric layers and hexagonal structure. The CNT could be organized in different coil modes, resulting in various diameters, microscopic structures, and distinct properties. Among carbon allotropes, CNTs stand out as the most promising and extensively studied. CNT are sp^2 hybridized structures with the most straightforward atomic bond configuration (GUPTA, Nikita; GUPTA; SHARMA, 2019). They are composed of graphene, with a radial dimension on the nanometer scale and an axial dimension on the micron scale, CNTs are hollow structures with both ends sealed (HAN et al., 2020). There are two main CNTs types: single-walled carbon nanotube (SWCNT) and multi-walled carbon nanotube (MWCNT) (DEVI, Rekha; GILL, 2021). MWCNT comprises multiple tubes rolled concentrically, forming a wall with more than one carbon atom thickness. In contrast, SWCNT is made of only one tube. The literature suggests an increasing order of effectiveness considering attainability and better physical, chemical, and conductive properties: simple CNT < SWCNT ≤ MWCNT (MEHRA; MISHRA; JAIN, 2014; MATOS et al., 2023; VAKHITOVA et al., 2023).

However, the effective dispersion of CNTs remains challenging due to their high natural agglomeration tendency, which limits their potential performance (CORREIA, António Alberto S.; CASALEIRO; RASTEIRO, 2015; DA LUZ *et al.*, 2019). This propensity

arises from their nanoscale dimensions and the action of adhesive or van der Waals forces between particles. Thus, materials incorporating CNTs often present agglomerates, which damages their geomechanical properties (KONSTA-GDOUTOS; METAXA; SHAH, 2010).

Addressing this challenge, achieving proper dispersion of CNTs in aqueous solutions is crucial for their effective utilization in composite materials. The most widely adopted dispersion approach involves advanced sonic treatments. However, large-scale implementation of this technique is hindered by demands for specialized equipment and the time required for the process. Alternatively, chemical functionalization presents a more practical and field-friendly dispersion technique, involving the addition of functional groups to the surfaces of CNTs (ABU AL-RUB *et al.*, 2012; CORREIA, António Alberto S.; CASALEIRO; RASTEIRO, 2015).

Alongside ultrasonic energy, the selection of surfactant and its concentration are crucial factors in obtaining a solution or sample with effective dispersion of CNTs (HASSANZADEH-AGHDAM et al., 2018; WANG, ZHONGKUN et al., 2019; CUI et al., 2023). Moreover, superplasticizer chemical admixtures have emerged as a promising solution for enhancing dispersion in mixtures containing carbon nanotubes, cement, and soil. These superplasticizers disrupt van der Waals forces and prevent agglomeration, improving the separation of CNTs in soil-cement composites (SHAH et al., 2009; CORREIA et al., 2021).

Superplasticizers in composites can be classified by their mechanism of action, with superplasticizers operating on the principle of steric repulsion induced by side chains and electrostatic repulsion facilitated by the main chain (IAN et al., 2019; LIN et al., 2021; TLI et al., 2022). Third-generation superplasticizers, often based on polycarboxylates, have been recognized as effective dispersants for improving the dispersion of MWCNTs in cement-based composites (DALAS *et al.*, 2015; PARVEEN *et al.*, 2017; STECHER; PLANK, 2019; XIANG; GAO; SHI, 2020). Figure 9 denotes the presence of long and neutral side chains and anionic carboxylate groups, contributing to the effectiveness of superplasticizer (ZOU et al., 2017; MA et al., 2023).

Figure 9 – Effect of the steric repulsion on particle dispersion due to the superplasticizer admixture

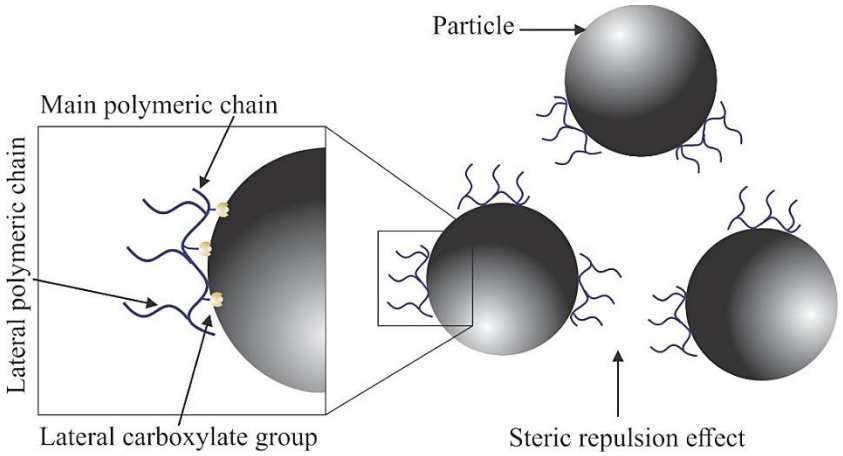

Source: The author.

Considering the demand for deep evaluations of soil-cement mixtures containing nanomaterials and their distinction and similarities with cement-based composites, assessing the effects of the current dispersion technique of MWCNTs with superplasticizer admixtures is mandatory. In the context of soil-cement composites, Correia *et al*. (2015) evaluated improvements in solutions containing a fixed value of superplasticizer and varying concentrations of MWCNTs compared to solutions of water and MWCNTs. Similarly, Figueiredo *et al*. (2015) employed two surfactants at concentrations ranging from 0.5 to 2.0%, with the dispersion method adjusted. Correia *et al*. (2021) analyzed the geomechanical behavior of soil chemically stabilized with carbon nanotubes using four types of surfactants, with concentrations ranging from 0.1 to 3%, and MWCNTs at concentrations of 0.001 and 0.01%. Correia *et al*. (2023) conducted performance tests by varying the concentration and type of surfactant, as well as the MWCNT concentration. These parameters play a significant role in enhancing soil-cement, requiring precise adjustment to achieve optimal concentrations. Overall, these studies collectively provide evidence supporting the development of cementitious composites reinforced with MWCNTs to enhance soil mechanical properties, while also identifying optimal concentrations and adjusting the dispersion method to achieve the desired efficacy.

This work investigates the effectiveness of three distinct types of superplasticizer admixtures as dispersing agents for MWCNTs in soil-cement composites. Then, several characterization techniques were employed involving soil-cement mixtures with different concentrations of admixtures, specifically 0.3%, 0.5% and 1.0% relative to the amount of

water, adequately dispersed in an aqueous medium, along with 0.001% de MWCNT, either individually or jointly.

3.2 Material Characterization and Experimental Procedures

3.2.1 Raw Materials

The MWCNTs, functionalized with carboxyl/hydroxyl groups and used in this research, were provided by CTNano (Center for Technology in Nanomaterials and Graphene, Federal University of Minas Gerais, Brazil). The physical properties of MWCNTs are described in Table 7.

Table 7 - Properties of the MWCNT used

Parameter	Values
Length range	0.5 to 15 μm
Average length	4.5 μm
Diameter range	8 to 45 nm
Average diameter	20 nm
Purity	≥ 95 %
Functionalization	9%

Source: The author.

This study compares three superplasticizer admixtures to determine the best dispersion capacity for MWCNTs in a soil-cement matrix. The chemical admixtures evaluated were Maxifluid 960H/1 (960H/1) and Maxifluid H 2085 (H2085), supplied by MatChem, and MC-PowerFlow 3100 (PF3100), provided by MC Bauchemie. Despite presenting the same chemical name and action mechanism, those three chemical admixtures are expected to have different performance that will contribute differently to the dispersion of MWCNTs. The specifications of these third-generation superplasticizer admixtures are detailed in Table 8.

Table 8 – Specifications of the superplasticizer admixtures

Specifications	960H/1	H2085	PF3100
Chemical name	RA2	RA2	RA2
Aspect	Colorless liquid	Red liquid	Brown liquid
Specific mass (g/cm³)	1.062 a 1.102	1.05 a 1.09	1.07
Solubility in water	Soluble	Soluble	Soluble
pH	3 to 5	3 to 5	4.7

Source: The author.

The Portland cement type II, with the addition of granulated blast furnace slag (CP II–E), produced in Brazil according to the ABNT NBR 16697:2018 (ABNT NBR 16697, 2018), was used in this study. This selection was based on sustainability and economic efficiency criteria, as the combination of Portland cement and granulated blast furnace slag has proven to be the most effective in improving unconfined compressive strength in different soil types (AHMAD *et al.*, 2013). The addition of granulated blast furnace slag corresponds to 19.71% of the mass of CPII–E. Table 9 shows the chemical composition in terms of the main constituents.

Table 9 – Chemical composition of cement content 5%

Composition	CaO	Al_2O_3	Fe_2O_3	K_2O	MgO	Na_2O	SiO_2	SO_3
Wt. (%)	55.27	5.84	2.29	0.85	3.14	0.18	21.79	3.73

Source: The author.

The soil used in the work was collected at a depth of 50 cm in the Geotechnics and Foundations Experimental Field of the Federal University of Ceará (CEGEF – UFC); on the Pici Campus. The material from the experimental field is sandy-silty granular soil, with around 16% fines (Figure 10). With a CNU (Coefficient of Uniformity) of 3.29 and a CC (Coefficient of Curvature) of 1.80, the sand can be classified as poorly graded and uniform.

Regarding the consistency of the soil, tests indicated a plasticity index with a null value, liquid limit equal to non-liquid, and plastic limit equal to non-plastic. The grain real density test provided a result of 2.61. According to the Highway Research Board - American Association of State Highway Officials (HRB-AASHO) and Unified Soil Classification System (USCS) classification, the soil is classified as A-2-4 and SM, respectively. These

values are aligned with other studies conducted in the experimental field (ALMEIDA *et al.*, 2020; MOURA *et al.*, 2021).

Figure 10 – Granulometric curve of soil

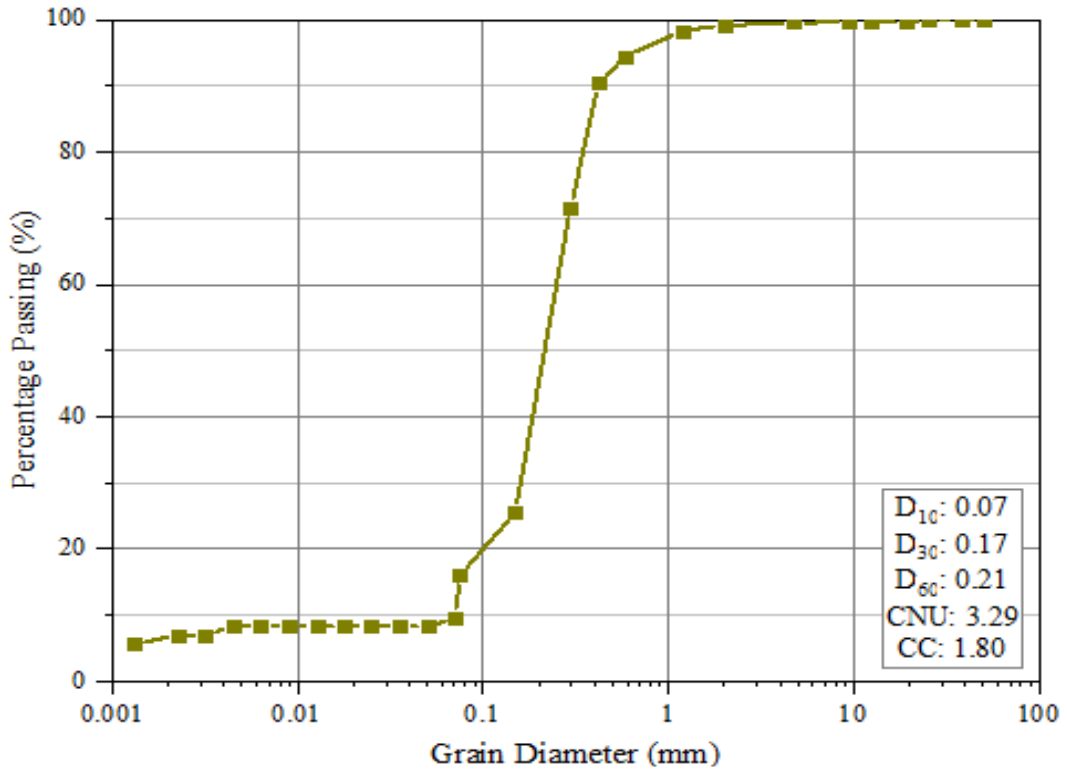

Source: The author.

For all characterizations and tests, only the percentage passing through the N° 40 sieve (425 µm opening) of the soil was used. This allows for a better visualization of the interaction of smaller particles with MWCNTs and superplasticizer admixtures, while preserving the inherent soil characteristics. Table 10 presents the examination of the chemical composition of the soil, indicating a significant presence of silica (SiO_2) and alumina (Al_2O_3). The fine texture of the soil combined with these chemical elements could mean pozzolanic properties.

Table 10 – Chemical composition of soil.

Composition	**CaO**	**Al_2O_3**	**Fe_2O_3**	**K_2O**	**P_2O_5**	**TiO_2**	**SiO_2**	**SO_3**
Wt. (%)	0.55	19.54	1.19	0.64	0.51	1.45	75.73	0.18

Source: The author.

According to the NBR 12253 (ABNT NBR 12253, 2012), the suggested cement content for the soil-cement compaction test corresponding to soil classification A-2 is 5%. Following the guidelines of NBR 12023 (ABNT NBR 12023, 2012), the soil compaction curve has a flatter shape (FIGURE 11), with maximum dry specific mass is 1.903 g/cm³, and the optimum moisture content is 10.45% for a cement content of 5%. This optimum moisture content increased by 0.5% to 1.0%, the amount of water addition sufficient to compensate for the water loss by evaporation (ABNT NBR 12024, 2012). This study defines the moisture content as 11.45% relative to the dry mixture.

Figure 11 – Compaction curve for the Normal Proctor energy of soil-cement with 5% cement content

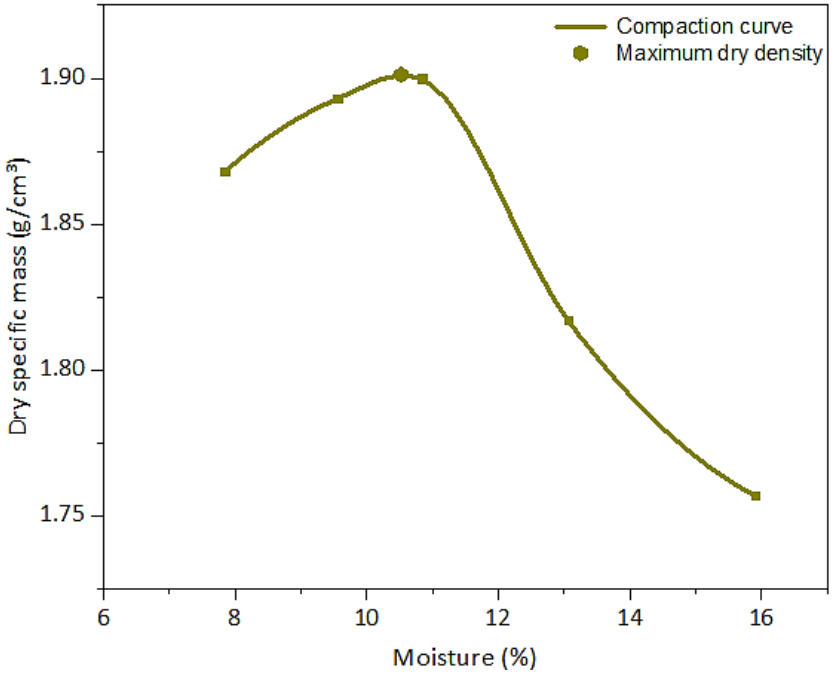

Source: The author.

3.2.2 Characterization techniques

A series of tests were performed to assess the properties of the used materials to support the understanding of possible interactions between them. Table 11 summarizes the characterization techniques used to investigate the properties of particles and materials at micro and nanoscales. In this section, each characterization method is explained in detail, minimizing redundancy, and optimizing the presentation of tests.

Table 11 - Physicochemical characterization techniques applied in the study

Material	Physicochemical test							
	Dz/PDI	**UV-Vis**	**Zeta**	**TG**	**FTIR**	**SEM**	**Raman**	**AFM**
MWCNTs solution	X		x					
Superplasticizer admixtures solution			x	x	x			
MWCNTs + superplasticizer admixtures solution	X	x						
Soil-cement samples		x				x	x	x

Source: The author.

The Z-average (Dz) and Polydispersity Index (PDI) are parameters related to the hydrodynamic diameter, evaluated through the Dynamic Light Scattering (DLS) method. The hydrodynamic diameter represents a dimension equivalent to the size of suspended particles, accounting for the interaction between particles and the surrounding fluid. The Z-average (Dz) characterizes the size distribution, also known as the cumulant mean, representing the optimal outcome of the hydrodynamic diameter distribution (MARLIERE *et al.*, 2023). The Polydispersity Index (PDI) is a metric that describes the uniformity of particle size distribution in a suspension (BHATTACHARJEE, 2016). The relationships between the quality of MWCNT-dispersion on the one hand and superplasticizer concentration on the other were determined using Dz/PDI. In each MWCNT and superplasticizer admixture solution, a hydrodynamic diameter analysis was applied in weeks 0 to 4 to assess variations and stabilities over time. The Dz and PDI were determined using the Nano Zetasizer equipment from Malvern®, model ZS 3600. The hydrodynamic diameter was measured with a laser at a wavelength of 633 nm and a fixed scattering angle of 173°.

Ultraviolet–visible spectroscopy (UV-Vis) measures the absorption of light by a sample due to electronic transitions, providing information about nanomaterials and analyzing the stability of solutions and samples over time (QUERAL-BELTRAN *et al.*, 2023). The UV-Vis equipment used was the Shimadzu UV-2600 spectrophotometer with an ISR-2600Plus integrating sphere and internal setup. The analyses of selected solutions and samples within the Eppendorf-type microtubes were conducted after 1st and 60th day of preparation.

The zeta potential (Zeta) of MWCNT solution and superplasticizer admixtures solutions was determined in the laboratory using the Electrophoretic Light Scattering (ELS) technique. Zeta potential is a critical parameter that determines electrostatic repulsion or

attraction, indicating the tendency of solid particles to aggregate in an aqueous medium (SRINIVASAN *et al.*, 2010). The Zeta was determined using the Nano Zetasizer model ZS 3600, with a scattering angle of 17°, conducted after 1st day of preparation.

The thermogravimetric analysis coupled with Fourier transform infrared spectroscopy (TG/FT-IR) is one of the most robust methods for investigating the thermal degradation of polymers. The temperature-mass variation curves obtained through TG provide insights into the thermal stability of the sample, the composition, and the residue composition of superplasticizer admixtures (SANCHES; CASSU; DUTRA, 2015). The TGA Q50 Instruments equipment was used for thermogravimetric tests. The experiments for superplasticizer admixtures were conducted in a synthetic air atmosphere with a 60 mL/min flow rate and a heating rate of 10°C/min from 25 to 900°C, conducted after preparation.

Fourier Transform Infrared (FT-IR) and Infrared spectroscopy (IR) were used for the analysis of the chemical and structural properties of third-generation superplasticizer admixtures based on specific molecular vibrations of the substances (DE OLIVEIRA *et al.*, 2023; HU; ZHAO; LIU, 2023). The infrared measurements of the samples were performed using an IR-Tracer100 spectrometer from Shimadzu with an attenuated total reflectance accessory. Liquid samples were directly placed on the crystal. The samples were also analyzed in the solid state, in the form of potassium bromide (KBr) pellets. Initially, they were ground in an agate mortar and then subjected to a pressure of 80 kN in a hydraulic press. All spectra were averaged from 64 scans, ranging from 600 to 4000 cm^{-1} with a resolution of 4 cm^{-1}.

The Scanning Electron Microscopes (SEM) were used for micro and nanoscale analyses and identification of MWCNTs, generating signals that are transformed into high-resolution images of the soil-cement sample surface (FELL *et al.*, 2023). The FEI-Quanta 450 high-resolution SEM (FEG-SEM) was used to examine pressed samples coated with a thin Ag film by cathodic spraying, conducted after 28th day of preparation.

Raman spectroscopies were used in soil-cement samples, from 28th day of preparation, to interpret specific functional groups through observed bands, providing insights into the molecular structure of MWCNTs present in the specimens (MUSSO *et al.*, 2009). The equipment used for Raman mapping experiments was the Oxford Instruments Witec Alpha 300 System, with a laser wavelength of 532 nm.

Atomic Force Microscopy (AFM) creates images of samples, allowing for precise information extraction regarding size, shape, and recognize particles of different specimens (CHENG *et al.*, 2021; JOSHUA; CHENG; LAU, 2023). The AFM equipment used was

Asylum MFP-3D-BIO from Oxford Instruments, operating in tapping mode. The tips were adjusted for a resonance frequency of 320 kHz, with K = 42 N/m, and an AFM tip radius of curvature of less than 8 nm. The soil-cement sample with the best dispersion and stability quality, as determined from the previous tests, was selected for AFM analysis.

3.2.3 Preparation for MWCNT dispersion

The characterization of the polycarboxylate-based additive employed in MWCNT dispersion was conducted through the evaluation of Dz, Zeta, and UV-Vis. All measurements were performed at least twice under the same conditions to ensure the reliability of the results. Based on previous studies and the facilities available in the laboratory, the procedure for preparing the dispersions was outlined (D'ALESSANDRO *et al.*, 2016; RAFAEL, 2017).

The dispersions containing MWCNTs were prepared by mixing deionized water with 0.001% of MWCNT. Dispersion was achieved through sonication using a needle-type agitator at a power of 20 W for 15 minutes. In turn, the superplasticizer admixtures dispersions were prepared by combining deionized water with concentrations of 0.3%, 0.5%, and 1.0% of each additive. Homogenization was achieved by magnetic stirring of the solution for 10 minutes at 500 rpm, followed by sonication of the sample for 2 minutes.

Subsequently, the dispersions containing superplasticizer admixtures with MWCNTs were obtained from deionized water solutions containing the determined concentrations of additives (0.3%, 0.5%, 1.0% relative to the solvent). After this step, the dispersion was subjected to magnetic stirring for 10 minutes at 500 rpm to ensure homogeneous dispersion, followed by sonication of the sample for 2 minutes. Then, 0.001% of MWCNTs was added to the dispersion, followed by additional sonication of the sample for 15 minutes. To minimize potential interferences, a 0.1 M NaCl solution was used as the solvent for Dz tests. The dispersions were filtered (0.20 μm for Dz, and 0.45 μm for Zeta) before being introduced into the test cell.

All mentioned concentrations were expressed in mass (for example, 1% corresponds to 1 g/100 mL). The results obtained guided the selection of optimal additive concentrations for the continuation of experiments. Figure 12 illustrates the scheme for the preparation of dispersions and Table 12 includes a summary of the test plan for the dispersions.

Figure 12 – Dispersion procedure and solution preparation method

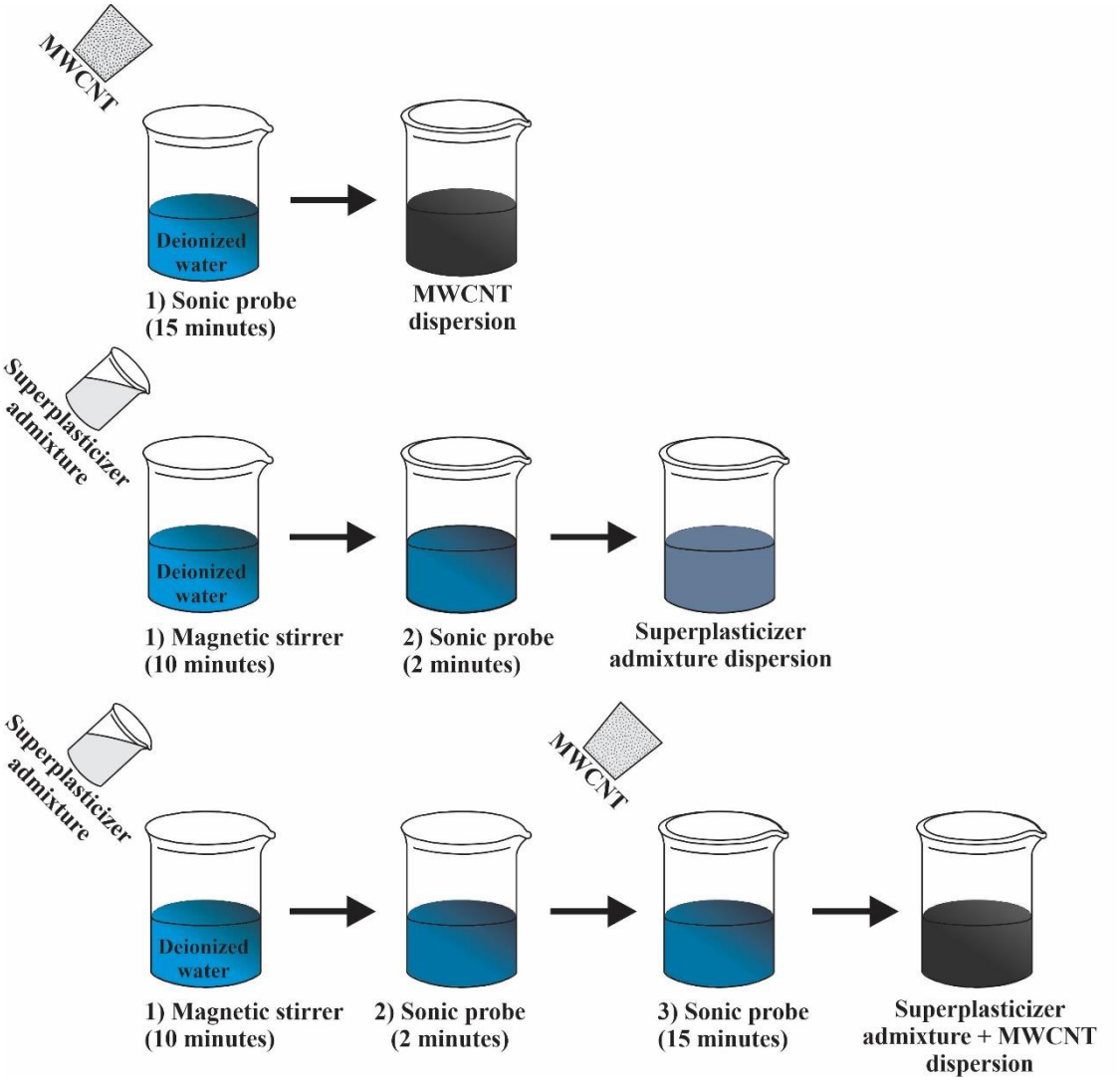

Source: The author.

Table 12 - Dispersions Test Plan

Superplasticizer admixture	Concentration	MWCNT
-	-	0.001%
960H/1	0.30%	0.001%
	0.50%	
	1.00%	
H2085	0.30%	0.001%
	0.50%	
	1.00%	
PF3100	0.30%	0.001%
	0.50%	
	1.00%	

Source: The author.

3.2.4 Samples preparation of soil-cement composites with MWCNT dispersions

Soil cement samples were prepared using the content that obtained the best dispersion obtained in the aqueous solutions tests, those assessing superplasticizer and MWCTs dispersion characterization. The preparation method for the specimens, based on the guidelines of Rafael (2017) and D'Alessandro *et al*. (2015), was as follows:

1) Manual dry mixing of 415.89 g of the analyzed soil, with 20.79 g of the cement, corresponding to a concentration of 5% of the soil mass, until homogeneity is obtained;

2) The mixture was mixed with 25 ml of the selected dispersion (half of the dispersions preparation, Topic 3.2.3) in the low-speed mechanical mixer (200 rpm) for 2 minutes;

3) The remaining 25 ml dispersions was included in the mixture in a medium-speed mechanical mixer (300 rpm) for 3 minutes;

4) Part of the fresh mixture was placed in Eppendorf-type microtubes, and the rest was separated to compression strength test in a hydraulic press for subsequent analyses.

The efficacy of superplasticizer admixtures in dispersing MWCNTs was confirmed through analyses conducted on various samples. These samples included soil-cement and water (SC), soil-cement, water, and MWCNTs without the application of a dispersant (SC MWCNT), as well as soil-cement samples treated with superplasticizer admixture dispersions and MWCNTs. The dispersion method developed in the study is schematically in Figure 13.

Figure 13 - MWCNT dispersion procedure, soil-cement paste preparation and specimens' apparatus

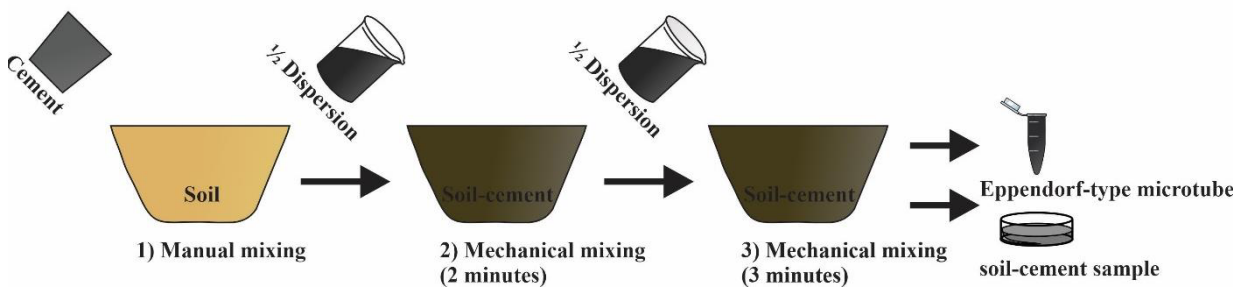

Source: The author.

The following concentrations described in Table 13 were performed to assess the efficiency of MWCNT dispersions with superplasticizer admixtures.

Table 13 – Proportions of the test plan for soil-cement samples

Material Constituents	**Mixtures proportions (kg/m³)**							
	SC	**SC MWCNT**	**SC PF3100**			**SC H2085**		**SC 960H/1**
			0.3%	**0.5%**	**1.0%**	**0.3%**	**0.5%**	**1.0%**
Soil (s)	16.270	16.270	16.265	16.262	16.253	16.265	16.262	16.253
Cement (c)	0.814	0.814	0.813	0.813	0.813	0.813	0.813	0.813
Water (w)	1.956	1.956	1.955	1.955	1.954	1.955	1.955	1.954
Superplasticizer admixtures (SP)	-	-	0.006	0.010	0.020	0.006	0.010	0.020
MWCNT	-	0.0002	0.0002	0.0002	0.0002	0.0002	0.0002	0.0002
Main ratios								
c/s	5%	5%	5%	5%	5%	5%	5%	5%
w/sc	11.45%	11.45%	11.45%	11.45%	11.45%	11.45%	11.45%	11.45%
SP/w	-	-	0.30%	0.50%	1.00%	0.30%	0.50%	1.00%
MWCNT/w	0.001%	0.001%	0.001%	0.001%	0.001%	0.001%	0.001%	0.001%

Source: The author.

3.3 Results and Discussion

3.3.1 Analysis of MWCNTs and superplasticizer admixtures dispersions

DLS was employed to determine the relationship between 0.001% of MWCNT dispersion quality and superplasticizer concentration. Weekly hydrodynamic diameter analysis over four weeks assessed variations and stability in each dispersion. The results, including PDI and Dz, are summarized in Tables 14 and 15, respectively.

Table 14 – PDI values of the dispersions

Superplasticizer admixtures	Concentration	Week				
		0	1	2	3	4
		PDI				
960H/1	0.30%	0.483	0.405	0.696	0.607	0.814
	0.50%	0.675	0.668	0.525	0.482	0.382
	1.00%	0.323	0.350	0.353	0.354	0.222
H2085	0.30%	0.590	0.550	0.558	0.785	0.667
	0.50%	0.193	0.727	0.706	0.732	0.629
	1.00%	0.610	0.224	0.608	0.546	0.764
PF3100	0.30%	0.255	0.242	0.282	0.325	0.363
	0.50%	0.673	0.660	0.813	0.896	0.979
	1.00%	0.946	0.998	1.000	1.000	1.000

Source: The author.

Table 15 - Dz values of the dispersions

Superplasticizer admixtures	Concentration	Week				
		0	1	2	3	4
		Dz (nm)				
960H/1	0.30%	146.40	240.90	590.70	472.30	459.80
	0.50%	89.99	145.10	157.10	177.30	126.90
	1.00%	93.50	153.10	123.10	104.80	94.42
H2085	0.30%	104.30	328.30	311.40	526.30	403.50
	0.50%	109.30	345.30	283.70	549.80	528.50
	1.00%	356.20	126.60	230.00	480.50	228.10
PF3100	0.30%	96.40	103.30	112.30	131.90	140.30
	0.50%	93.82	165.20	190.70	143.70	126.80
	1.00%	32.22	44.93	53.45	34.96	52.43

Source: The author.

Table 14 shows an increase in PDI over the 4 weeks analyzed in all concentrations of PF3100 and H2085 and for 0.3% content of 960H/1. On the other hand, 960H/1 0.5% and

1.0% show a significant decrease over the weeks, considering the initial and final PDI values. For the PF3100 superplasticizer, there is a tendency for an increase in the PDI as the concentration increases. In the case of H2085 and 960H/1, it is impossible to distinguish a behavior trend increasing concentration.

Regarding the Dz value, all dispersions containing the superplasticizer PF3100 obtained the lowest values (less than 191 nm) and lower variations. Despite the high PDI of PF3100, the 1.0% concentration reached the lowest Dz values. The behavior of Dz for H2085 follows the same trend as PDI, in terms of increasing or decreasing data over the weeks. For 960H/1, Dz and PDI have similar behavior for 0.5% and 1.0%, with slight reductions and variations (less than 178 nm). However, the 960H/1 0.3% concentration had a significant increase and variation over time.

Hydrodynamic diameter tests in MWCNT dispersion obtained a Dz value of 240.8 nm and a PDI of 0.316. Figure 14 shows the size distribution of nanotubes after the dispersion process on deionized water.

Figure 14 – Size distribution by intensity for MWCNT

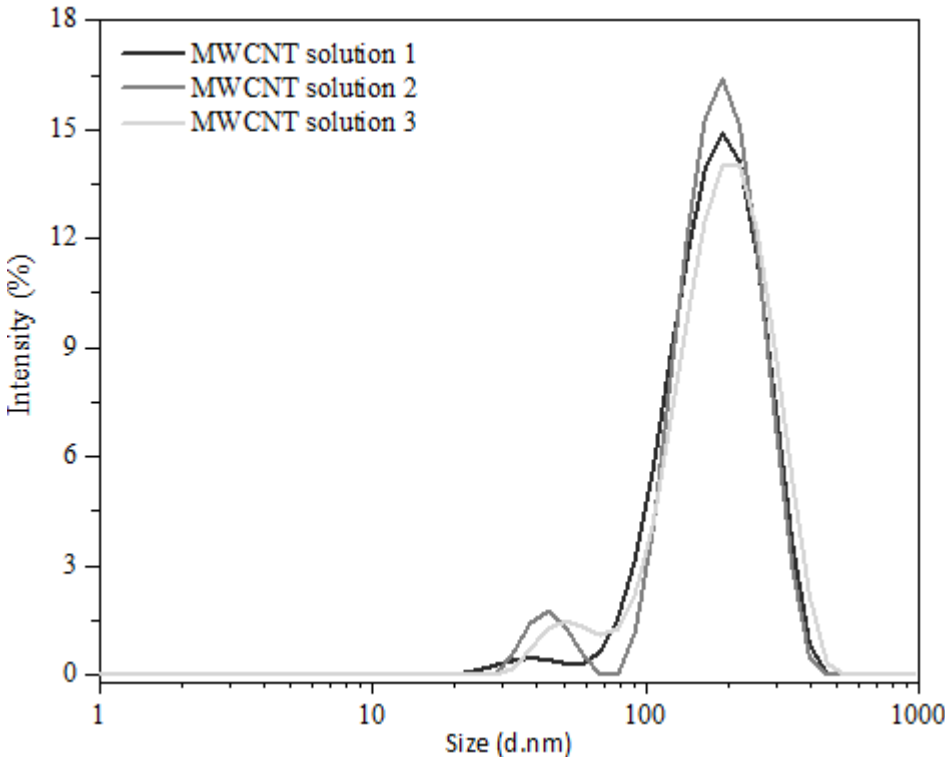

Source: The author.

Figure 14 indicates that, during the mixing and preparation of the aqueous solution, MWCNT agglomerate into large filaments. Thus, superplasticizer admixtures are

considered adequate if they achieve lower values of Dz in the dispersion with only MWCNT, keeping a certain degree of consistency over time. For comparison, at least one concentration of each of the superplasticizers studied was selected for comparisons. The most efficient concentrations are 0.3%, 0.5%, and 1.0% of PF3100, 0.3% of H2085, 0.5% and 1.0% of 960H/1. The evolution of Dz analysis over the weeks are illustrated in Figure 15.

Figure 15 – Evolution of the Dz of selected concentrations

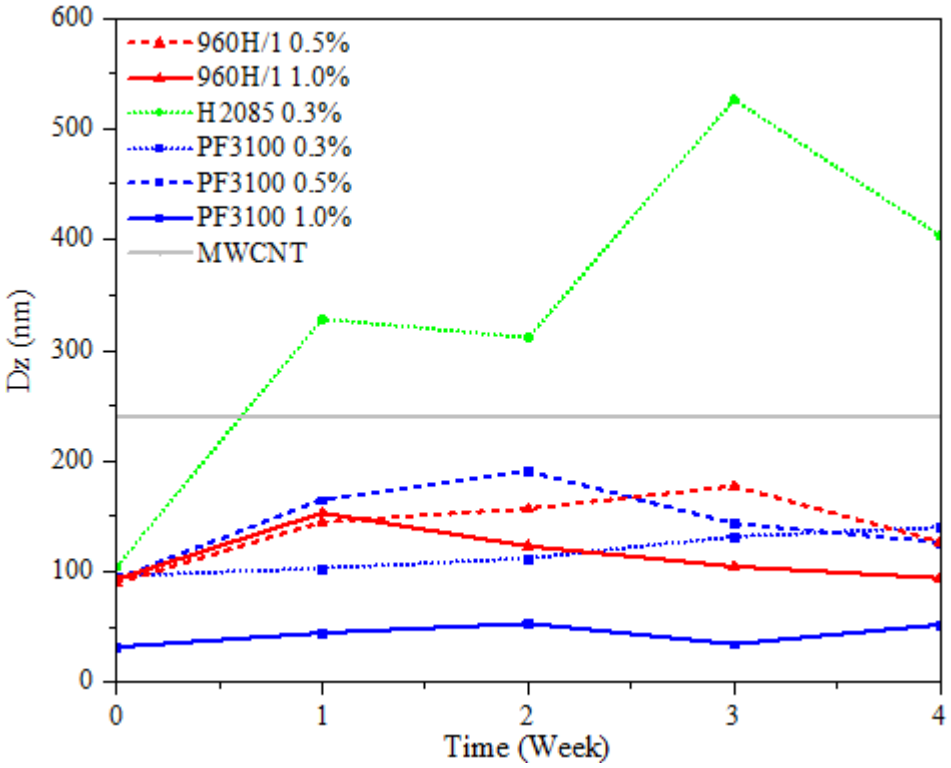

Source: The author.

Figure 16 describes the characterization of the most efficient dispersion of CNTs and superplasticizer admixtures in aqueous solution using UV-Vis. The observation of an increase in intensity is attributed to π to π transitions, indicating effective interaction between the molecules of the studied components. Thus, there is an absence of changes in the electronic behavior of the samples over time, suggesting significant stability. This stability of the samples is an important aspect, as it indicates that the physicochemical properties of the dispersions remain consistent over time. It is noted that there was no degradation or agglomeration of the MWCNTs during the study period.

Figure 16 – Liquid UV-Vis with added CNTs and (a) 960H/1 0.5%, (b) 960H/1 1.0%, (c) H2085 0.3%, (d) PF3100 0.3%, (e) PF3100 0.5%, and (f) PF3100 1.0%

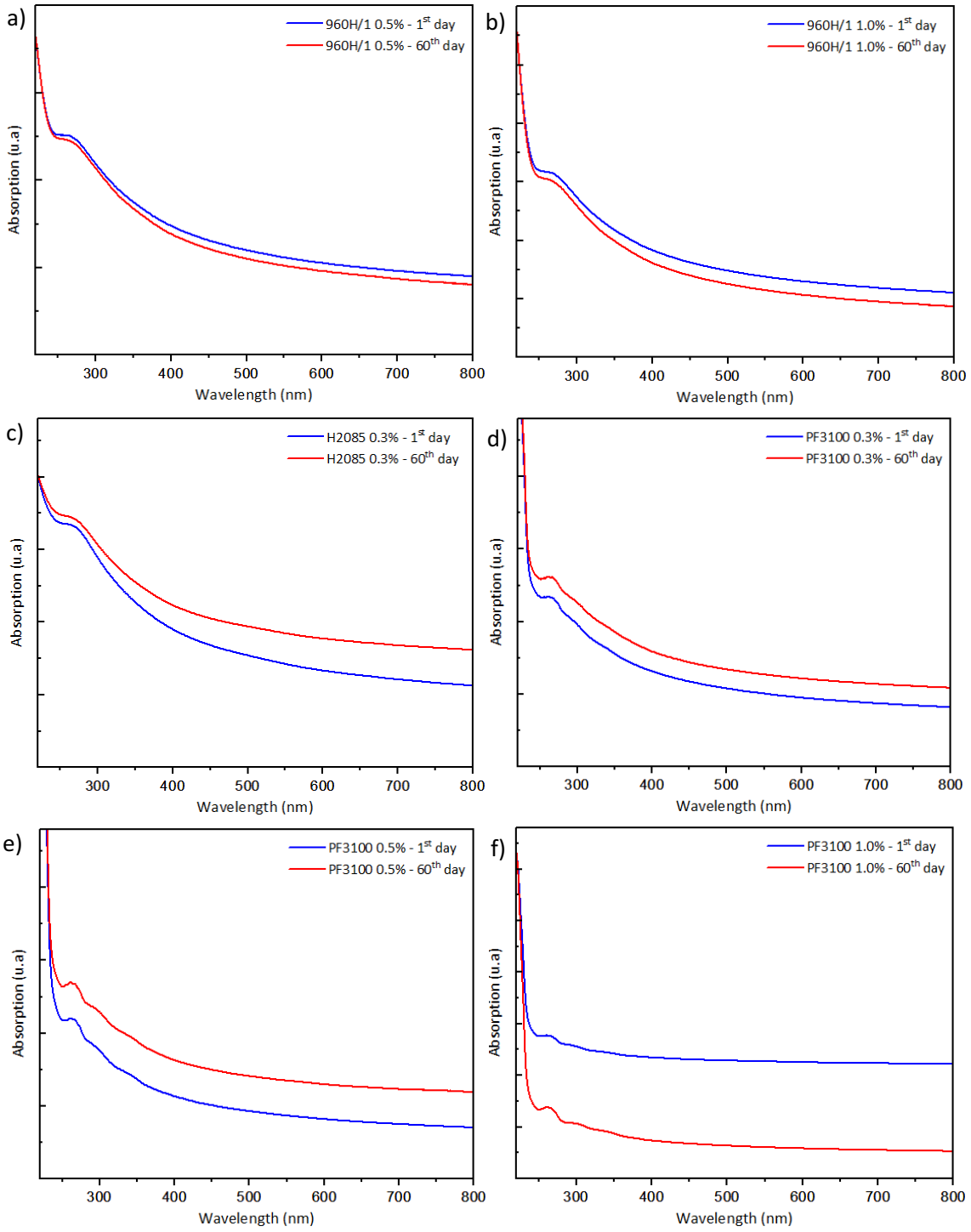

Source: The author.

Figure 17 shows the samples on the 1st and 60th day. Visibly, the samples do not exhibit any significant change in coloration or sedimentation after days, which is consistent with the results obtained from UV-Vis analyses.

Figure 17 – Photographs of the MWCNT on the 1st and 60th days after preparation under static conditions: a) H2085 0.3%, 960H/1 0.5%, and 960H/1 1.0%, on the 1st day; b) H2085 0.3%, 960H/1 0.5%, and 960H/1 1.0%, on the 60th day; c) PF3100 0.3%, PF3100 0.5%, and PF3100 1.0%, on the 1st day; d) PF3100 0.3%, PF3100 0.5%, and PF3100 1.0%, on the 60th day

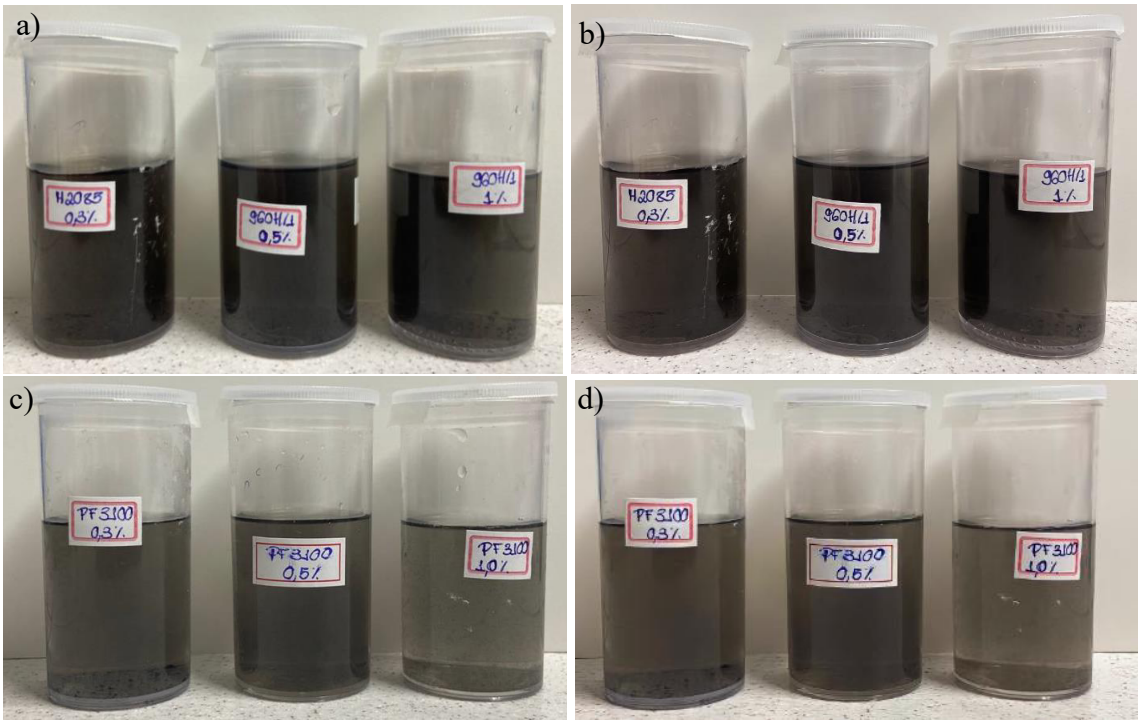

Source: The author.

Table 16 describes the Zeta results for the selected superplasticizer dispersions.

Table 16 – Zeta potential values of the selected concentrations

Superplasticizer admixtures	Concentration	Zeta Potential
960H/1	0.50%	-37.0 mV
	1.00%	-16.5 mV
H2085	0.30%	-36.9 mV
PF3100	0.30%	-23.3 mV
	0.50%	-22.9 mV
	1.00%	-19.9 mV

Source: The author.

The highest zeta potentials, in absolute terms, were obtained by the 0.5 content of 960H/1 and H2085, registering -37.0 and -36.9 mV, respectively. The lowest zeta potential,

corresponding to -16.5 mV, was achieved by 960H/1 1.0%. Also, the increase in PF3100 concentrations reduces the zeta potential. Regarding the incorporation of superplasticizer admixtures, although there is a reduction in the zeta potential, there is an increase in steric stability. This stability acts on the particle repulsion provided by the polymer chain. Furthermore, while elongating the side chain leads to a decrease in anionic charge density, the pronounced steric hindrance effect becomes evident, enhancing the dispersion of cement particles and decreasing the slurry's viscosity and shear yield stress (BURGOS-MONTES *et al.*, 2012; LIU, Ming *et al.*, 2015). This justifies the decrease in the zeta potential of the additives compared to the zeta potential of MWCNTs alone in aqueous solution, which corresponds to -39.4 mV.

Figure 18 shows the TG and DTG curves for the superplasticizers analyzed to identify the functional groups.

Figure 18 – TG and DTG curves for superplasticizer admixtures in a synthetic air atmosphere at a rate of 10°C/min

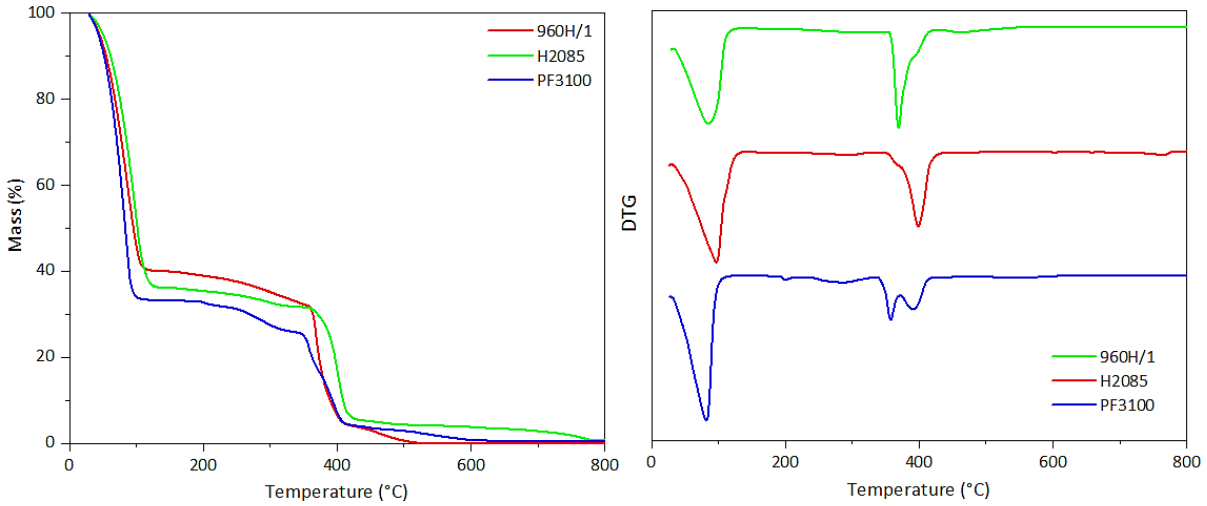

Source: The author.

Through the TG and DTG curves, it is observed that superplasticizer admixtures undergo two degradation events. It is assumed that around 60% to 70% of the composition of the superplasticizers consists of water, with the first decomposition occurring around 100°C. The second degradation is between 350 and 400°C since the superplasticizer admixtures are polymers. The thermal decomposition of polymers is related to the breakdown of molecular chains, starting with the rupture of weak or secondary bonds, such as hydrogen bonds and dipole interactions, until the main bonds of the polymeric chains begin to break. The 960H/1, H2085, and PF3100 chemical admixtures presented 0.117%, 0.830% and 0.688%,

respectively, of inorganic residue. These values indicate the amount of non-volatile material that remains after thermal decomposition of chemical admixtures up to 800°C.

The spectra of the three additives exhibited similar behaviors and were effective in confirming the presence of functional groups that characterize polycarboxylate-based additives, as can be observed in Figure 19.

Figure 19 - FTIR spectra of superplasticizer admixtures

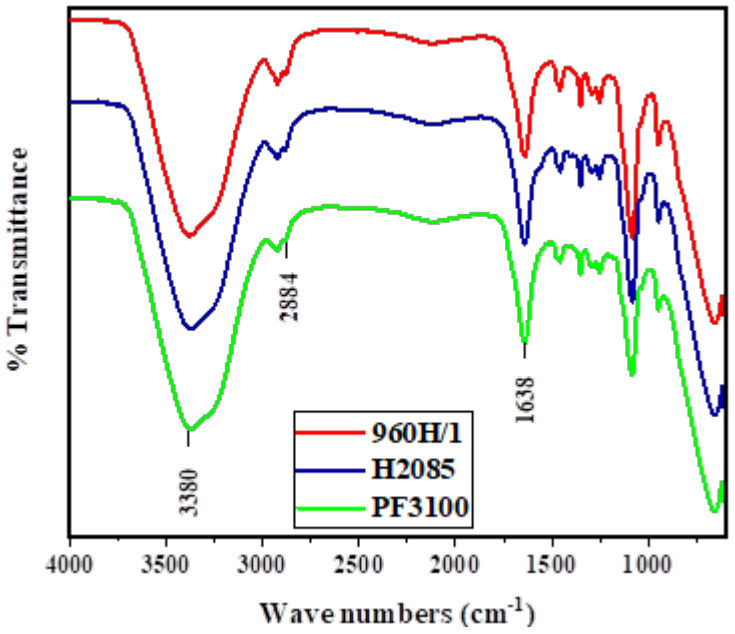

Source: The author.

The stretching vibrations of CH (ν C-H) in aliphatic molecules are found at approximately 2884 cm^{-1} corresponding to CH and CH_2 groups. This band at 2887 cm^{-1} is classified it as an aliphatic hydrophobic group (JANOWSKA-RENKAS, 2015). A broad band was seen at approximately 3380 cm^{-1}, attributed to the stretching vibrations of OH (ν O-H), and at 1638 cm^{-1}, a band from the deformation modes of water molecules (δ H2O) was observed (KHAOULAF et al., 2017). Thus, it is probable that the plasticizers are dispersed in water, hence, making it difficult to visualize the intense carbonyl band, observed from 1760-1690 cm^{-1}, which is a characteristic functional group of polycarboxylate-based additives.

For a better characterization of the material, it was necessary to heat these additives to check for bands that are overlapped by the intense bands characteristic of water (Figure 20). With the reduction of the 1638 cm^{-1} band, corresponding to water vibration modes, an intense band is observed at 1730 cm^{-1} in the characteristic spectral range of carbonyl, which could be related to carboxylic acid carbonyl (1725-1700 cm^{-1}) and ester

carbonyl (1750-1730 cm^{-1}) (PAVIA *et al.*, 2014). A stretching vibration of COC (ν C-O-C) was seen at 1112 cm^{-1} indicating the presence of ether function in the additives, confirming the occurrence of characteristic functional groups of the additives.

Figure 20 - FTIR spectra of superplasticizer admixtures after heating

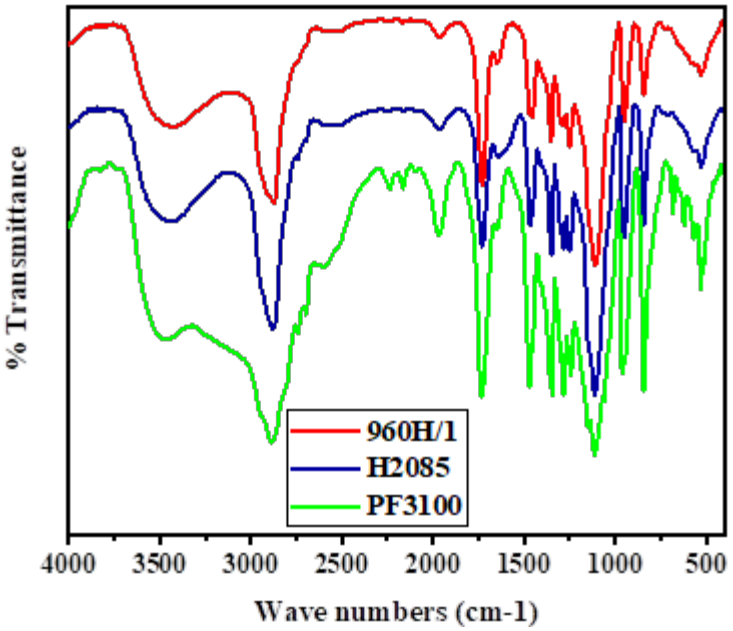

Source: The author.

3.3.2 Analyses of soil-cement composites

Figure 21 presents the soil-cement sample's microstructure without the incorporation of MWCNTs (Figure 21-a), adding untreated dispersed MWCNTs (Figure 21-b), and those fabricated with the MWCNT and superplasticizer selected dispersions (Figure 21-c to 21-h). Figure 21-a shows particles of various sizes overlapping without a specific orientation, but without interconnections between them. Figure 21-b to 21-h illustrate the random distribution of MWCNTs within the soil-cement samples.

Figure 21 – Optical scanning microscopy on soil-cement sample surfaces: (a) SC, (b) SC MWCNT, (c) SC 960H/1 0.5%, (d) SC 960H/1 1.0%, (e) SC H2085 0.3%, (f) SC PF3100 0.3%, (g) SC PF3100 0.5%, (h) SC PF3100 1.0%

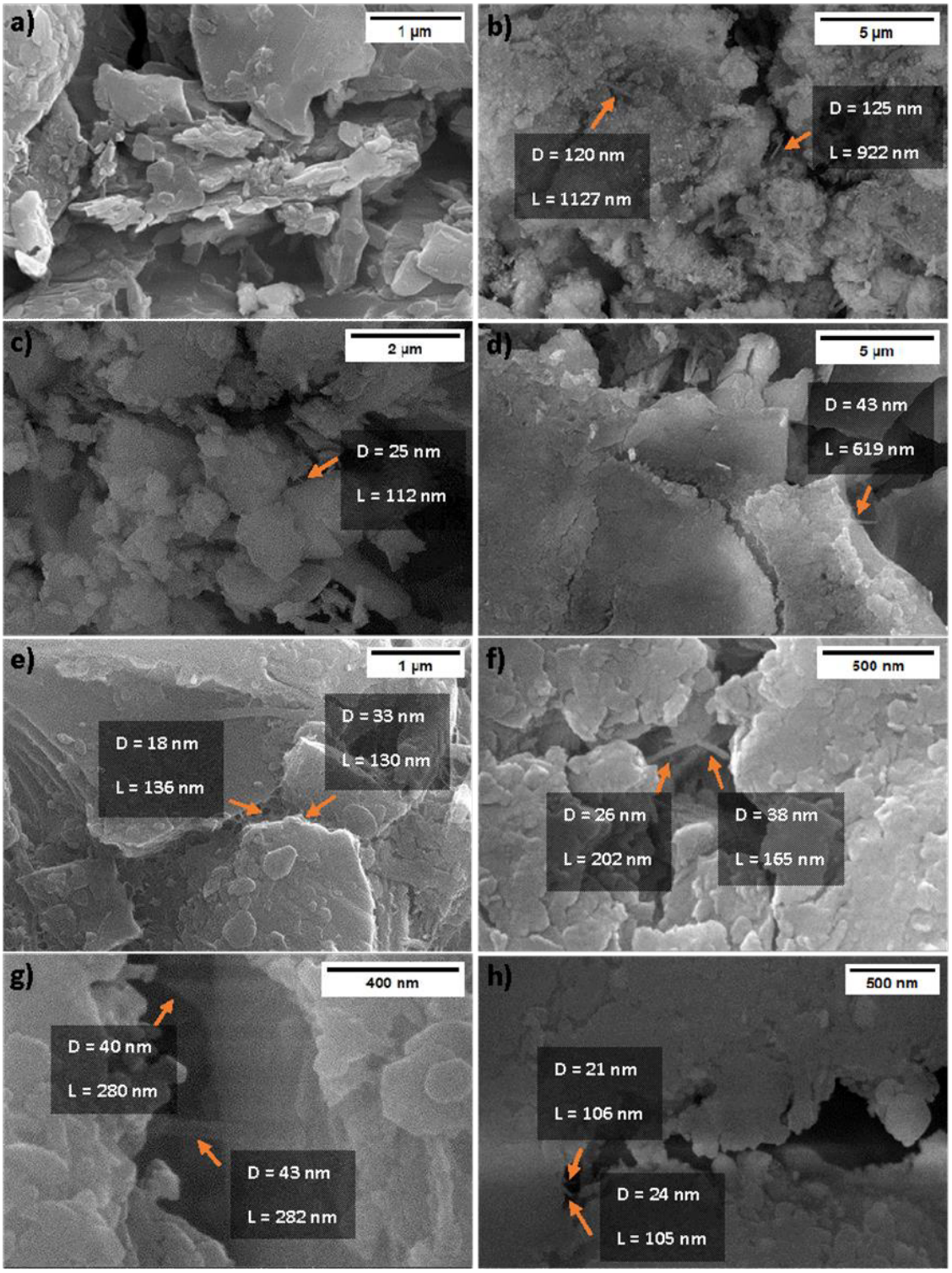

Source: The author.

These images reveal that MWCNTs serve as connectors between microparticles, which appear as the darkest areas in the SEM images (TORABIAN; LI; REDAELLI, 2016).

However, it's worth noting that some MWCNTs exhibited a significantly larger diameter, approximately 120 nm as seen in Figure 21-b, due to agglomeration resulting from the absence of a dispersant in the sample. This observation highlights the crucial influence of the dispersant on the proper dispersion of MWCNTs within the soil-cement matrix. (MESQUITA et al., 2023). The diameter of the MWCNTs dispersed in the superplasticizers was found to be in the nanometric range, typically ranging from 18 to 43 nm, as observed in micrographs (Figure 21-c to Figure 21-h). These findings are consistent with the properties reported in Table 7. Regarding the length of the MWCNTs, the average was approximately 221 nm, slightly surpassing the hydrodynamic diameter results obtained in the 4th analyzed week. This disparity could be attributed to the presence of longer MWCNTs, such as those measuring 619 nm in SC 960H/1 1.0% (Figure 21-d), which were not fully captured in the Dz measurements.

From the micrographs in Figure 21-c, d, e, g, h, it is noticeable that there is no significant difference between the uses and concentrations of the additives, proving the effective dispersion method of MWCNTs evident through the analyzed diameters and lengths. In Figure 21-e, the micrographs reveal well-connected microparticles, contributing to the smaller diameter observed and consequently, to the reduced agglomeration of MWCNTs. Therefore, considering the presence of microparticle bonds, the sample prepared with SC PF3100 0.3% demonstrated itself as the most effective MWCNT dispersant in this study. Saidumov *et al*. (2019) emphasize that MC-PowerFlow stands out among the analyzed additives due to the high stability of the water-binder-plasticizer system, suitable viscosity of the mixture, and persistence.

The characterization of the most efficient dispersions of MWCNTs and superplasticizers in soil-cement composites through UV-Vis spectroscopy is elaborately discussed in Figure 22. Remarkably, no alterations in the electronic behavior of the samples were observed. Furthermore, the long-term stability of MWCNT and superplasticizer dispersions is crucial to ensure the long-term integrity and resistance to degradation of construction materials. The absence of changes in the behavior of the composites over a period of 60 days suggests that these dispersions can support their beneficial properties for an extended period, which is crucial for long-lasting infrastructure applications (GARCEZ *et al.*, 2024).

Figure 22 – Solid UV-Vis: (a) SC, (b) SC 960H/1 0.5%, (c) SC 960H/1 1.0%, (d) SC H2085 0.3%, (e) SC PF3100 0.3%, (f) SC PF3100 0.5%, (g) SC PF3100 1.0%

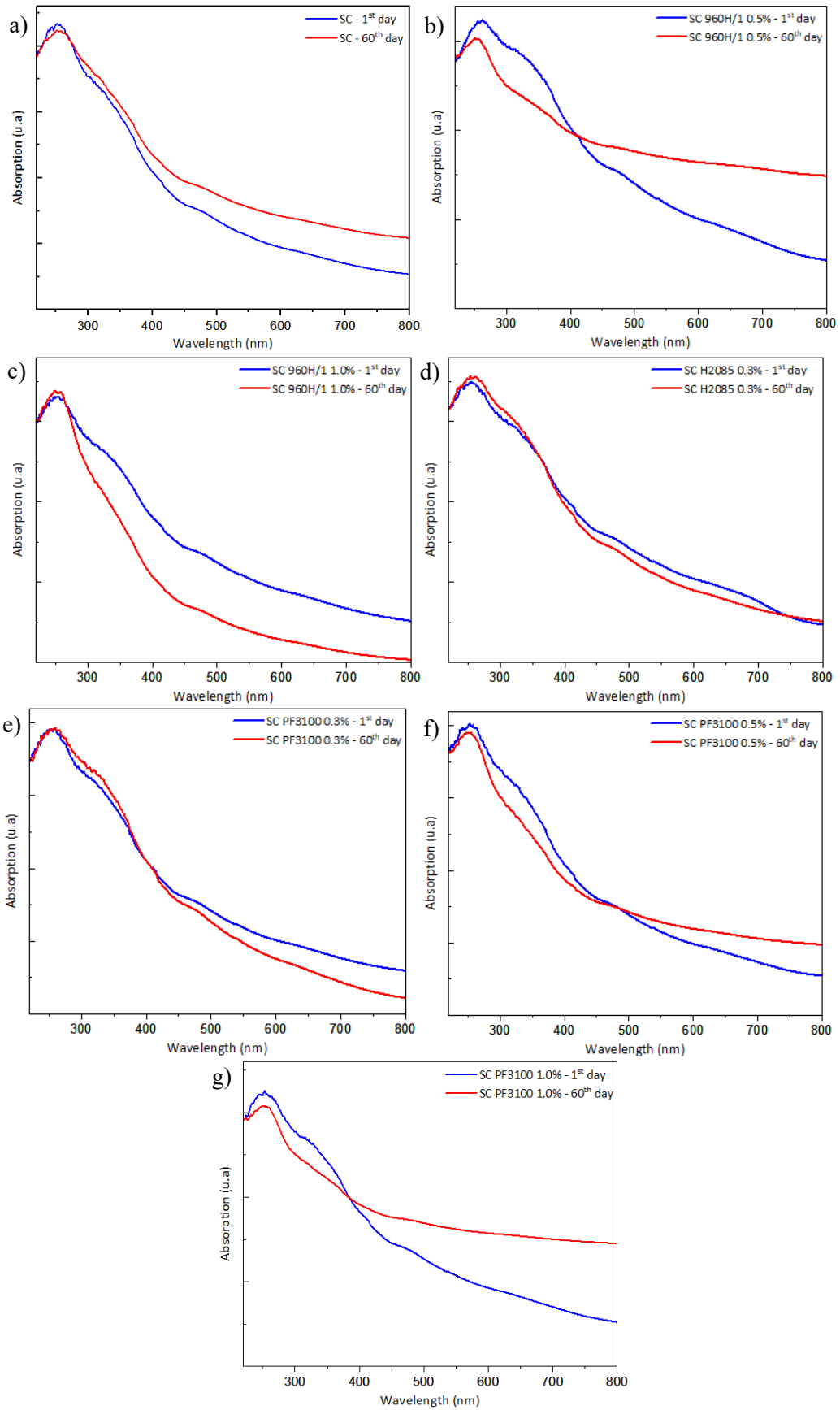

Source: The author.

Figure 23 displays the Raman mapping captures obtained in the study. The spectral analyses conducted confirms the presence of MWCNTs within the darkest regions of the samples, which appear to have an apparent absence of particles on the surface, as also observed in the SEM images. The spectral performance across both the darker and lighter areas of the sections further corroborate this observation.

Figure 23 - Images from spectral mapping using Raman spectroscopy: a) darkest region, b) lighter region

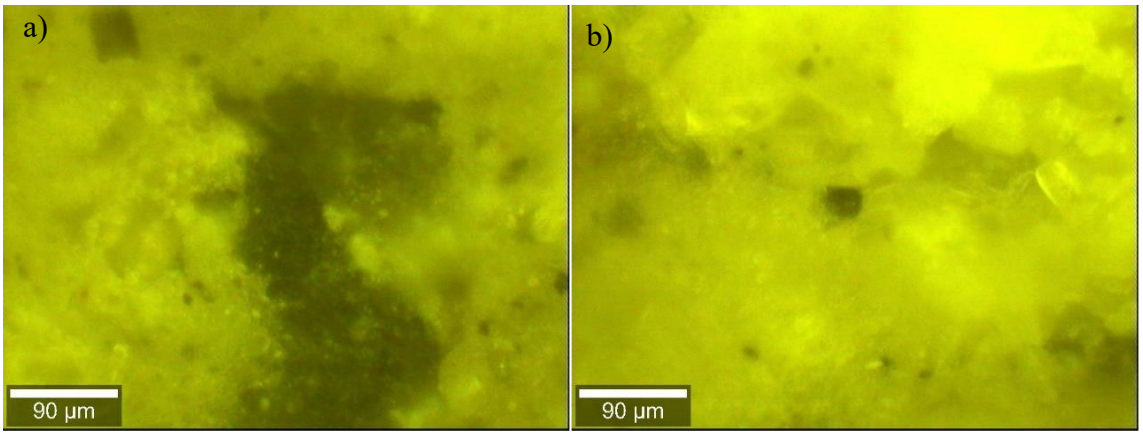

Source: The author.

Figure 24 shows the Raman spectra obtained from the eight soil-cement composites. The spectral profiles of carbon nanotubes reveal two inherent peaks: the D band, with a peak around 1344 cm^{-1}; and G band, with a peak around 1591 cm^{-1}. The D band results from the phononic mode induced by disorder, attributed to vacancies and lattice defects resulting from the combination of Sp^2 and Sp^3 bonds. The G band is associated with allowed Raman phononic mode, indicating the presence of Sp^2 vibrational bonds (carbon–carbon) attributed to the graphene-type bonds. The evaluation of the structural ordering is still given by the analysis of the intensity ratio of the D and G band (I_D/I_G). It is assumed that I_D decreases as the defect density decreases (LAURA et al., 2022; LI et al., 2023).

The reference spectrum is attributed to mapping in the brighter region, where it indicates the presence of significant luminescence. Luminescence is detected in all samples, but it is more moderate in the soil-cement with MWCNT (SC MWCNT) and in the soil-cement alone (SC) samples, as these mixtures do not contain superplasticizers. It is attributed to the composition of additives, which include 40% more water, as confirmed by the TG analyses, and to the soil-cement produced at greatest moisture.

Figure 24 – Raman mapping on the samples

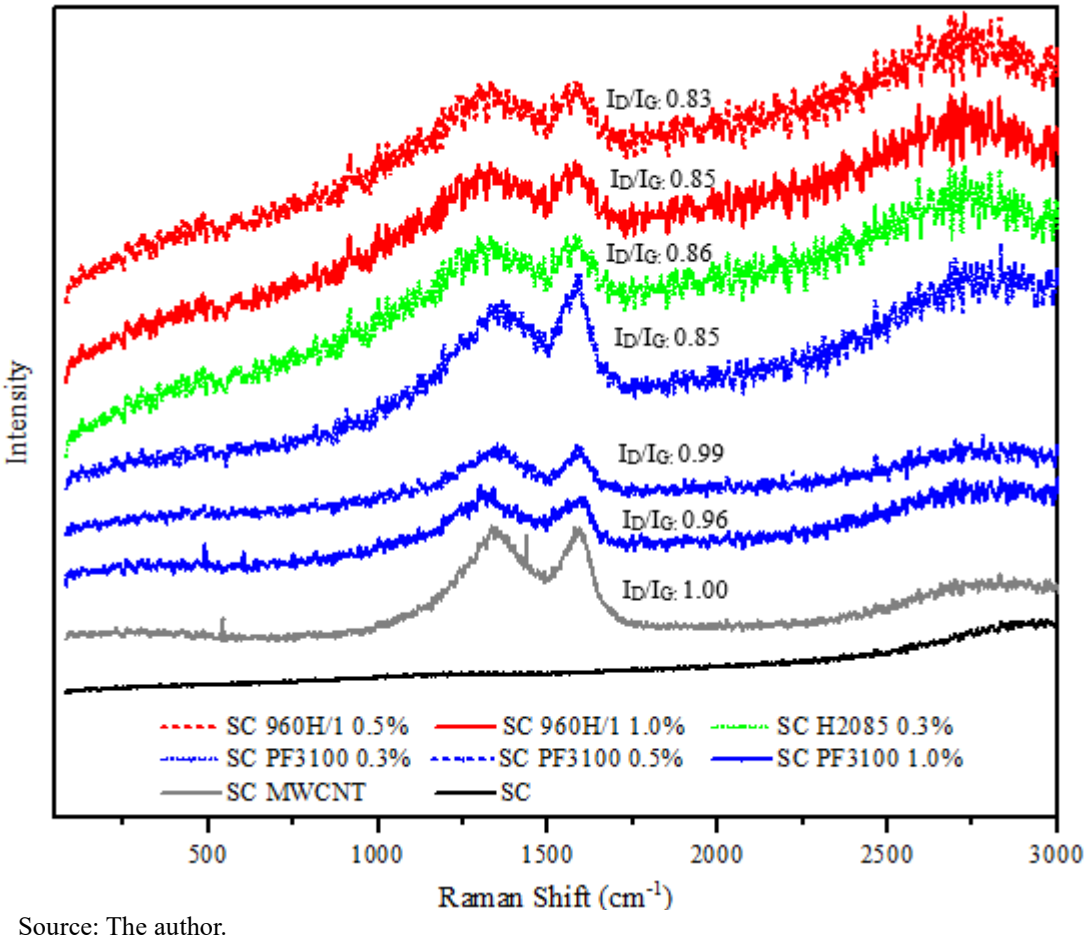

Source: The author.

The D and G bands are evident in all samples containing MWCNT. For the composites containing the 960H/1 additive, the lower the concentration of the additive, the lower the defect density in this study. However, for the SC PF3100 samples, no clear pattern between concentration and defect density is observable. The samples SC 960H/1 0.5%, SC PF3100 0.3%, and SC 960H/1 1.0% show the lowest intensity ratios of the D and G bands, with 0.83, 0.85, 0.85, respectively. It is evident that the sample containing CNT without additives obtained the highest I_D/I_G among the specimens (1.00), as expected. This suggests that superplasticizer additives play a crucial role in ensuring the integrity and functionality of MWCNTs within the composites. Additionally, the concentration of superplasticizers appears to directly impact the degree of dispersion and the density of defects in the MWCNTs (LIU et al., 2015; RAFAEL, 2017; LI et al., 2022).

Based on the alignment of the analyzed results, SC PF3100 0.3% was chosen for AFM analysis. Through AFM, the morphology of the specimen is revealed, as depicted in Figure 18. At the scale of tens of nanometers, it becomes apparent that van der Waals forces

typically govern the interaction between particles in the analyzed sample (CHENG *et al.*, 2021). These forces are known to be attractive, confirming the action of MWCNTs in the composite material.

The 3D height portrait (Figure 25-a) reveals crest and valley regions, providing insight into the surface morphology of the specimen. Notably, connections between valleys are discernible, suggesting potential structural features.

Figure 25 – Retrace of SC PF3100 0.3% in: a) 3D representation of AFM height data; b) corresponding AFM amplitude image and graph; c) corresponding AFM phase image and graph

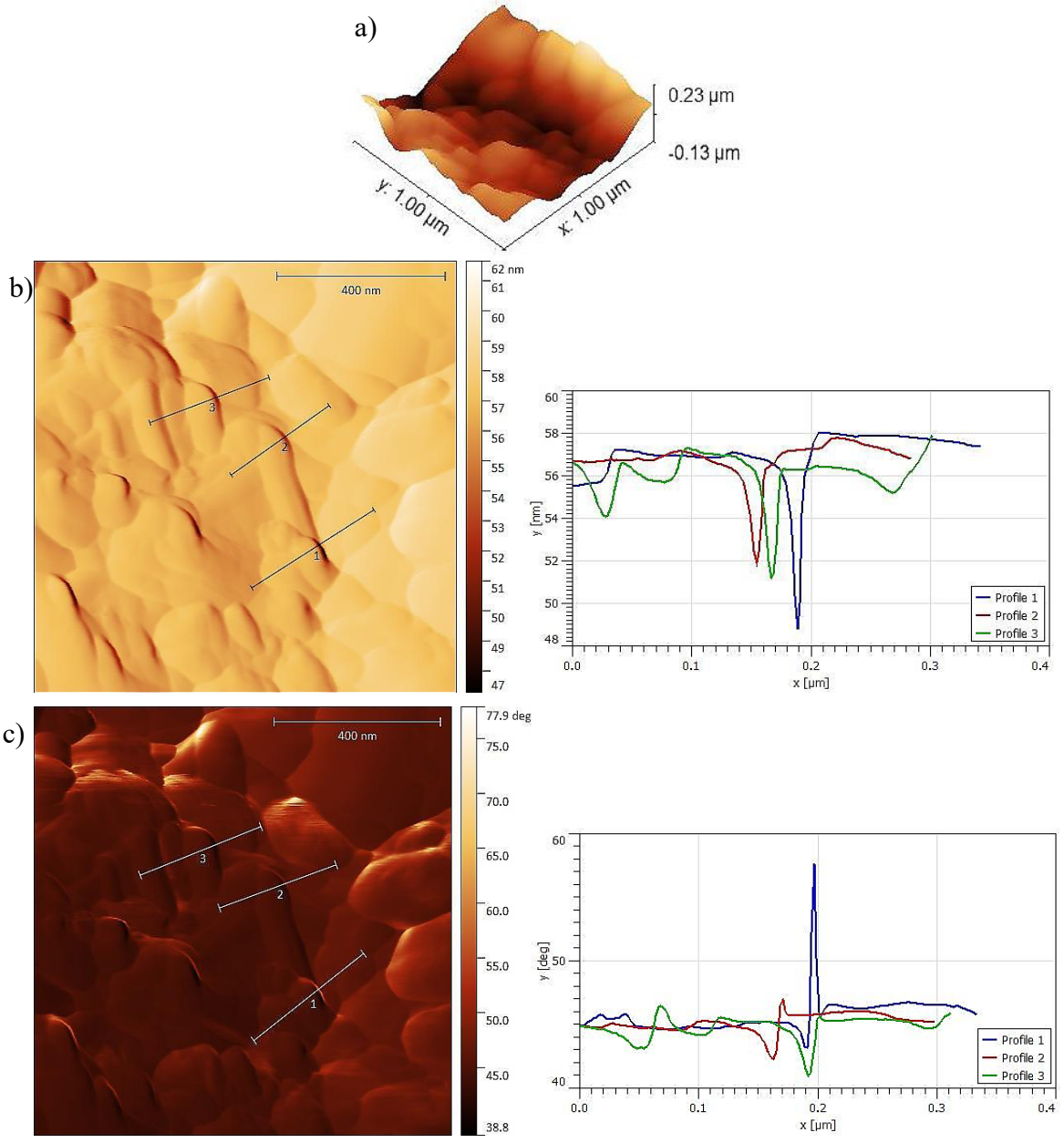

Source: The author.

Through analyses of the amplitude and phase distribution in segments of these connections, visual discrepancies become plain compared to the rest of the capture (Figure 25-b). Furthermore, significant peaks highlighted in the graphs indicate variations in material composition and mechanical properties. Specifically, the phase graph (Figure 25-c) reflects changes in mechanical properties, while the amplitude graph shows differences in adhesion and variations in viscoelasticity.

3.4 Final comments

In this work, the physicochemical characterization of MWCNT dispersion in superplasticizer admixtures for use in soil-cement composites is the initial step to validate and verify applications in engineering. Particle size, polydispersity index, stability over time, structural configuration, chemical composition, zeta potential, and defect tendency were determined in dispersions and/or composite samples. This contributed to selecting the most effective superplasticizer and concentrations for dispersing MWCNTs. Based on the results, the following conclusions can be outlined:

The study found that superplasticizers, especially when used at concentrations of 0.3%, 0.5%, and 1.0% of McPowerFlow 3100, 0.3% of MaxiFluid H2085, and 0.5% and 1.0% of MaxiFluid 960H/1, effectively dispersed MWCNTs. This was evidenced by consistent hydrodynamic diameter analyses over several weeks. Furthermore, dispersions and soil-cement composites maintained their structural stability over time, as confirmed by UV-Vis spectroscopy, indicating no loss of capacity or properties during their useful life. Scanning electron microscopy images and Raman mapping revealed that the addition of superplasticizer admixtures contributed to a more uniform dispersion of MWCNTs in soil-cement composites, leading to a lower probability of defects. Particularly noteworthy was the effective dispersion achieved with the PF3100 additive. Additionally, zeta potential analyses confirmed the steric repulsion effect of superplasticizer admixtures, further supporting their role in enhancing MWCNT dispersion and stability. Finally, MWCNTs in soil-cement served as connectors between microparticles, as evidenced by peaks in amplitudes and phases in AFM analyses, highlighting their presence and structural influence.

Therefore, the results obtained confirmed the highlighted concentrations of superplasticizer admixtures proved efficient in MWCNT dispersion in soil-cement composites, showing stability over time and improving the uniformity of nanotubes

distribution. These results are crucial for developing composites with enhanced properties in various civil engineering applications.

4. SELF-MONITORING OF SOIL-CEMENT COMPOSITES: AN ANALYSES OF ELECTRICAL CHARACTERISTICS

4.1 Introduction

Geotechnical materials play a fundamental role as a foundation for many civil structures, making their properties and behavior crucial considerations in construction projects. In the context of infrastructure systems, the incorporation of additives such as cement ensures improvement in soil properties. This practice aims to enhance the capacity and stabilize the soil mass, making it more suitable to withstand the demands of the structures built upon it (LIU et al., 2023; GARCEZ et al., 2024; YU et al., 2024). However, issues in soil composites stabilized with a percentage of cement address settlement analyses and stability or rupture analyses. Static or cyclic pressures, whether from thermal or mechanical factors, initiate microcracks in the composites that propagate gradually, coalesce, and produce macrocracks. Therefore, these macrocracks lead to instability, reducing the load-bearing capacity, resulting in the collapse of structures (CASTELLI et al., 2022; LIU et al., 2022; FATEHI et al., 2023; AGYEMANG et al., 2023). This analytical approach is essential to understand the integrity and safety of soil-cement infrastructure.

The evaluation of the actual performance of soil-based infrastructures requires an appropriate monitoring program during construction and after completion. The Structural Health Monitoring (SHM) system is an emerging and essential technology for measuring responses and capturing structural behavior changes resulting from these microcracks. Its main objective is to evaluate the safety and reliability of structures and infrastructures by detecting and quantifying any damage. SHM involves the collection, transmission, storage, and analyses of structural data throughout its life cycle (DING, Yang; YE; GUO, 2023; FAN; HE; LI, 2023; SALEHI *et al.*, 2023; YANG, Yanping; ZHU; AU, 2023). When conducted continuously, SHM enables timely interventions within the designed structural performance margin under various conditions and mitigates potential defects early on (YU et al., 2023; MARIANI et al., 2024).

In general, the data collected by SHM comes from optical sensors, vibrating wires, extensometers, accelerometers, and non-destructive techniques such as laser scanning and digital image correlation. However, such conventional methods are expensive, difficult to install, and lack precision in addressing analyses needs (PARIDA; MOHARANA, 2023; XU et al., 2023). The adoption of new SHM technologies provides a promising path to enhance

diagnostic and prognostic capabilities. In this regard, self-sensing smart materials address the deficiencies found in traditional sensors (DINESH; KARTHICK; RAMKUMAR, 2022; JAWED et al., 2023; FERGUSON et al., 2024).

Nanomaterials, such as carbon microfibers, graphite powder, carbon nanotubes, in combinations with composites, produce self-sensing materials. Among self-sensing materials, composites doped with multi-walled carbon nanotubes (MWCNTs) stand out as promising for SHM purposes, especially in sustainable and resilient infrastructure applications (HAO *et al.*, 2023; SARMADI *et al.*, 2023). MWCNTs, composed of multiple tubes with high aspect ratio, besides possessing unique structures and physical, chemical, and mechanical enhancements, piezoresistive properties and electrical conductivity to cement-based and soil-cement materials. MWCNTs added to the surface or inserted into the mixture, when subjected to static loads or slow cyclic loadings, exhibit a significant relationship between changes in resistivity and load changes (MATOS et al., 2023; SHI et al., 2023; VAKHITOVA et al., 2023). They are expected to offer deformation measurements in structures with precision and detection capability up to 3.5 times greater than regular extensometers, while conforming to infrastructure durability. Although initially more costly than other nanomaterials, they require a much smaller quantity for the same level of monitoring efficiency, achieving better cost-effectiveness (MATERAZZI; UBERTINI; D'ALESSANDRO, 2013).

Improvements in electrical properties are linked to MWCNT concentration. Below the optimal concentration, electrical conductivity in CNTs occurs through tunneling effect. Without mechanical contact between them, electron transfer occurs through quantum tunneling mechanisms. As the concentration of CNTs approaches the percolation threshold (critical concentration), contact conductivity becomes predominant. The distance between CNTs reduces until direct contact occurs, resulting in a conductive network. Under loads, structural deformation, or microcracking in the material, nanocomposites undergo deformations, affecting tunnel distance, and consequently reinforcing or weakening tunnel conductivity. This variation in conductivity makes them suitable for deformation detection, revealing a piezoresistive behavior (GARCÍA-MACÍAS et al., 2018; RAO; SASMAL, 2022; LI et al., 2023). This electrical sensivity of CNTs to external physical parameters such as voltage, deformation, force, displacement, and pressure makes them ideal for structural monitoring applications (DEVI; VIJAYALAKSHMI, 2020; DING et al., 2022; SIAHKOUHI et al., 2023).

The effective medium theory postulates that each composite particle is immersed in an effective medium with the same electrical conductivity. The shape and spatial

distribution of conductive particles, as well as their interconnections, are influenced by the volumetric fraction and exponential coefficient (WANG, Jialiang *et al.*, 2023). Thus, the proper functioning of MWCNT is directly linked to its dispersion. As they are nanometric structures, where van der Waals forces prevail, there is a natural tendency to agglomerate. In the literature, various types of dispersion are described, such as sonication treatments, mineral additives, and surfactants (CORREIA; LOPES; REIS, 2022; GARCÍA-MACÍAS et al., 2017; LI et al., 2023). Additives based on polycarboxylates or superplasticizers at optimal concentrations, through the steric and electrostatic effect of polymeric chains, constitute excellent dispersants to obtain individual MWCNTs in composites (XIANG; GAO; SHI, 2020; CORREIA; FIGUEIREDO; RASTEIRO, 2023; MA et al., 2023).

Vasconcelos *et al.* (2024) investigates the effectiveness of three different types of superplasticizer admixtures as dispersing agents for the content of 0.001% of MWCNT in soil-cement composites. Through physicochemical characterization, optimal concentrations are obtained for each superplasticizer used. Based on this work, the main objective of this study is to examine the self-sensing characteristics of soil-cementitious composites developed with selected superplasticizer admixtures.

4.2 Materials and Experimental Methods

The research focuses on the analyses of electrical and sensing properties of soil-cement composites, incorporating different quantities of additives and a fixed content of MWCNTs. MWCNT dispersion is achieved through an aqueous solution of polycarboxylate-based additives, which is subsequently added to the soil-cement composites during production. The electrical properties of the samples are evaluated statically through a planned experimental campaign.

4.2.1 Primary materials

The soil used in the study was collected at a depth of 50 cm in the Geotechnics and Foundations Experimental Field of the Federal University of Ceará (CEGEF – UFC), located on the Pici Campus. The material is sandy-silty granular soil, with approximately 16% fines (Figure 10). With a Coefficient of Uniformity (CNU) of 3.29 and a Coefficient of Curvature (CC) of 1.80, the sand can be classified as poorly graded and uniform. The grain real density test provided a result of 2.61. According to the Highway Research Board -

American Association of State Highway Officials (HRB-AASHO) and Unified Soil Classification System (USCS) classification, the soil is classified as A-2-4 and SM, respectively (ALMEIDA *et al.*, 2020; MOURA *et al.*, 2021).

Figure 26 - Soil particle size distribution curve

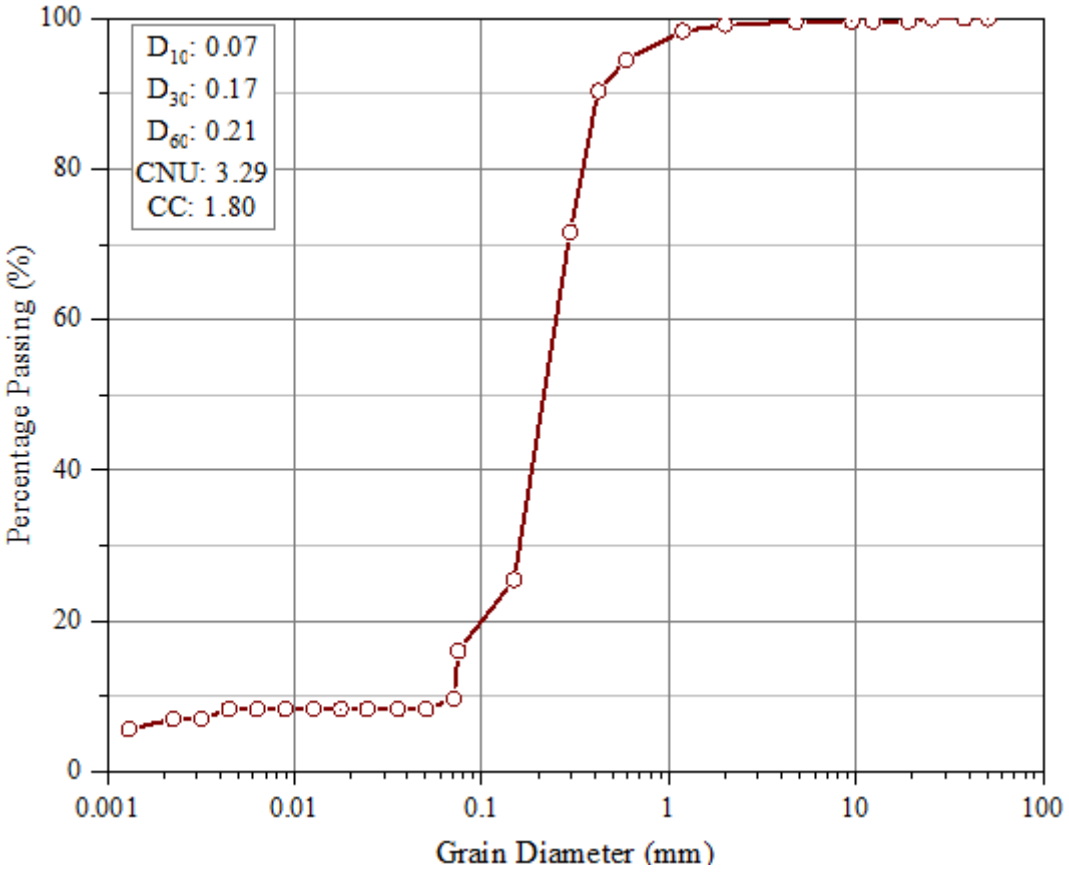

Source: The author.

Only the portion of soil passing through sieve N° 40 (with an opening of 425 μm) was utilized for all characterizations. This method ensures a clearer examination of the interaction between smaller particles and MWCNTs and superplasticizer admixtures, while preserving the soil's intrinsic properties. According to NBR 12253 (2012), the recommended cement content for soil-cement compaction testing corresponding to soil classification A-2 is 5%. The soil compaction curve exhibits a flatter shape, with a maximum dry unit weight of 1.903 g/cm³ and an optimum moisture content of 10.45% for a cement content of 5%. To compensate for water loss due to evaporation, the optimum moisture content is increased by 0.5% to 1.0% (ABNT NBR 12024, 2012). In this study, the moisture content is defined as 11.45% relative to the dry mixture. The chemical analysis provided in Table 17.

Table 17 – Soil's chemical composition

Composition	CaO	Al_2O_3	Fe_2O_3	K_2O	P_2O_5	TiO_2	SiO_2	SO_3
Wt. (%)	0.55	19.54	1.19	0.64	0.51	1.45	75.73	0.18

Source: The author.

The MWCNTs, functionalized with carboxyl/hydroxyl groups and used in this research, were provided by CTNano (Center for Nanomaterials and Graphene Technology, Federal University of Minas Gerais, Brazil). The physical properties of the MWCNTs are described in Table 18.

Table 18 – Properties of MWCNTs

Lenght range	Average lenght	Diameter range	Average diameter	Purity	Funcionalization
0.5 to 15.0 μm	4.5 μm	8 to 45 nm	20 nm	≥ 95 %	9 %

Source: The author.

The polycarboxylate-base additives under evaluation were Maxifluid 960H/1 (960H/1) and Maxifluid H 2085 (H2085), supplied by MatChem, and MC-PowerFlow 3100 (PF3100), provided by MC Bauchemie. The specifications of these third-generation superplasticizer admixtures are outlined in Table 19.

Table 19 – Superplasticizer admixture specifications

Superplasticizer admixture	Chemical name	Liquid aspect	Specific mass (g/cm^3)	Solubility in water	pH
960H/1	RA2	Colorless	1.062 to 1.102	Soluble	3.0 to 5.0
H2085	RA2	Red	1.050 to 1.090	Soluble	3.0 to 5.0
PF3100	RA2	Brown	1.070	Soluble	4.7

Source: The author.

Portland cement type II, with the addition of granulated blast furnace slag (CP II-E), produced in Brazil, was used in this study (ABNT NBR 16697, 2018). The addition of granulated blast furnace slag corresponds to 19.71% of the mass of CP II-E. Table 20 shows the chemical composition in terms of the main constituents.

Table 20 – Chemical composition of cement

Composition	CaO	Al_2O_3	Fe_2O_3	K_2O	MgO	Na_2O	SiO_2	SO_3
Wt. (%)	55.27	5.84	2.29	0.85	3.14	0.18	21.79	3.73

Source: The author.

4.2.2 Electrical Test

In this study, the behavior of MWCNT with selected superplasticizer admixtures and their impact in the electrical properties of soil-cement composites are investigated. The two-probe method is employed for static measurements Although the four-probe method minimizes the electrode resistance impact through the analyses, the decision is made to use two electrodes for its simplicity, practicality, and higher precision at higher voltage (YOU et al., 2017; LI et al., 2023).

The test involves connecting the electrodes of the prismatic specimens to a voltage source applying a continues potential difference, “V”, and to a digital multimeter to measure the current “I” at the center of the sample. The central zone, between two electrodes with distance “d”, is modeled as a parallel arrangement of a capacitor, “C”, and a resistor, “R”. An initial internal capacitance and resistance are assumed, measured from the current generated by the potential difference without load application. It is also emphasized that there is a resistance inherent to the wires and connectors.

Materials based on soil-cement, due to their dielectric properties, exhibit polarization effects when exposed to electric field. It is determined that the measurements reach a satisfactory level of polarization stability in the area section A of the material after a time t = tp =3,000 s to 10,000 s of continuous application of V. This allows for the determination of the electrical resistance of the samples, represented by “Rt”, and conductivity, symbolized by σ (MATERAZZI; UBERTINI; D’ALESSANDRO, 2013; D’ALESSANDRO et al., 2016; MEONI et al., 2022), governed by Ohm's Law (Eq. 1 e 2, respectively):

$$R_t = V/I(t)_{t=t_p} \quad (1)$$

$$\sigma = (R_{t=t_p} * A/d)^{-1} \quad (2)$$

For static test, the current is measured on all cubic specimens using a digital multimeter (model 34465A 6 1⁄2, Keysight, Brazil), applying a continuous voltage of 1.5 V through a power supply (model HF-3005S, HIKARI, Brazil), on days 1, 3, 7, 14 e 28 after molding. During measurements, the current was stabilized to mitigate polarization effects. The configuration of the electrical setup is presented in the Figure 27.

Figure 27 – Experimental setup of the electrical testing

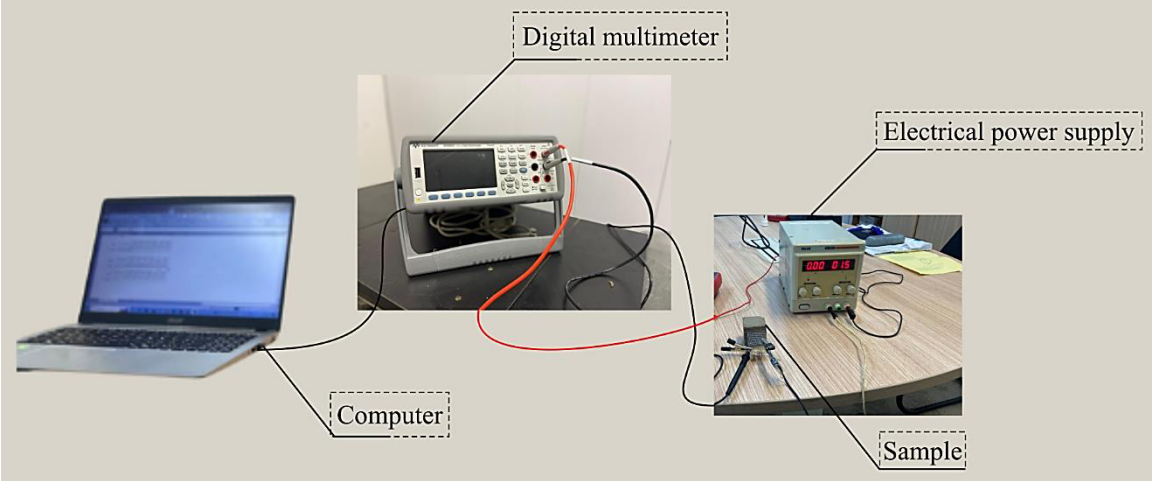

Source: The author.

4.2.3 Specimens production

Samples to electrical tests were prepared into test specimens, utilizing the best dispersions results of MWCNTs achieved in aqueous solutions, following the method described by Vasconcelos *et al.* (2024). The Table 21 contains the test plan proportion specifications for each soil-cement sample.

Table 21 – Specifications of the proportions within the test plan for soil-cement samples

Sample	Additive	Superplasticizer	MWCNT	Soil	Cement	Water
		Kg/m³				
SC	-	-	-	16.270	0.814	1.956
SC CNT	-	-	0.0002	16.270	0.814	1.956
SC 960H/1 0.5%	960H/1	0.010	0.0002	16.262	0.813	1.955
SC 960H/1 1.0%		0.020		16.262	0.813	1.954
SC H2085 0.3%	H2085	0.006	0.0002	16.253	0.813	1.955
SC PF3100 0.3%	PF3100	0.006	0.0002	16.265	0.813	1.956
SC PF3100 0.5%		0.010		16.262	0.813	1.955
SC PF3100 1.0%		0.020		16.253	0.813	1.954

Source: The author.

The procedure for preparing the test specimens was follows:

a) Preparation of a deionized water solution as the solvent and defined concentrations of polycarboxylate-based additives;
b) Agitation of the prepared dispersions for 10 minutes at a speed of 500 rpm to obtain a homogeneous dispersion;
c) Subjecting the sample to 2 minutes of sonication using a sonicator with a needle-type probe, cyclically at a power of 20 W;
d) Inclusion of 0.001% MWCNTs in the dispersions;
e) Subjecting the sample to 15 minutes of sonication using a sonicator with a needle-type probe, cyclically at a power of 20 W;
f) Dry manual mixing of 415.89 g of the analyzed soil, passing through sieve N° 40, with 20.79 g of cement, corresponding to a concentration of 5% of the soil mass, until homogeneity is achieved;
g) Inclusion of the prepared mixture together with 25 ml of the selected dispersion in a low-speed mechanical mixer (200 rpm) for 2 minutes;
h) Inclusion of the remaining 25 ml of the dispersion into the mechanical mixer at medium speed (300 rpm) for 3 minutes;
i) Molding of the test specimens with dimensions of 4x4x4 cm and immersion of electrodes.

Figure 28 illustrates the methodology employed in the study.

Figure 28 - Procedure for dispersing MWCNTs, preparation of soil-cement paste, and apparatus for specimen testing

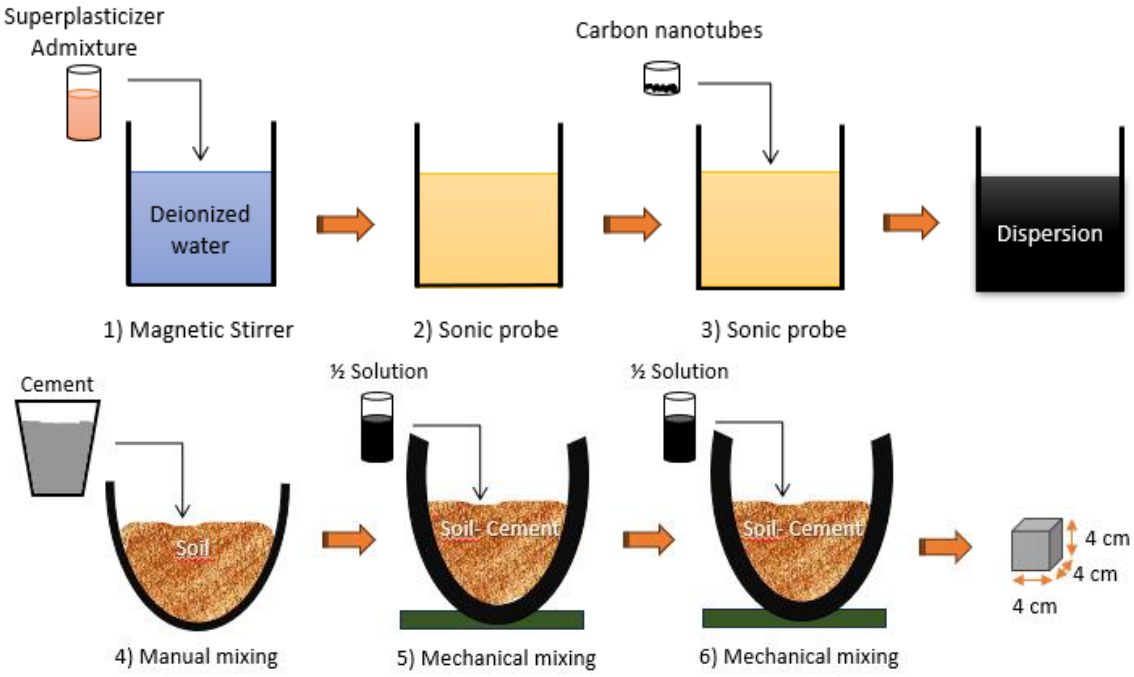

Source: The author.

The electrodes were embedded in the specimen during its molding, ensuring the integrity of both the electrode and the composite. The distance between the electrodes was set to 20 mm in the central region of each sample to apply a potential difference and measure the electrical current (Figure 29).

Figure 29 - Dimensions (mm) of the soil-cement-based sensor with carbon nanotubes: (a) side view and (b) front view

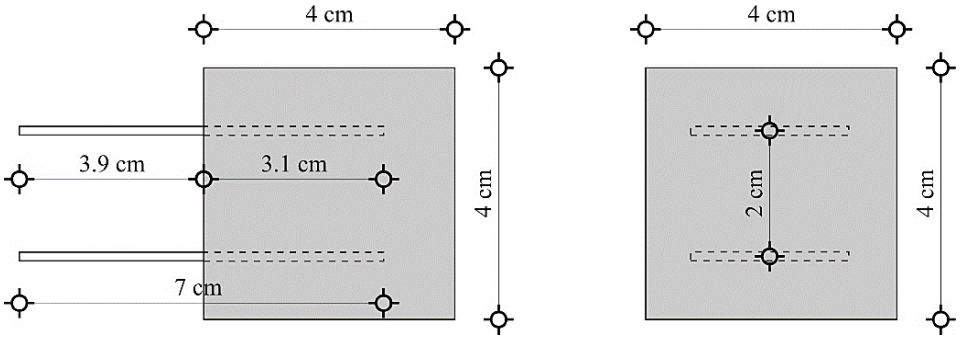

Source: The author.

Prior to measurements, all samples were allowed to acclimate to ambient conditions for 24 hours. The 24 samples produced is illustrates in Figure 30.

Figure 30 – Samples produced for the static test

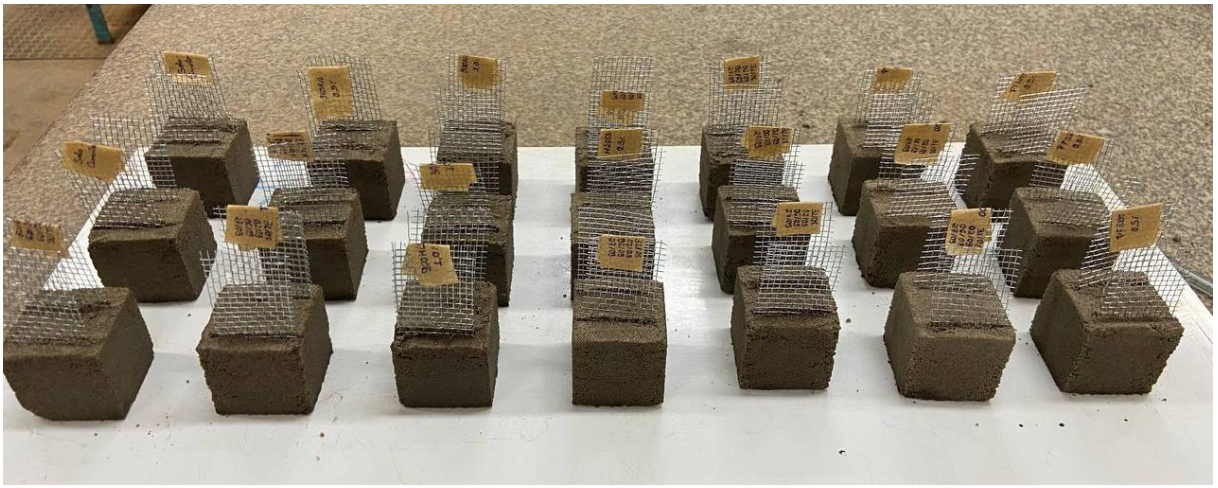

Source: The author.

4.3 Results and discussions

The correlation between the conductivity of each sample measured through the static test over 28 days is present in Figure 31. It is noted that the inclusion of nanotubes increases the conductivity values shortly after the first 24 hours of curing (D'ALESSANDRO *et al.*, 2021). The conductivity of soil-cement composites varies between 1.21E-3 $(\Omega\text{cm})^{-1}$, for samples without MWCNTs, to 4,72E-3 $(\Omega\text{cm})^{-1}$, for samples with carbon nanotubes without any dispersant. This phenomenon is due to the electrical properties of CNTs and their agglomeration in samples where there is no dispersant (MESQUITA et al., 2023).

For samples using the PF3100 additive, conductivity varied from 3.46E-3 to 1.88E-5 for concentration of 0.3%, and for concentrations of 0.5% and 1.0%, there was a decrease from 1.49E-3 and 2.67-3 $(\Omega\text{cm})^{-1}$ to 1.41E-5 and 1.26E-5 $(\Omega\text{cm})^{-1}$, respectively. Similarly, for samples containing the 960H/1 superplasticizer agent at concentrations of 0.5% and 1.0%, conductivity decreased from 1.87E-3 and 2.77E-3 $(\Omega\text{cm})^{-1}$ to 1.43E-5 and 1.27E-5 $(\Omega\text{cm})^{-1}$. This indicates that increasing the concentration of additives does not result in a significant difference in conductivity (LI, Shaojie *et al.*, 2021). With the H2085 additive at a concentration of 0.3%, the samples followed the same pattern as the others over time (2.13E-3 to 1.36E-5 $(\Omega\text{cm})^{-1}$).

Figure 31 - Evolution of the electrical conductivity of the composite soil-cement with different concentrations of hyperplastic additives and fixed CNT along the curing time, with electrical characterization performed with direct current, with supplied electrical voltage of 1.5V

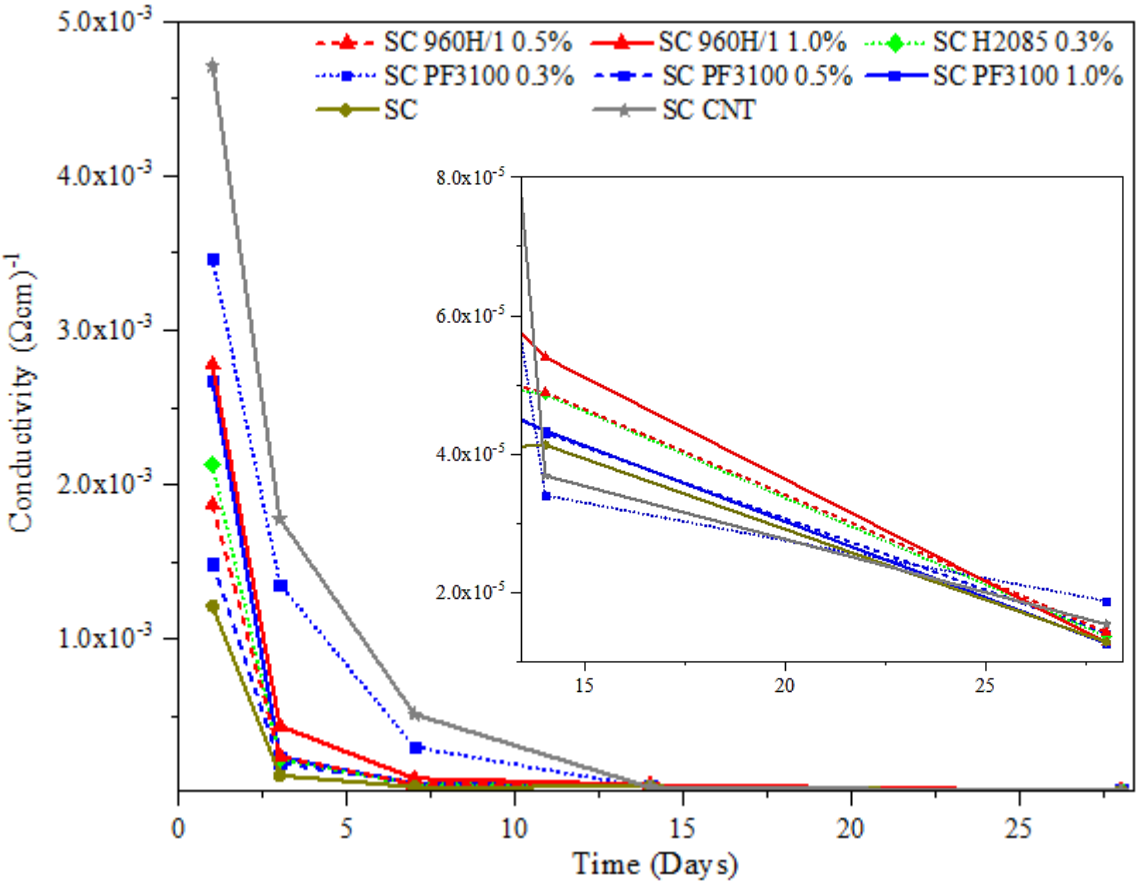

Source: The author.

The soil-cement reference samples showed a decreased from 1.21E-3 to 1.28E-5 $(\Omega cm)^{-1}$, while SC MWCNT decreased from 4.72E-3 to 1.54E-5 $(\Omega cm)^{-1}$. These two samples showed the lowest and highest decrease over the analyzed time, respectively. It is highlighted that the SC CNT and SC PF3100 0.3% samples show significant conductivity on the 3rd and 7th days compared to other analyzed samples. At the 14th and 28th day, samples with superplasticizer admixtures and CNTs do not show considerable effects compared to the soil-cement reference. The samples also exhibit a decline in conductivity as the days progress, attributed to the hydration process of cement. This occurrence results in the conductivity of the soil-cement reference sample decreasing after 28 days (DALLA *et al.*, 2016; TAFESSE *et al.*, 2021).

The difference in the use of superplasticizer admixture and their respective concentrations also promotes higher conductivity among all samples. The result suggests that

it is necessary to use a greater quantity than 0.001% of CNTs to reach the electrical percolation threshold and achieve better conductivity compared to not using carbon nanotubes (DANOGLIDIS; KONSTA-GDOUTOS; SHAH, 2019; TAFESSE *et al.*, 2021).

Figure 32 illustrates the resistivity obtained in the samples over the 28 days analyzed. Resistivity shows an increase over the days. In the first 24 hours after curing, the highest resistivity is found in the soil-cement sample with 8.26 Ωm. This pattern repeats on the 3rd (88.22 Ωm) and 7th (255.26 Ωm). The SC PF3100 0.3% sample followed by the SC CNT sample obtained the lowest final resistivity values, ranging from 2.89 and 2.12 Ωm on the 1st day after curing to 533.15 and 650.85 Ωm on the 28th day. It is emphasized that the lower the electrical resistivity, the greater the chance of application in monitoring the health of structural components (DINESH; SUDHARSAN; HARIBALA, 2021; DINESH; KARTHICK; RAMKUMAR, 2022; SARANYA et al., 2022).

Figure 32 - Evolution of the resistivity of the composites soil-cement with concentrations of hyperplastic additives and fixed MWCNT along the curing time, with electrical characterization performed with direct current, with supplied electrical voltage of 1.5V

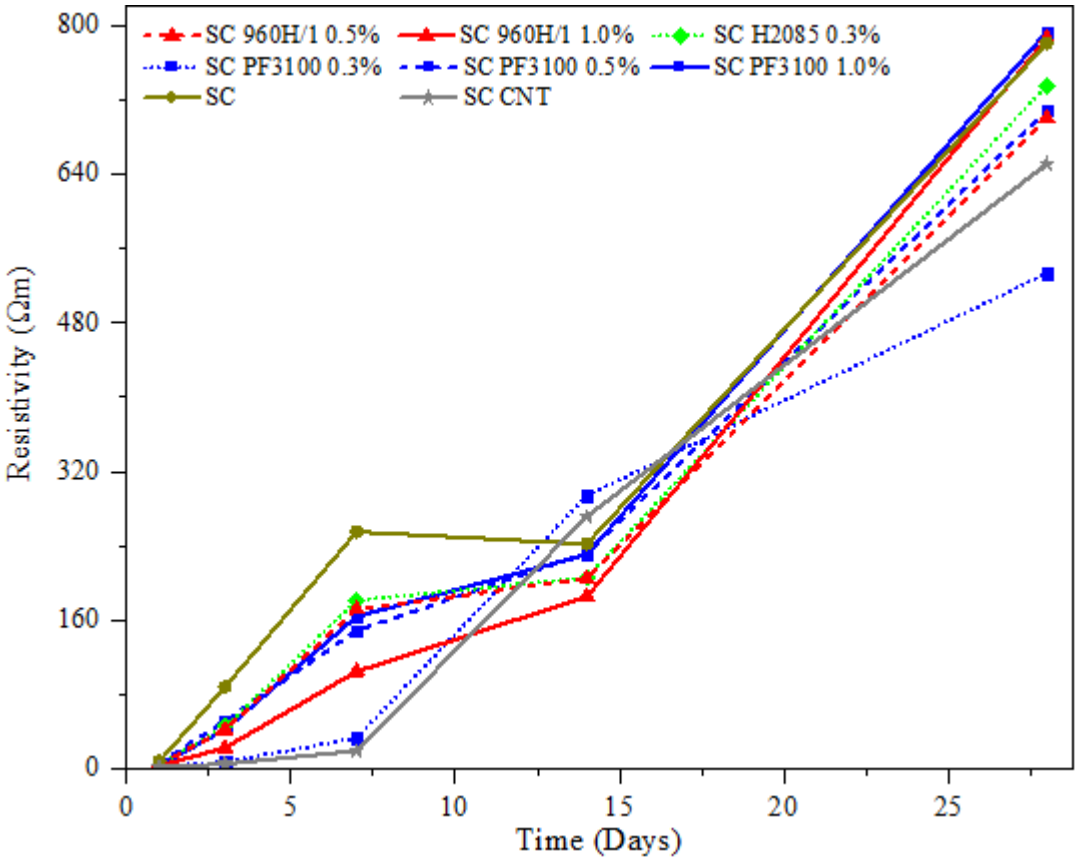

Source: The author.

The three highest resistivities measured correspond to the SC PF3100 1.0%, SC 960H/1 1.0% e SC samples, with 792.79, 785.65 e 780.60 Ωm, respectively. It is confirmed that a higher concentration of additive/MWCNT ends up nullifying the effect of MWCNT, resulting in its behavior, in terms of resistivity, being equal to that of the reference sample. This confirmation can be justified by the formation of micelles, small aggregates formed by surfactant molecules with greater affinity for each other than for the aqueous medium, instead of being adsorbed on the surface of MWCNT (COSTA; RASTEIRO; CORREIA, 2016).

Based on the data from Figure 32, three clear patterns of resistivity behavior are observed: 1) the soil-cement, with a constant and pronounced increase until the 7th day, a slight decrease until the 14th day, and a again a pronounced increase until the 28th day; 2) samples SC PF3100 0.5%, SC PF3100 1.0%, SC H2085 0.3%, SC 960H/1 0.5% and SC 960H/1 1,0%, with slight increases until the 14th day and significant increase at 28 days; 3) samples SC PF3100 0.3% and SC CNT, with discrete increases until the 7th day, a pronounced increase at the 14th day, reaching the highest values among the analyzed groups, and a smaller increase on the 28th day. The process of increasing resistivity analyzed in the samples doped with CNTs may be associate with the water consumed during the cement hydration and the inherent property of carbon nanotubes (NALON et al., 2021; HONG et al., 2022; MESQUITA et al., 2023).

Analyzing in terms of conductivity and resistivity, the behaviors observed are not significantly different from samples lacking CNTs and/or superplasticizer additives. This suggests that mixtures containing 0.001% MWCNTs may be classified as sub-percolated, implying that the quantity of nanosensors hasn't reached the optimal concentration, known as the percolation threshold. This fact does not significantly enhance the sensitivity of the composite to small variations in deformation (D'ALESSANDRO et al., 2016; SIAHKOUHI et al., 2021; DINESH et al., 2023).

4.4 Final comments

Composite materials doped with MWCNTs exhibit piezoresistive properties and electrical conductivity, making them suitable for SHM applications. The study focused on analyzing the resistivity and conductivity of soil-cement samples throughout the curing process, including measurements at 28 days, using selected concentrations of superplasticizer admixtures.

The analysis of conductivity over 28 days reveals notable trends. Samples SC CNT show increased conductivity shortly after 24 hours of curing, attributed to CNTs' electrical properties and agglomeration in samples lacking dispersants. However, the addition of superplasticizer additives like PF3100, 960H/1, and H2085 doesn't significantly affect conductivity. The conductivity of soil-cement reference samples decreases over time due to the hydration process of cement.

Similarly, resistivity increases over time for all samples. Notably, SC PF3100 0.3% and SC CNT samples exhibit the lowest final resistivity values. Higher concentrations of additives in relation of MWCNTs lead to higher resistivity, nullifying the effect of MWCNTs and resembling the behavior of reference samples. Three distinct patterns of resistivity behavior emerge: constant and pronounced increase, slight increases until 14 days followed by significant increases at 28 days, and discrete increases until 7 days, pronounced increase at 14 days, and smaller increase at 28 days.

Overall, the behaviors observed in terms of conductivity and resistivity suggest that mixtures containing 0.001% MWCNTs are sub-percolated, indicating the need for higher concentrations to reach the percolation threshold and enhance sensitivity to deformation. The study provides valuable insights into optimizing MWCNT dispersion and understanding its impact on soil-cement composite properties, laying a foundation for further research in SHM and sustainable infrastructure development.

5 CONCLUSIONS

In the realm of structural monitoring, traditional methods are often costly and short-lived. However, the emergence of self-sensing materials offers clear advantages over conventional monitoring technologies, particularly within the realm of smart materials. These innovative materials, when integrated into structures, provide enhanced compatibility and durability akin to traditional civil works.

A literature review conducted through the Preferred Reporting Items for Systematic Review and Meta-Analysis methodology indicates a growing significance of self-sensing materials in civil engineering, as evidenced by their increasing adoption in SHM practices. Journals like Construction and Building Materials have become pivotal in this research area, with a notable surge observed since 2014, suggesting their increasing effectiveness in continuous SHM. Globally, interest in self-sensing materials is apparent, with China, the United States, and Italy leading in contributions. Hence, smart and self-sensing materials are crucial in various engineering constructions such as pavements, bridges, high-rise buildings, dams, and tunnels. Through quantitative studies, carbon-based materials have garnered increased attention as conductive additives owing to their superior electrical conductivity and operational stability. Particularly, CNTs have garnered interest in recent years due to their exceptional mechanical and transport properties, indicating their suitability for high-performance and self-sensing composites. Most of these composites are primarily composed of cementitious materials and are subjected to frequent service loads and harsh environmental conditions. In this context, intrinsic self-sensing materials would serve as a valuable complement to existing sensing technologies, enabling long-term, widespread, and cost-effective monitoring of infrastructures.

The physicochemical characterization of MWCNT dispersion with superplasticizer additives for use in soil-cement composites was the first step to validate and assess engineering applications. Based on the results, we highlight those superplasticizers, particularly at concentrations of 0.3%, 0.5%, and 1.0% of McPowerFlow 3100, 0.3% of MaxiFluid H2085, and 0.5% and 1.0% of MaxiFluid 960H/1, were effective in dispersing MWCNTs, as evidenced by consistent analyses over several weeks. Additionally, dispersions and soil-cement composites maintain their structural stability over time, without loss of capacity or properties during their lifespan. The steric repulsion effect of superplasticizer additives contributed to a more uniform dispersion and reduced likelihood of defects in MWCNTs, especially with the PF3100 additive, which demonstrated effective dispersion.

Furthermore, MWCNTs in soil-cement acted as connectors between microparticles, ensuring better mechanical and electrical conductivity.

Through the fabrication of soil-cement composite samples with selected concentrations, the results indicated an increase in conductivity shortly after curing, attributed to the electrical properties of MWCNTs. Significant conductivity was observed in samples with specific superplasticizer additives and MWCNTs, suggesting their potential to improve electrical properties. Resistivity analyses demonstrated varied patterns among the samples, influenced by additive concentrations and MWCNT content. While some samples showed consistent increases in resistivity, others exhibited discrete variations, indicating complex interactions within the composites. Mixtures with 0.001% MWCNTs were considered sub-percolated, implying that the nanosensor concentration did not reach the optimal percolation threshold. This finding underscores the importance of MWCNT quantity in enhancing the composite's sensitivity to deformation. Overall, the study contributes valuable insights into optimizing MWCNT dispersion and understanding its impact on the self-detection properties of soil-cement composites, laying the groundwork for further research in structural health monitoring and sustainable infrastructure development.

As a proposal for future studies, to validate the soil-cement composite with MWCNTs as an SHM sensor, it is necessary to conduct cyclic tests and measure its piezoresistive properties. Furthermore, optimizing the dispersion methods of MWCNTs in field-replicable soil-cement composites may be crucial for their development and practical application. Additionally, considering the increasing importance of sustainability in civil engineering, it would be beneficial to conduct comprehensive studies on the life cycle, durability under environmental conditions, and cost-benefit analyses of the developed composites.

REFERENCES

ABEDI, Mohammadmahdi; GOMES CORREIA, António; FANGUEIRO, Raul. Geotechnical and piezoresistivity properties of sustainable cementitious stabilized sand reinforced with recycled fibres. **Transportation Engineering**, [*s. l.*], v. 6, p. 1-14, dec. 2021. Available at: https://www.sciencedirect.com/science/article/pii/S2666691X2100052X. Accessed on: 14 nov. 2023.

ABEDI, Mohammadmahdi; HASSANSHAHI, Omid; BARROS, Joaquim A.O.; GOMES CORREIA, António; FANGUEIRO, Raul. Three-dimensional braided composites as innovative smart structural reinforcements. **Composite Structures**, [*s. l.*], v. 297, p. 1-24, oct. 2022. Available at: https://www.sciencedirect.com/science/article/pii/S0263822322006742. Accessed on: 28 apr. 2024.

BRAZILIAN ASSOCIATION OF TECHNICAL STANDARDS. **ABNT NBR 12023**: Soil-cement - Compaction testing - Method of test, Rio de Janeiro, 1992.

BRAZILIAN ASSOCIATION OF TECHNICAL STANDARDS. **ABNT NBR 12024**: Soil-cement — Molding and curing of cylindric specimens — Procedure, Rio de Janeiro, 2012.

BRAZILIAN ASSOCIATION OF TECHNICAL STANDARDS. **ABNT NBR 12253**: Soil-cement — Mixture for use in pavement layer — Procedure, Rio de Janeiro, 2012.

BRAZILIAN ASSOCIATION OF TECHNICAL STANDARDS. **ABNT NBR 16697**: Portland cement — Requirements, Rio de Janeiro, 2018.

ABU AL-RUB, Rashid K.; TYSON, Bryan M.; YAZDANBAKHSH, Ardavan; GRASLEY, Zachary. Mechanical properties of nanocomposite cement incorporating surface-treated and untreated carbon nanotubes and carbon nanofibers. **Journal of Nanomechanics and Micromechanics**, [*s. l.*], v. 2, n 1, p. 1–6, mar. 2012. Available at: https://www.researchgate.net/publication/234834021_Mechanical_Properties_of_Nanocomposite_Cement_Incorporating_Surface-Treated_and_Untreated_Carbon_Nanotubes_and_Carbon_Nanofibers. Accessed on: 28 nov. 2023.

AGYEMANG, Isaac Osei; ZHANG, Xiaoling; ADJEI-MENSAH, Isaac; ACHEAMPONG, Daniel; FIASAM, Linda Delali; SEY, Collins; YUSSIF, Sophyani Banaamwini; EFFAH, Derrick. Automated vision-based structural health inspection and assessment for post-construction civil infrastructure. **Automation in Construction**, [*s. l.*], v. 156, p. 1-18, dec. 2023. Available at: https://www.sciencedirect.com/science/article/pii/S0926580523004132. Accessed on: 03 sep. 2023.

AHMAD, Kamarudin; ALI, N; KHARI, Mahdy; ALIMOHAMMADI, Payman; DEHGHANBANADAKI, Ali; ALI, Nazri; LATIFI, Nima. Stabilization of soft soils with deep mixed soil columns-general perspective. **Electronic Journal of Geotechnical Engineering**, [*s. l.*], v. 18, p. 295–306, jan. 2013. Available at: https://www.researchgate.net/publication/260390275. Accessed on: 04 jan. 2024.

AHMED, Osama; WANG, Xin; TRAN, Manh Vu; ISMADI, Mohd Zulhilmi. Advancements in fiber-reinforced polymer composite materials damage detection methods: Towards achieving energy-efficient SHM systems. **Composites Part B: Engineering**, [*s. l.*], v. 223, p. 1-18, oct. 2021. Available at: https://www.sciencedirect.com/science/article/pii/S1359836821005205. Accessed on: 4 may 2024.

ALAO, Joseph Omeiza. Determination of the geophysical signature of soft-clay and hard lateritic soils and the implications on geotechnical works using electrical resistivity imaging. **Results in Earth Sciences**, [*s. l.*], v. 2, p. 1-7, 1 dec. 2024. Available at: https://linkinghub.elsevier.com/retrieve/pii/S2211714824000128. Accessed on: 8 may 2024.

ALAVI, Amir H.; HASNI, Hassene; LAJNEF, Nizar; CHATTI, Karim. Damage growth detection in steel plates: Numerical and experimental studies. **Engineering Structures**, [*s. l.*], v. 128, p. 124–138, dec. 2016. Available at: https://www.sciencedirect.com/science/article/pii/S0141029616305995. Accessed on: 11 apr. 2024.

ALEXAKIS, Haris; LIU, Han; DEJONG, Matthew J. Damage identification of brick masonry under cyclic loading based on acoustic emissions. **Engineering Structures**, [*s. l.*], v. 221, p. 1-13, oct. 2020. Available at: https://www.sciencedirect.com/science/article/pii/S0141029619350837. Accessed on: 15 apr. 2024.

ALMEIDA, Marcela M.da R.; FILHO, Francisco C.da S.; LOPES, Elis Ferreira; MOURA, Alfran Sampaio. Evaluation of bearing capacity methods for shallow foundations in unsaturated soils. **Geotecnia**, [*s. l.*], n. 150, p. 87–106, nov. 2020. Available at: https://www.researchgate.net/publication/347550246_Evaluation_of_bearing_capacity_methods_for_shallow_foundations_in_unsaturated_soils. Accessed on: 06 jan. 2024.

AZHARI, Faezeh; BANTHIA, Nemkumar. Cement-based sensors with carbon fibers and carbon nanotubes for piezoresistive sensing. **Cement and Concrete Composites**, [*s. l.*], v. 34, n. 7, p. 866–873, aug. 2012. Available at: https://www.sciencedirect.com/science/article/pii/S0958946512000960. Accessed on: 19 feb. 2024.

BANDARRA, B. S.; MONTEIRO, L.; VELOSO, G.; ABREU, P.; SOUSA, H.; MARTINS, R. C.; PEREIRA, J. L.; COELHO, P. A.L.F.; QUINA, M. J. Evaluation of MSW incineration bottom ash for environmentally safe geotechnical applications. **Construction and Building Materials**, [*s. l.*], v. 427, p. 1-14, may 2024. Available at: https://www.sciencedirect.com/science/article/pii/S0950061824011528. Accessed on: 8 may 2024.

BHALLA, Suresh; KAUR, Naveet. Prognosis of low-strain fatigue induced damage in reinforced concrete structures using embedded piezo-transducers. **International Journal of Fatigue**, [*s. l.*], v. 113, p. 98–112, aug. 2018. Available at: https://www.sciencedirect.com/science/article/pii/S0142112318301324. Accessed on: 15 apr. 2024.

BHATTACHARJEE, Sourav. DLS and zeta potential - What they are and what they are not? **Journal of Controlled Release**, [*s. l.*], v. 235, p. 337–351, aug. 2016. Available at: https://www.sciencedirect.com/science/article/pii/S0168365916303832. Accessed on: 04 nov. 2023.

BIRGIN, Hasan Borke; GARCÍA-MACÍAS, Enrique; D'ALESSANDRO, Antonella; UBERTINI, Filippo. Self-powered weigh-in-motion system combining vibration energy harvesting and self-sensing composite pavements. **Construction and Building Materials**, [*s. l.*], v. 369, p. 1-15, mar. 2023. Available at: https://www.sciencedirect.com/science/article/pii/S0950061823002490. Accessed on: 17 dec. 2023.

BROWN, Lesa; SANCHEZ, Florence. Influence of carbon nanofiber clustering on the chemo-mechanical behavior of cement pastes. **Cement and Concrete Composites**, [*s. l.*], v. 65, p. 101–109, jan. 2016. Available at: https://www.sciencedirect.com/science/article/pii/S095894651530038X. Accessed on: 18 dec. 2023.

BUI TIEN, Thanh; VU QUANG, Tuyen; NGUYEN NGOC, Lan; TRAN NGOC, Hoa. Time series data recovery in SHM of large-scale bridges: Leveraging GAN and Bi-LSTM networks. **Structures**, [*s. l.*], v. 63, p. 1-12, may 2024. Available at: https://www.sciencedirect.com/science/article/pii/S2352012424005204. Accessed on: 07 may 2024.

BURGOS-MONTES, Olga; PALACIOS, Marta; RIVILLA, Patricia; PUERTAS, Francisca. Compatibility between superplasticizer admixtures and cements with mineral additions. **Construction and Building Materials**, [*s. l.*], v. 31, p. 300–309, jun. 2012. Available at: https://www.sciencedirect.com/science/article/pii/S0950061811007823. Accessed on: 11 dec. 2023.

CARDOSO, Josué; FERREIRA, Adelino; ALMEIDA, Arminda; SANTOS, João. Incorporation of plastic waste into road pavements: A systematic literature review on the fatigue and rutting performances. **Construction and Building Materials**, [*s. l.*], v. 407, p. 1-13, dec. 2023. Available at: https://www.sciencedirect.com/science/article/pii/S0950061823031586. Accessed on: 26 jan. 2024.

CASTAÑEDA-SALDARRIAGA, Diego L.; ALVAREZ-MONTOYA, Joham; MARTÍNEZ-TEJADA, Vladimir; SIERRA-PÉREZ, Julián. Toward structural health monitoring of civil structures based on self-sensing concrete nanocomposites: A validation in a reinforced-concrete beam. **International Journal of Concrete Structures and Materials**, [*s. l.*], v. 15, n. 1, p. 1–18, dec. 2021. Available at: https://link.springer.com/articles/10.1186/s40069-020-00451-8. Accessed on: 28 apr. 2024.

CASTELLI, Simone; BELLERI, Andrea; GRAZIOSI, Luca Rota; LOCATELLI, Lorenzo; ZIRPOLI, Adalgisa; SVALUTO, Gabriele. Integrated BIM-SHM techniques for the assessment of seismic damage. *In*: XIX ANIDIS CONFERENCE, SEISMIC ENGINEERING IN ITALY, 19., 2022, Torino. **Procedia Structural Integrity** [...]. [*S. l.*]: Elsevier B.V., 2022. p. 846–853. Available at:

https://www.sciencedirect.com/science/article/pii/S2452321623001178. Accessed on: 26 jan. 2024.

CHAKRABORTY, Joyraj; KATUNIN, Andrzej; KLIKOWICZ, Piotr; SALAMAK, Marek. Embedded ultrasonic transmission sensors and signal processing techniques for structural change detection in the Gliwice bridge. *In*: INTERNATIONAL CONFERENCE ON STRUCTURAL INTEGRITY, 3., 2019, Funchal. **Procedia Structural Integrity** [...]. [*S. l.*]: Elsevier B.V., 2019. p. 387–394. Available at: https://www.sciencedirect.com/science/article/pii/S2452321619302550. Accessed on: 15 apr. 2024.

CHENG, Biyao; YANG, Shuming; LI, Wei; LI, Shi; SHAFIQUE, Shareen; WU, Dong; JI, Shengyun; SUN, Yu; JIANG, Zhuangde. Controlled growth of a single carbon nanotube on an AFM probe. **Microsystems and Nanoengineering**, [*s. l.*], v. 7, n. 1, dec. 2021. Available at: https://www.nature.com/articles/s41378-021-00310-w. Accessed on: 21 feb. 2024

CHU, Hongqiang; QIN, Zhaoqiao; ZHANG, Yingzhong; XI, Xiang; ZHU, Zhengyu; JIANG, Linhua. Magnetic field enhancing preferred orientation of nickel-cobalt plated carbon fibers in cement paste, with relevance to compression self-sensing. **Measurement**, [*s. l.*], v. 220, p. 1-16, oct. 2023. Available at: https://www.sciencedirect.com/science/article/pii/S0263224123009600. Accessed on: 24 feb. 2024.

CORREIA, António Alberto S.; CASALEIRO, Pedro D.F.; FIGUEIREDO, Diogo T.R.; MOURA, Marta S.M.R.; RASTEIRO, Maria Graça. Key-parameters in chemical stabilization of soils with multiwall carbon nanotubes. **Applied Sciences (Switzerland)**, [*s. l.*], v. 11, n. 18, p. 1-17, 1 set. 2021. Available at: https://www.mdpi.com/2076-3417/11/18/8754. Accessed on: 25 feb. 2024.

CORREIA, António Alberto S.; CASALEIRO, Pedro D.F.; RASTEIRO, Maria Graça B.V. Applying multiwall carbon nanotubes for soil stabilization. *In*: WORLD CONGRESS ON PARTICLE TECHNOLOGY, 7., 2014, Beijing. **Procedia Engineering** [...]. [*S. l.*]: Elsevier Ltd, 2015. p. 1766–1775. Available at: https://www.sciencedirect.com/science/article/pii/S187770581500332X. Accessed on: 25 feb. 2024.

CORREIA, António Alberto S.; FIGUEIREDO, Diogo; RASTEIRO, Maria G. An experimental design methodology to evaluate the key parameters on dispersion of carbon nanotubes applied in soil stabilization. **Applied Sciences (Switzerland)**, [*s. l.*], v. 13, n. 8, apr. 2023. Available at: https://www.mdpi.com/2076-3417/13/8/4880. Accessed on: 26 feb. 2024.

CORREIA, António A.S.; LOPES, Luis; REIS, Marco S. Advanced predictive modelling applied to the chemical stabilisation of soft soils. **Proceedings of the Institution of Civil Engineers: Geotechnical Engineering**, [*s. l.*], v. 175, n. 5, p. 461–471, oct. 2022. Available at: https://www.sciencedirect.com/org/science/article/pii/S1353261820000150. Accessed on: 26 feb. 2024.

COSTA, Daniela C. **Chemical stabilization of soils using carbon nanotubes**. 2016. 102 f. Master's thesis (Chemical Engineering) - Department of Chemical Engineering, Faculty of

Science and Technology, University of Coimbra, Coimbra, 2016. Available at: https://estudogeral.uc.pt/bitstream/10316/81632/1/Chemical%20stabilization%20of%20soils%20using%20carbon%20nanotubes.pdf. Accessed on: 13 aug. 2023.

CUI, Kai; LIANG, Kaikang; JIANG, Ting; ZHANG, Jixin; LAU, Denvid; CHANG, Jun. Understanding the role of carbon nanotubes in low-carbon concrete: From experiment to molecular dynamics. **Cement and Concrete Composites**, [*s. l.*], v. 142, p. 1-13, sep. 2023. Available at: https://www.sciencedirect.com/science/article/pii/S0958946523002639. Accessed on: 16 jan. 2024.

DA LUZ, Graziele; GLEIZE, Philippe Jean Paul; BATISTON, Eduardo Roberto; PELISSER, Fernando. Effect of pristine and functionalized carbon nanotubes on microstructural, rheological, and mechanical behaviors of metakaolin-based geopolymer. **Cement and Concrete Composites**, [*s. l.*], v. 104, p. 1-7, nov. 2019. Available at: https://www.sciencedirect.com/science/article/pii/S0958946518307054. Accessed on: 16 jan. 2024.

DALAS, Florent; POURCHET, Sylvie; NONAT, André; RINALDI, David; SABIO, Serge; MOSQUET, Martin. Fluidizing efficiency of comb-like superplasticizers: The effect of the anionic function, the side chain length and the grafting degree. **Cement and Concrete Research**, [*s. l.*], v. 71, p. 115–123, mar. 2015. Available at: https://www.sciencedirect.com/science/article/pii/S0008884615000435?via%3Dihub. Accessed on: 08 feb. 2024.

D'ALESSANDRO, Antonella; RALLINI, Marco; UBERTINI, Filippo; MATERAZZI, Annibale Luigi; KENNY, Josè Maria. Investigations on scalable fabrication procedures for self-sensing carbon nanotube cement-matrix composites for SHM applications. **Cement and Concrete Composites**, [*s. l.*], v. 65, p. 200–213, jan. 2016. Available at: https://www.sciencedirect.com/science/article/pii/S0958946515300512. Accessed on: 23 nov. 2023.

D'ALESSANDRO, Antonella; TIECCO, Matteo; MEONI, Andrea; UBERTINI, Filippo. Improved strain sensing properties of cement-based sensors through enhanced carbon nanotube dispersion. **Cement and Concrete Composites**, [*s. l.*], v. 115, p. 1-9, jan. 2021. Available at: https://www.sciencedirect.com/science/article/pii/S0958946520303474. Accessed on: 11 may 2024.

DALLA, Panagiota T.; DASSIOS, Konstantinos G.; TRAGAZIKIS, Ilias K.; EXARCHOS, Dimitrios A.; MATIKAS, Theodore E. Carbon nanotubes and nanofibers as strain and damage sensors for smart cement. **Materials Today Communications**, [*s. l.*], v. 8, p. 196–204, set. 2016. Available at: https://www.sciencedirect.com/science/article/pii/S2352492816300691. Accessed on: 11 may 2024.

DANOGLIDIS, Panagiotis A.; KONSTA-GDOUTOS, Maria S.; GDOUTOS, Emmanuel E.; SHAH, Surendra P. Strength, energy absorption capability and self-sensing properties of multifunctional carbon nanotube reinforced mortars. **Construction and Building Materials**, [*s. l.*], v. 120, p. 265–274, sep. 2016. Available at: https://www.sciencedirect.com/science/article/pii/S0950061816307747. Accessed on: 24 feb. 2024.

DANOGLIDIS, Panagiotis A.; KONSTA-GDOUTOS, Maria S.; SHAH, Surendra P. Relationship between the carbon nanotube dispersion state, electrochemical impedance and capacitance and mechanical properties of percolative nanoreinforced OPC mortars. **Carbon**, [*s. l.*], v. 145, p. 218–228, apr. 2019. Available at: https://www.sciencedirect.com/science/article/pii/S0008622318312223. Accessed on: 11 may 2024.

DE IULIIS, Melissa; CARDONI, Alessandro; PAOLO CIMELLARO, Gian. Resilience and safety of civil engineering systems and communities: A bibliometric analysis for mapping the state-of-the-art. **Safety Science**, [*s. l.*], v. 174, p. 1-18, jun. 2024. Available at: https://www.sciencedirect.com/science/article/pii/S0925753524000602. Accessed on: 7 may 2024.

DE OLIVEIRA, Andrielli Morais; OLIVEIRA, Ana Paula; VIEIRA, Janine Domingos; JUNIOR, Alex Neves; CASCUDO, Oswaldo. Study of the development of hydration of ternary cement pastes using X-ray computed microtomography, XRD-Rietveld method, TG/DTG, DSC, calorimetry and FTIR techniques. **Journal of Building Engineering**, [*s. l.*], v. 64, p. 1-17, abr. 2023. Available at: https://www.sciencedirect.com/science/article/pii/S2352710222016229. Accessed on: 13 jan. 2024.

DENG, Yang; ZHAO, Yingjie; JU, Hanwen; YI, Ting Hua; LI, Aiqun. Abnormal data detection for structural health monitoring: State-of-the-art review. **Developments in the Built Environment**, [*s. l.*], v. 17, p. 1-18, mar. 2024. Available at: https://www.sciencedirect.com/science/article/pii/S2666165924000188. Accessed on: 7 may 2024.

DEVI, G. Nagamani; VIJAYALAKSHMI, M.M. Smart structural health monitoring in civil engineering: A survey. *In:* INTERNATIONAL CONFERENCE ON MECHANICAL, ELECTRONICS AND COMPUTER ENGINEERING: MATERIALS SCIENCE, 2020, Kancheepuram. **Materials Today: Proceedings** [...]. [*S. l.*]: Elsevier Ltd, 2021, p. 7143-7146. Available at: https://www.sciencedirect.com/science/article/pii/S2214785321011573. Accessed on: 12 dez. 2023.

DEVI, Rekha; GILL, Sandeep Singh. A squared bossed diaphragm piezoresistive pressure sensor based on CNTs for low pressure range with enhanced sensitivity. **Microsystem Technologies**, [*s. l.*], v. 27, n. 8, p. 3225–3233, aug. 2021. Available at: https://link.springer.com/article/10.1007/s00542-020-05208-7. Accessed on: 13 dez. 2023.

DINESH, A.; ASHWATHI, R.; KAMAL, B.; AKASH, C.; SUJITH, S. Influence of carbon nanotube on the mechanical and electrical characteristics of concrete – A review. *In:* INTERNATIONAL CONFERENCE ON ADVANCES IN CONSTRUCTION MATERIALS AND STRUCTURES, 2022, [s. l.]. **Materials Today: Proceedings** [...]. [*S. l.*]: Elsevier Ltd, 2023. p. 1-8. Available at: https://doi.org/10.1016/j.matpr.2021.02.095. Accessed on: 20 dez. 2023.

DINESH, A.; KARTHICK, A.; RAMKUMAR, S. Structural health monitoring of infrastructures using sensors as smart materials– Review and perspective. *In:* SUSTAINABLE MATERIALS AND SMART PRACTICES, 2021, [*s. l.*]. **Materials Research Proceedings** [...]. Washington: Association of American Publishers, 2022. p. 255–

268. Available at: https://www.researchgate.net/publication/360613091_Structural_Health_Monitoring_of_Infrastructures_Using_Sensors_as_Smart_Materials-_Review_and_Perspective. Accessed on: 22 nov. 2023.

DINESH, A.; SUDHARSAN, S. T.; HARIBALA, S. Self-sensing cement-based sensor with carbon nanotube: Fabrication and properties - A review. *In*: INTERNATIONAL CONFERENCE ON ADVANCES IN MATERIALS SCIENCE, COMMUNICATION AND MICROELECTRONICS, 2021, [*s. l.*]. **Materials Today: Proceedings** [...]. [*S. l.*]: Elsevier Ltd, 2021. p. 5801–5807. Available at: https://www.sciencedirect.com/science/article/pii/S2214785321018757. Accessed on: 20 dez. 2023.

DINESH, A.; SUJI, D.; PICHUMANI, Moorthi. Performance evaluation of graphite-integrated smart-engineered cementitious composite for health monitoring of structural components. **Journal of Building Engineering**, [*s. l.*], v. 69, p. 1-16, jun. 2023. Available at: https://www.sciencedirect.com/science/article/pii/S2352710223004072. Accessed on: 29 jul. 2023.

DING, Siqi; RUAN, Yanfeng; YU, Xun; HAN, Baoguo; NI, Yi Qing. Self-monitoring of smart concrete column incorporating CNT/NCB composite fillers modified cementitious sensors. **Construction and Building Materials**, [*s. l.*], v. 201, p. 127–137, mar. 2019. Available at: https://www.sciencedirect.com/science/article/pii/S0950061818332008. Accessed on: 28 apr. 2024.

DING, Siqi; XIANG, Yu; NI, Yi Qing; THAKUR, Vijay Kumar; WANG, Xinyue; HAN, Baoguo; OU, Jinping. In-situ synthesizing carbon nanotubes on cement to develop self-sensing cementitious composites for smart high-speed rail infrastructures. **Nano Today**, [*s. l.*], v. 43, p. 1-15, apr. 2022. Available at: https://www.sciencedirect.com/science/article/pii/S1748013222000652. Accessed on: 13 feb. 2024.

DING, Yang; YE, Xiao Wei; GUO, Yong. Copula-based JPDF of wind speed, wind direction, wind angle, and temperature with SHM data. **Probabilistic Engineering Mechanics**, [*s. l.*], v. 73, p. 1-10, jul. 2023. Available at: https://www.sciencedirect.com/science/article/pii/S0266892023000723. Accessed on: 14 feb. 2024.

DONG, Wei; HUANG, Yimiao; LEHANE, Barry; MA, Guowei. An artificial intelligence-based conductivity prediction and feature analysis of carbon fiber reinforced cementitious composite for non-destructive structural health monitoring. **Engineering Structures**, [*s. l.*], v. 266, p. 1-13, sep. 2022. Available at: https://www.sciencedirect.com/science/article/pii/S0141029622006812. Accessed on: 24 feb. 2024.

DONG, Wei; HUANG, Yimiao; LEHANE, Barry; MA, Guowei. Multi-objective design optimization for graphite-based nanomaterials reinforced cementitious composites: A data-driven method with machine learning and NSGA-II. **Construction and Building Materials**, [*s. l.*], v. 331, p. 1-16, may 2022. Available at:

https://www.sciencedirect.com/science/article/pii/S0950061822008789. Accessed on: 27 feb. 2024.

DONG, Wenkui; LI, Wengui; WANG, Kejin; SHAH, Surendra P.; SHENG, Daichao. Multifunctional cementitious composites with integrated self-sensing and self-healing capacities using carbon black and slaked lime. **Ceramics International**, [*s. l.*], v. 48, n. 14, p. 19851–19863, jul. 2022. Available at: https://www.sciencedirect.com/science/article/pii/S0272884222010690. Accessed on: 24 feb. 2024.

DONG, Wenkui; LI, Wengui; ZHU, Xinqun; SHENG, Daichao; SHAH, Surendra P. Multifunctional cementitious composites with integrated self-sensing and hydrophobic capacities toward smart structural health monitoring. **Cement and Concrete Composites**, [*s. l.*], v. 118, p. 1-14, apr. 2021. Available at: https://www.sciencedirect.com/science/article/pii/S0958946521000329. Accessed on: 28 apr. 2024.

DROUGKAS, Anastasios; SARHOSIS, Vasilis; BASHEER, Muhammed; D'ALESSANDRO, Antonella; UBERTINI, Filippo. Design of a smart lime mortar with conductive micro and nano fillers for structural health monitoring. **Construction and Building Materials**, [*s. l.*], v. 367, p. 1-11, feb. 2023. Available at: https://www.sciencedirect.com/science/article/pii/S0950061822036807. Accessed on: 21 apr. 2024.

FAN, Gao; HE, Zhengyan; LI, Jun. Structural dynamic response reconstruction using self-attention enhanced generative adversarial networks. **Engineering Structures**, [*s. l.*], v. 276, p. 1-13, feb. 2023. Available at: https://www.sciencedirect.com/science/article/pii/S0141029622014109. Accessed on: 09 mar. 2024.

FATEHI MARJI, Mohammad; YOUSOFIAN, Hatef; SOLTANIAN, Hamid; POURMAZAHERI, Yaser; ABDOLLAHIPOUR, Abolfazl. Superior crack propagation inhibitory effectiveness of MWCNT reinforced SBS toward improving oil/gas well cement integrity. **Construction and Building Materials**, [*s. l.*], v. 403, p. 1-11, nov. 2023. Available at: https://www.sciencedirect.com/science/article/pii/S095006182302888X. Accessed on: 11 mar. 2024.

FELL, Jonas; PAULY, Christoph; MAISL, Michael; ZABLER, Simon; MÜCKLICH, Frank; HERRMANN, Hans-Georg. Three-dimensional imaging of microstructural evolution in SEM-based nano-CT. **Tomography of Materials and Structures**, [*s. l.*], v. 2, p. 1-9, jun. 2023. Available at: https://www.sciencedirect.com/science/article/pii/S2949673X23000074. Accessed on: 09 mar. 2024.

FERGUSON, Alan J.; O'HIGGINS, Connor; HESTER, David; WOODS, Roger. Sampling methods based on expected traffic-volume information for long-term rotation-based bridge SHM in resource-constrained environments. **Mechanical Systems and Signal Processing**, [*s. l.*], v. 208, p. 1-24, feb. 2024. Available at: https://www.sciencedirect.com/science/article/pii/S0888327023008415. Accessed on: 13 mar. 2024.

FROTA, De Albuquerque Landi; FABIANI, C.; D'ALESSANDRO, A.; UBERTINI, F.; PISELLO, A. L. Life cycle assessment of a novel fired smart clay brick monitoring system for masonry buildings. **Sustainable Energy Technologies and Assessments**, [*s. l.*], v. 50, p. 1-16, mar. 2022. Available at: https://www.sciencedirect.com/science/article/abs/pii/S2213138821007591. Accessed on: 22 apr. 2024.

FUGGINI, Clemente; ZANGANI, Donato; WOSNIOK, Aleksander; KREBBER, Katerina; FRANITZA, Petra; GABINO, Luciano; WEIGAND, Frank. Innovative approach in the use of geotextiles for failures prevention in railway embankments. *In*: TRANSPORT RESEARCH ARENA, 6., 2016, Warsaw. **Transportation Research Procedia** [...]. [*S. l.*]: Elsevier B.V., 2016. p. 1875–1883. Available at: https://www.sciencedirect.com/science/article/pii/S2352146516301557. Accessed on: 23 jan. 2024.

GABEN, Mahdi; GOLDFELD, Yiska. Self-sensory carbon-based textile reinforced concrete beams – Characterization of the structural-electrical response by AC measurements. **Sensors and Actuators A: Physical**, [*s. l.*], v. 334, p. 1-14, feb. 2022. Available at: https://www.sciencedirect.com/science/article/pii/S0924424721007858. Accessed on: 28 apr. 2024.

GAO, Yuan; ZHU, Xingyi; CORR, David J.; KONSTA-GDOUTOS, Maria S.; SHAH, Surendra P. Characterization of the interfacial transition zone of CNF-Reinforced cementitious composites. **Cement and Concrete Composites**, [*s. l.*], v. 99, p. 130–139, may 2019. Available at: https://www.sciencedirect.com/science/article/pii/S095894651830444X. Accessed on: 12 jan. 2024.

GARCEZ, Lilyanne Rocha; BALESTRA, Carlos Eduardo Tino; MONTEIRO, Nathalie Barbosa Reis; MELO FILHO, João de Almeida; RAMIREZ GIL, Miguel Angel. Mechanical strength and life cycle assessment (LCA) of soil-cement: comparison between mixtures of soil with ASTM type III cement, LC3, and the incorporation of by products and agroindustrial residues. **Construction and Building Materials**, [*s. l.*], v. 411, p. 1-13, jan. 2024. Available at: https://www.sciencedirect.com/science/article/abs/pii/S0950061823040497. Accessed on: 13 jan. 2024.

GARCÍA-MACÍAS, Enrique; CASTRO-TRIGUERO, Rafael; FRISWELL, Michael I.; ADHIKARI, Sondipon; SÁEZ, Andrés. Metamodel-based approach for stochastic free vibration analysis of functionally graded carbon nanotube reinforced plates. **Composite Structures**, [*s. l.*], v. 152, p. 183–198, sep. 2016. Available at: https://www.sciencedirect.com/science/article/pii/S0263822316305013. Accessed on: 26 apr. 2024.

GARCÍA-MACÍAS, Enrique; CASTRO-TRIGUERO, Rafael; SÁEZ, Andrés; UBERTINI, Filippo. 3D mixed micromechanics-FEM modeling of piezoresistive carbon nanotube smart concrete. **Computer Methods in Applied Mechanics and Engineering**, [*s. l.*], v. 340, p. 396–423, oct. 2018. Available at: https://www.sciencedirect.com/science/article/pii/S0045782518302895. Accessed on: 23 nov. 2023.

GARCÍA-MACÍAS, Enrique; D'ALESSANDRO, Antonella; CASTRO-TRIGUERO, Rafael; PÉREZ-MIRA, Domingo; UBERTINI, Filippo. Micromechanics modeling of the uniaxial strain-sensing property of carbon nanotube cement-matrix composites for SHM applications. **Composite Structures**, [*s. l.*], v. 163, p. 195–215, mar. 2017. Available at: https://www.sciencedirect.com/science/article/pii/S0263822316322693. Accessed on: 24 nov. 2023.

GLASHIER, Theo; KROMANIS, Rolands; BUCHANAN, Craig. An iterative regression-based thermal response prediction methodology for instrumented civil infrastructure. **Advanced Engineering Informatics**, [*s. l.*], v. 60, p. 1-17, abr. 2024. Available at: https://doi.org/10.1016/j.aei.2023.102347. Accessed on: 7 may 2024.

GRABOWSKI, Krzysztof; SRIVATSA, Shreyas; VASHISTH, Aniruddh; MISHNAEVSKY, Leon; UHL, Tadeusz. Recent advances in MXene-based sensors for structural health monitoring applications: A review. **Measurement**, [*s. l.*], v. 189, p. 1-18, feb. 2022. Available at: https://doi.org/10.1016/j.measurement.2021.110575. Accessed on: 4 may 2024.

GULISANO, Federico; ABEDI, Mohammadmahdi; JURADO-PIÑA, Rafael; APAZA, Freddy Richard Apaza; ROSHAN, Mohammad Jawed; FANGUEIRO, Raul; CORREIA, António Gomes; GALLEGO, Juan. Stress and damage-sensing capabilities of asphalt mixtures incorporating graphene nanoplatelets. **Sensors and Actuators A: Physical**, [*s. l.*], v. 359, p. 1-14, sep. 2023. Available at: https://doi.org/10.1016/j.sna.2023.114494. Accessed on: 3 may 2024.

GUPTA, Nikita; GUPTA, Shipra Mital; SHARMA, S. K. Carbon nanotubes: synthesis, properties and engineering applications. **Carbon Letters**, [*s. l.*], v. 29, n. 5, p. 419–447, oct. 2019. Available at: https://link.springer.com/article/10.1007/s42823-019-00068-2. Accessed on: 03 nov. 2023.

GUPTA, Sumit; LIN, Yun An; LEE, Han Joo; BUSCHECK, Jeff; WU, Rongzong; LYNCH, Jerome P.; GARG, Navneet; LOH, Kenneth J. In situ crack mapping of large-scale self-sensing concrete pavements using electrical resistance tomography. **Cement and Concrete Composites**, [*s. l.*], v. 122, p. 1-14, sep. 2021. Available at: https://doi.org/10.1016/j.cemconcomp.2021.104154. Accessed on: 03 may 2024.

HAN, Jinsheng; PAN, Jinlong; CAI, Jingming; LI, Xiaopeng. A review on carbon-based self-sensing cementitious composites. **Construction and Building Materials**, [*s. l.*], v. 265, p. 1-14, dez. 2020. Available at: https://doi.org/10.1016/j.conbuildmat.2020.120764. Accessed on: 22 nov. 2023.

HAO, Hong; BI, Kaiming; CHEN, Wensu; PHAM, Thong M.; LI, Jun. Towards next generation design of sustainable, durable, multi-hazard resistant, resilient, and smart civil engineering structures. **Engineering Structures**, [*s. l.*], v. 277, p. 1-20, feb. 2023. Available at: https://doi.org/10.1016/j.engstruct.2022.115477. Accessed on: 23 nov. 2023.

HAQ, Moinul; BHALLA, Suresh; NAQVI, Tabassum. Fatigue damage and residual fatigue life assessment in reinforced concrete frames using PZT-impedance transducers. **Cement and Concrete Composites**, [*s. l.*], v. 114, p. 1-16, nov. 2020. Available at: https://doi.org/10.1016/j.cemconcomp.2020.103771. Accessed on: 12 may 2024.

HASNI, Hassene; ALAVI, Amir H.; CHATTI, Karim; LAJNEF, Nizar. A self-powered surface sensing approach for detection of bottom-up cracking in asphalt concrete pavements: Theoretical/numerical modeling. **Construction and Building Materials**, [*s. l.*], v. 144, p. 728–746, jul. 2017. Available at: https://doi.org/10.1016/j.conbuildmat.2017.03.197. Accessed on: 01 may 2024.

HASNI, Hassene; JIAO, Pengcheng; ALAVI, Amir H.; LAJNEF, Nizar; MASRI, Sami F. Structural health monitoring of steel frames using a network of self-powered strain and acceleration sensors: A numerical study. **Automation in Construction**, [[*s. l.*], v. 85, p. 344–357, jan. 2018. Available at: https://doi.org/10.1016/j.autcon.2017.10.022. Accessed on: 12 may 2024.

HASSANZADEH-AGHDAM, M. K.; ANSARI, R.; MAHMOODI, M. J.; DARVIZEH, A.; HAJATI-MODARAEI, A. A comprehensive study on thermal conductivities of wavy carbon nanotube-reinforced cementitious nanocomposites. **Cement and Concrete Composites**, [*s. l.*], v. 90, p. 108–118, jul. 2018. Available at: https://doi.org/10.1016/j.cemconcomp.2017.09.021. Accessed on: 23 dez. 2023.

HONG, Geuntae; CHOI, Seongcheol; YOO, Doo Yeol; OH, Taekgeun; SONG, Yooseob; YEON, Jung Heum. Moisture dependence of electrical resistivity in under-percolated cement-based composites with multi-walled carbon nanotubes. **Journal of Materials Research and Technology**, [*s. l.*], v. 16, p. 47–58, jan. 2022. Available at: https://doi.org/10.1016/j.jmrt.2021.11.151. Accessed on: 11 may 2024.

HU, Pingfang; ZHAO, Li; LIU, Hai. Infrared spectral super-resolution model with linear canonical transforms regularization for spectral signals. **Infrared Physics and Technology**, [*s. l.*], v. 133, p. 1-8, sep. 2023. Available at: https://doi.org/10.1016/j.infrared.2023.104850. Accessed on: 11 may 2024.

HUANG, Yu; WANG, Lin. Experimental studies on nanomaterials for soil improvement: a review. **Environmental Earth Sciences**, [*s. l.*], v. 75, n. 6, p. 1-13, mar. 2016. Available at: https://doi.org/10.1007/s12665-015-5118-8. Accessed on: 13 may 2024.

HUSSAIN, Abasal; XIANG, Yu; YU, Tao; ZOU, Fangxin. Nanocarbon black-based ultra-high-performance concrete (UHPC) with self-strain sensing capability. **Construction and Building Materials**, [*s. l.*], v. 359, p. 1-15, dez. 2022. Available at: https://doi.org/10.1016/j.conbuildmat.2022.129496. Accessed on: 24 feb. 2024.

JANOWSKA-RENKAS, Elzbieta. The influence of the chemical structure of polycarboxylic superplasticizers on their effectiveness in cement pastes. *In*: SCIENTIFIC-TECHNICAL CONFERENCE MATERIAL PROBLEMS IN CIVIL ENGINEERING, 7., 2015, Lviv. **Procedia Engineering** [...]. [*S. l.*]: Elsevier Ltd, 2015. p. 575–583. Available at: https://doi.org/10.1016/j.proeng.2015.06.180. Accessed on: 15 dez. 2023.

JAWED ROSHAN, Mohammad; ABEDI, Mohammadmahdi; GOMES CORREIA, António; FANGUEIRO, Raul. Application of self-sensing cement-stabilized sand for damage detection. **Construction and Building Materials**, [*s. l.*], v. 403, p. 1-24, nov. 2023. Available at: https://doi.org/10.1016/j.conbuildmat.2023.133080. Accessed on: 14 dez. 2023.

JOHN BRITTO, J. Jerold; VASANTHANATHAN, A.; NAGARAJ, P. Finite element modeling and simulation of condition monitoring on composite materials using piezoelectric transducers - ANSYS®. *In*: INTERNATIONAL CONFERENCE ON EMERGING TRENDS IN MATERIALS AND MANUFACTURING ENGINEERING, 2017, Tamil Nadu. **Materials Today: Proceedings** [...]. [*S. l.*]: Elsevier Ltd, 2018. p. 6684–6691. Available at: https://doi.org/10.1016/j.matpr.2017.11.325. Accessed on: 12 may 2024.

JOSHUA, A. M.; CHENG, G.; LAU, E. V. Soft matter analysis via atomic force microscopy (AFM): A review. **Applied Surface Science Advances**, [*s. l.*], v. 17, p. 1-14, oct. 2023. Available at: https://doi.org/10.1016/j.apsadv.2023.100448. Accessed on: 14 jan. 2024.

KANG, Zehao; ASLANI, Farhad; HAN, Baoguo. Prediction of mechanical and electrical properties of carbon fibre-reinforced self-sensing cementitious composites. **Case Studies in Construction Materials**, [*s. l.*], v. 20, p. 1-21, jul. 2024. Available at: https://doi.org/10.1016/j.cscm.2023.e02716. Accessed on: 24 feb. 2024.

KELLY, Richard. A view on the state of practice in transportation geotechnics in Australia. **Transportation Geotechnics**, [*s. l.*], v. 46, p. 1-33, may 2024. Available at: https://doi.org/10.1016/j.trgeo.2024.101259. Accessed on: 8 may 2024.

KHAOULAF, R.; BROUZI, K.; ENNACIRI, A.; HARCHARRAS, M.; ELHAFIANE, F. Vibrational spectra of dizincate sodium triphosphte nonahydrate. **Journal of Materials and Environmental Sciences**, [*s. l.*], v. 8, n. 8, p. 2884–2893, 2017. Available at: https://www.jmaterenvironsci.com/Document/vol8/vol8_N8/287-JMES-3240-Khaoulaf.pdf. Accessed on: 25 feb. 2024.

KIM, Jeong Tae; PARK, Jae Hyung; HONG, Dong Soo; PARK, Woo Sun. Hybrid health monitoring of prestressed concrete girder bridges by sequential vibration-impedance approaches. **Engineering Structures**, [*s. l.*], v. 32, n. 1, p. 115–128, jan. 2010. Available at: https://doi.org/10.1016/j.engstruct.2009.08.021. Accessed on: 15 apr. 2024.

KIM, Min Kyoung; KIM, Dong Joo; AN, Yun Kyu. Electro-mechanical self-sensing response of ultra-high-performance fiber-reinforced concrete in tension. **Composites Part B: Engineering**, [*s. l.*], v. 134, p. 254–264, feb. 2018. Available at: https://doi.org/10.1016/j.compositesb.2017.09.061. Accessed on: 24 feb. 2024.

KIM, Sang Yeob; YUN KWON, Da; JANG, Arum; JU, Young K.; LEE, Jong Sub; HONG, Seungkwan. A review of UAV integration in forensic civil engineering: From sensor technologies to geotechnical, structural and water infrastructure applications. **Measurement**, [*s. l.*], v. 224, p. 1-14, jan. 2024. Available at: https://doi.org/10.1016/j.measurement.2023.113886. Accessed on: 8 may 2024.

KIM, Tae Uk; LE, Huy Viet; PARK, Jong Woong; EOCK, Seung Kim; JANG, Yun; KIM, Dong Joo. Development of a smart concrete block with an eccentric load sensing capacity. **Construction and Building Materials**, [*s. l.*], v. 306, p. 1-15, nov. 2021. Available at: https://doi.org/10.1016/j.conbuildmat.2021.124881. Accessed on: 23 apr. 2024.

KONSTA-GDOUTOS, Maria S.; DANOGLIDIS, Panagiotis A.; FALARA, Maria G.; NITODAS, Stephanos F. Fresh and mechanical properties, and strain sensing of nanomodified cement mortars: The effects of MWCNT aspect ratio, density and functionalization. **Cement**

and Concrete Composites, [*s. l.*], v. 82, p. 137–151, sep. 2017. Available at: https://doi.org/10.1016/j.cemconcomp.2017.05.004. Accessed on: 08 nov. 2023.

KONSTA-GDOUTOS, Maria S.; METAXA, Zoi S.; SHAH, Surendra P. Highly dispersed carbon nanotube reinforced cement based materials. **Cement and Concrete Research**, [*s. l.*], v. 40, n. 7, p. 1052–1059, jul. 2010. Available at: https://doi.org/10.1016/j.cemconres.2010.02.015. Accessed on: 09 nov. 2023.

KULPA, Maciej; HOWIACKI, Tomasz; WIATER, Agnieszka; SIWOWSKI, Tomasz; SIEŃKO, Rafał. Strain and displacement measurement based on distributed fibre optic sensing (DFOS) system integrated with FRP composite sandwich panel. **Measurement**, [*s. l.*], v. 175, p. 1-14, apr. 2021. Available at: https://doi.org/10.1016/j.measurement.2021.109099. Accessed on: 15 apr. 2024.

LAURA, Echeverry Cardona; RAFAEL, Cabanzo; JORGE, Quintero Orozco; HARVI ALIRIO, Castillo Cuero; LAURA VICTORIA, Rodríguez Restrepo; ELISABETH, Restrepo Parra. Effects of molarity and storage time of MWCNTs on the properties of cement paste. **Materials**, [*s. l.*], v. 15, n. 24, p. 1-17, dez. 2022. Available at: https://doi.org/10.3390/ma15249035. Accessed on: 23 nov. 2023.

LE, Huy Viet; KIM, Min Kyoung; KIM, Dong Joo; PARK, Jongwoong. Electrical properties of smart ultra-high performance concrete under various temperatures, humidities, and age of concrete. **Cement and Concrete Composites**, [*s. l.*], v. 118, p. 1-14, apr. 2021. Available at: https://doi.org/10.1016/j.cemconcomp.2021.103979. Accessed on: 24 feb. 2024.

LEE, Eunji; KIM, Dong-Joo. Review— Recent exploration of two-dimensional mxenes for gas sensing: From a theoretical to an experimental view. **Journal of The Electrochemical Society**, [*s. l.*], v. 167, n. 3, p. 1-12, jan. 2020. Available at: https://iopscience.iop.org/article/10.1149/2.0152003JES. Accessed on: 4 may 2024.

LEE, Seon Yeol; LE, Huy Viet; KIM, Dong Joo. Self-stress sensing smart concrete containing fine steel slag aggregates and steel fibers under high compressive stress. **Construction and Building Materials**, [*s. l.*], v. 220, p. 149–160, sep. 2019. Available at: https://doi.org/10.1016/j.conbuildmat.2019.05.197. Accessed on: 12 apr. 2024.

LI, Lin; WEI, Huan; HAO, Yazhen; LI, Yizheng; CHENG, Wei; ISMAIL, Yusuf Abshir; LIU, Zhuangzhuang. Carbon nanotube (CNT) reinforced cementitious composites for structural self-sensing purpose: A review. **Construction and Building Materials**, [*s. l.*], v. 392, p. 1-16, aug. 2023. Available at: https://doi.org/10.1016/j.conbuildmat.2023.131384. Accessed on: 17 nov. 2023.

LI, Shaojie; ZHANG, Yuling; CHENG, Chen; WEI, Han; DU, Shiguo; YAN, Jun. Surface-treated carbon nanotubes in cement composites: Dispersion, mechanical properties and microstructure. **Construction and Building Materials**, [*s. l.*], v. 310, p. 1-11, dez. 2021. Available at: https://doi.org/10.1016/j.conbuildmat.2021.125262. Accessed on: 11 may 2024.

LI, Wengui; DONG, Wenkui; GUO, Yipu; WANG, Kejin; SHAH, Surendra P. Advances in multifunctional cementitious composites with conductive carbon nanomaterials for smart infrastructure. **Cement and Concrete Composites**, [*s. l.*], v. 128, p. 1-19, apr. 2022. Available at: https://doi.org/10.1016/j.cemconcomp.2022.104454. Accessed on: 02 may 2024.

LI, Zheling; DENG, Libo; KINLOCH, Ian A.; YOUNG, Robert J. Raman spectroscopy of carbon materials and their composites: Graphene, nanotubes and fibres. **Progress in Materials Science**, [*s. l.*], v. 135, p. 1-58, jun. 2023. Available at: https://doi.org/10.1016/j.pmatsci.2023.101089. Accessed on: 23 nov. 2023.

LIN, Tzu Hsuan; PUTRANTO, Alan; WANG, Yan Ting. Smart sensor tags for seepage sensing protected by 3D-printed case for embedding in concrete structures. **Construction and Building Materials**, [*s. l.*], v. 284, p. 1-17, may 2021. Available at: https://doi.org/10.1016/j.conbuildmat.2021.122784. Accessed on: 21 apr. 2024.

LIN, Xiuju; PANG, Hao; WEI, Daidong; LU, Mangeng; LIAO, Bing. Effect of the cross-linker structure of cross-linked polycarboxylate superplasticizers on the behavior of cementitious mixtures. **Colloids and Surfaces A: Physicochemical and Engineering Aspects**, [*s. l.*], v. 608, p. 1-8, jan. 2021. Available at: https://doi.org/10.1016/j.colsurfa.2020.125437. Accessed on: 22 sep. 2023.

LIU, Chunhui; ZHANG, Qing; ZHAO, Chaoqun; DENG, Lijun; FANG, Qinghe. Assessment of strength development of soil stabilized with cement and nano SiO2. **Construction and Building Materials**, [*s. l.*], v. 409, p. 1-12, dez. 2023. Available at: https://doi.org/10.1016/j.conbuildmat.2023.133889. Accessed on: 24 sep. 2023.

LIU, Ming; LEI, Jiaheng; BI, Yao; DU, Xiaodi; ZHAO, Qinglin; ZHANG, Xuqing. Preparation of polycarboxylate-based superplasticizer and its effects on zeta potential and rheological property of cement paste. **Journal of Wuhan University of Technology-Mater. Sci. Ed.**, Wuhan, v. 30, n. 5, p. 1008–1012, oct. 2015. Available at: http://link.springer.com/10.1007/s11595-015-1265-8. Accessed on: 23 sep. 2023.

LIU, Yi; VAN VLIET, Tim; TAO, Yinping; BUSFIELD, James J.C.; PEIJS, Ton; BILOTTI, Emiliano; ZHANG, Han. Sustainable and self-regulating out-of-oven manufacturing of FRPs with integrated multifunctional capabilities. **Composites Science and Technology**, [*s. l.*], v. 190, p. 1-9, apr. 2020. Available at: https://doi.org/10.1016/j.compscitech.2020.108032. Accessed on: 28 apr. 2024.

LIU, Ying; ZHAO, Yongzhe; ZHANG, Deng; LIU, Zhiyong. The long-term mechanical performance of geogrid-reinforced soil retaining walls under cyclic footing loading. **Case Studies in Construction Materials**, [*s. l.*], v. 17, p. 1-17, dez. 2022. Available at: https://doi.org/10.1016/j.cscm.2022.e01642. Accessed on: 22 apr. 2024.

LOBIANCO, Alessandro Lubrano; DEL ZOPPO, Marta; DI LUDOVICO, Marco. Correlation of local and global structural damage state for SHM. *In:* XIX ANIDIS CONFERENCE, SEISMIC ENGINEERING IN ITALY, 19., 2022, Torino. **Procedia Structural Integrity** [...]. [*S. l.*]: Elsevier B.V., 2022. p. 910–917. Available at: https://doi.org/10.1016/j.prostr.2023.01.118. Accessed on: 17 jan. 2024.

LUO, Zhongtao; ZHI, Tianyi; LIU, Xiaohai; YIN, Kunpeng; PAN, Han; FENG, Hu; SONG, Yatao; SU, Yanfeng. Effects of different nanomaterials on the early performance of ultra-high performance concrete (UHPC): C–S–H seeds and nano-silica. **Cement and Concrete Composites**, [*s. l.*], v. 142, p. 1-12, sep. 2023. Available at: https://doi.org/10.1016/j.cemconcomp.2023.105211. Accessed on: 17 feb. 2024.

LYNGDOH, Gideon A.; DAS, Sumanta. Integrating multiscale numerical simulations with machine learning to predict the strain sensing efficiency of nano-engineered smart cementitious composites. **Materials & Design**, [*s. l.*], v. 209, p. 1-15, nov. 2021. Available at: https://doi.org/10.1016/j.matdes.2021.109995. Accessed on: 24 feb. 2024.

MA, Ran; WANG, Yinbin; LI, Hui; BAI, Yang. Progress in the polycarboxylate superplasticizer and their structure-activity relationship – A review. **Materials Today Communications**, [*s. l.*], v. 35, p. 1-14, jun. 2023. Available at: https://doi.org/10.1016/j.mtcomm.2023.105838. Accessed on: 14 nov. 2023.

MARIANI, S.; KALANTARI, A.; KROMANIS, R.; MARZANI, A. Data-driven modeling of long temperature time-series to capture the thermal behavior of bridges for SHM purposes. **Mechanical Systems and Signal Processing**, [*s. l.*], v. 206, p. 1-13, jan. 2024. Available at: https://doi.org/10.1016/j.ymssp.2023.110934. Accessed on: 10 jan. 2024.

MARLIERE, Claire; PERRIN, Sylvie; FROT, Didier; LEFEBVRE, Xavier; LÉCOLIER, Eric. New design of microchip for in-situ DLS measurement of colloidal suspensions. **JCIS Open**, [*s. l.*], v. 11, p. 1-8, oct. 2023. Available at: https://doi.org/10.1016/j.jciso.2023.100086. Accessed on: 12 nov. 2023.

MATERAZZI, Annibale Luigi; UBERTINI, Filippo; D'ALESSANDRO, Antonella. Carbon nanotube cement-based transducers for dynamic sensing of strain. **Cement and Concrete Composites**, [*s. l.*], v. 37, n. 1, p. 2–11, mar. 2013. Available at: https://doi.org/10.1016/j.cemconcomp.2012.12.013. Accessed on: 22 sep. 2023.

MATOS, Ryan A.; NASCIMENTO FILHO, Luis Carlos; GUILHEM, Isabela; FREITAS, Vytórya; MOURA, Jerfson; MESQUITA, Esequiel. An electrical modeling approach for analysis of the behavior of carbon nanotubes cement-based composite. **Journal of Building Pathology and Rehabilitation**, [*s. l.*], v. 8, n. 1, p. 1–9, jun. 2023. Available at: https://link.springer.com/article/10.1007/s41024-023-00314-1. Accessed on: 21 sep. 2023.

MD NUJID, Masyitah; THOLIBON, Duratul Ain; MUKHLISIN, Muhammad. Geotechnical and structural assessment on estimated bearing capacity of strip footing resting on silty sand incorporating moisture content effect. **Case Studies in Construction Materials**, [*s. l.*], v. 20, p. 1-17, jul. 2024. Available at: https://doi.org/10.1016/j.cscm.2024.e03106. Accessed on: 8 may 2024.

MEHRA, Neelesh Kumar; MISHRA, Vijay; JAIN, N. K. A review of ligand tethered surface engineered carbon nanotubes. **Biomaterials**, [*s. l.*], v. 35, n. 4, p. 1267–1283, jan. 2014. Available at: https://doi.org/10.1016/j.biomaterials.2013.10.032. Accessed on: 03 nov. 2023.

MEONI, A.; D'ALESSANDRO, A.; KRUSE, R.; DE LORENZIS, L.; UBERTINI, F. Strain field reconstruction and damage identification in masonry walls under in-plane loading using dense sensor networks of smart bricks: Experiments and simulations. **Engineering Structures**, [*s. l.*], v. 239, p. 1-21, jul. 2021. Available at: https://doi.org/10.1016/j.engstruct.2021.112199. Accessed on: 23 apr. 2024.

MEONI, A.; D'ALESSANDRO, A.; UBERTINI, F. Characterization of the strain-sensing behavior of smart bricks: A new theoretical model and its application for monitoring of

masonry structural elements. **Construction and Building Materials**, [*s. l.*], v. 250, p. 1-12, jul. 2020. Available at: https://doi.org/10.1016/j.conbuildmat.2020.118907. Accessed on: 23 apr. 2024.

MEONI, A.; FABIANI, C.; D'ALESSANDRO, A.; PISELLO, A. L.; UBERTINI, F. Strain-sensing smart bricks under dynamic environmental conditions: Experimental investigation and new modeling. **Construction and Building Materials**, [*s. l.*], v. 336, p. 1-13, jun. 2022. Available at: https://doi.org/10.1016/j.conbuildmat.2022.127375. Accessed on: 23 apr. 2024.

MEONI, Andrea; D'ALESSANDRO, Antonella; FALOPE, Federico Oyedeji; TARANTINO, Angelo Marcello; UBERTINI, Filippo. An experimental study on smart-earth samples for structural applications. *In:* XIX ANIDIS CONFERENCE, SEISMIC ENGINEERING IN ITALY, 19., 2022, Torino. **Procedia Structural Integrity** [...]. [*S. l.*]: Elsevier B.V., 2022. p. 1632–1639. Available at: https://doi.org/10.1016/j.prostr.2023.01.209. Accessed on: 03 feb. 2024.

MESQUITA, Esequiel; SOUSA, Israel; VIEIRA, Mylene; MATOS, Ana Mafalda; SANTOS, Luis P.M.; SILVESTRO, Laura; SALVADOR, Renan; D'ALESSANDRO, Antonella; UBERTINI, Filippo. Investigation of the electrical sensing properties of cementitious composites produced with multi-wall carbon nanotubes dispersed in NaOH. **Journal of Building Engineering**, [*s. l.*], v. 77, p. 1-16, oct. 2023. Available at: https://doi.org/10.1016/j.jobe.2023.107496. Accessed on: 01 jul. 2023.

METAXA, Zoi S.; KONSTA-GDOUTOS, Maria S.; SHAH, Surendra P. Carbon nanofiber cementitious composites: Effect of debulking procedure on dispersion and reinforcing efficiency. **Cement and Concrete Composites**, [*s. l.*], v. 36, p. 25–32, feb. 2013. Available at: https://doi.org/10.1016/j.cemconcomp.2012.10.009. Accessed on: 02 jul. 2023.

MIN, Jiyoung; PARK, Seunghee; YUN, Chung Bang; LEE, Chang Geun; LEE, Changgil. Impedance-based structural health monitoring incorporating neural network technique for identification of damage type and severity. **Engineering Structures**, [*s. l.*], v. 39, p. 210–220, jun. 2012. Available at: https://doi.org/10.1016/j.engstruct.2012.01.012. Accessed on: 15 apr. 2024.

MONTEIRO, André O.; CACHIM, Paulo B.; COSTA, Pedro M.F.J. Self-sensing piezoresistive cement composite loaded with carbon black particles. **Cement and Concrete Composites**, [*s. l.*], v. 81, p. 59–65, aug. 2017. Available at: https://doi.org/10.1016/j.cemconcomp.2017.04.009. Accessed on: 24 feb. 2024.

MOURA, Alfran Sampaio; RAMOS, Mônica Rodrigues; JUNIOR, Edno Cerqueira; FILHO, Francisco Pinheiro Lima; MENEZES, Pedro Henrique Lustosa Bezerra de. Preliminary geotechnical characterization of the subsoil of the Geotechnical and Foundation Experimental Field of the Federal University of Ceará (CEGEF - UFC). **Brazilian Journal of Development**, [*s. l.*], v. 7, n. 4, p. 33781–33796, apr. 2021. Available at: https://ojs.brazilianjournals.com.br/ojs/index.php/BRJD/article/view/27606/21835. Accessed on: 30 jul. 2023.

MUSSO, Simone; TULLIANI, Jean Marc; FERRO, Giuseppe; TAGLIAFERRO, Alberto. Influence of carbon nanotubes structure on the mechanical behavior of cement composites.

Composites Science and Technology, [*s. l.*], v. 69, n. 11/12, p. 1985–1990, set. 2009. Available at: https://doi.org/10.1016/j.compscitech.2009.05.002. Accessed on: 04 aug. 2023.

NALON, Gustavo Henrique; RIBEIRO, José Carlos Lopes; PEDROTI, Leonardo Gonçalves; ARAÚJO, Eduardo Nery Duarte de; CARVALHO, José Maria Franco de; LIMA, Gustavo Emilio Soares de; GUIMARÃES, Luciano de Moura. Residual piezoresistive properties of mortars containing carbon nanomaterials exposed to high temperatures. **Cement and Concrete Composites**, [*s. l.*], v. 121, p. 1-23, aug. 2021. Available at: https://doi.org/10.1016/j.cemconcomp.2021.104104. Accessed on: 11 may 2024.

NALON, Gustavo H.; RIBEIRO, José Carlos Lopes; PEDROTI, Leonardo Gonçalves; SILVA, Roberto Márcio da; ARAÚJO, Eduardo Nery Duarte de; LIMA, Gustavo Emílio Soares de. Smart laying mortars for masonry structures: effects of lime/cement ratio and carbon nanomaterials content on self-sensing behavior. **Cement and Concrete Composites**, [*s. l.*], v. 145, p. 1-22, jan. 2024. Available at: https://doi.org/10.1016/j.cemconcomp.2023.105351. Accessed on: 10 apr. 2024.

NALON, Gustavo Henrique; RIBEIRO, José Carlos Lopes; ARAÚJO, Eduardo Nery Duarte de; PEDROTI, Leonardo Gonçalves; CARVALHO, José Maria Franco de; SANTOS, Rodrigo Felipe; APARECIDO-FERREIRA, Alex. Effects of different kinds of carbon black nanoparticles on the piezoresistive and mechanical properties of cement-based composites. **Journal of Building Engineering**, [*s. l.*], v. 32, p. 1-12, nov. 2020. Available at: https://doi.org/10.1016/j.jobe.2020.101724. Accessed on: 02 may 2024.

NALON, Gustavo Henrique; RIBEIRO, José Carlos Lopes; DA SILVA, Roberto Marcio; PEDROTI, Leonardo Gonçalves; ARAÚJO, Eduardo Nery Duarte de. Self-sensing concrete masonry structures with intrinsic abilities of strain monitoring and damage detection. **Structures**, [*s. l.*], v. 59, p. 1-25, jan. 2024. Available at: https://doi.org/10.1016/j.istruc.2023.105760. Accessed on: 23 apr. 2024.

NGUYEN, Duy Liem; NGOC-TRA LAM, My; KIM, Dong Joo; SONG, Jiandong. Direct tensile self-sensing and fracture energy of steel-fiber-reinforced concretes. **Composites Part B: Engineering**, [*s. l.*], v. 183, p. 1-19, feb. 2020. Available at: https://doi.org/10.1016/j.compositesb.2019.107714. Accessed on: 24 feb. 2024.

NOSENZO, Giorgio; WHELAN, B. E.; BRUNTON, M.; KAY, Daryl; BUYS, Henk. Continuous monitoring of mining induced strain in a road pavement using fiber Bragg grating sensors. **Photonic Sensors**, [*s. l.*], v. 3, n. 2, p. 144–158, jun. 2013. Available in:. https://link.springer.com/article/10.1007/s13320-012-0077-0. Accessed on: 28 apr. 2024.

PARIDA, Lukesh; MOHARANA, Sumedha. A comprehensive review on piezo impedance based multi sensing technique. **Results in Engineering**, [*s. l.*], v. 18, p. 1-11, jun. 2023. Available at: https://doi.org/10.1016/j.rineng.2023.101093. Accessed on: 18 jan. 2024.

PARVEEN, Shama; RANA, Sohel; FANGUEIRO, Raul; PAIVA, Maria Conceição. A novel approach of developing micro crystalline cellulose reinforced cementitious composites with enhanced microstructure and mechanical performance. **Cement and Concrete Composites**, [*s. l.*], v. 78, p. 146–161, apr. 2017. Available at: https://doi.org/10.1016/j.cemconcomp.2017.01.004. Accessed on: 16 jan. 2024.

PAVIA, D. L.; LAMPMAN, G. M.; KRIZ, G. S.; VYVYAN, J. A. **Introduction to Spectroscopy**. 5. ed. Ohio: Cengage Learning, 2014.

PRASAD, Sneha; KUMAR, David; KALRA, Sumit; KHANDELWAL, Arpit. A real-time feature-based clustering approach for vibration-based SHM of large structures. **Measurement**, [*s. l.*], v. 227, p. 1-16, mar. 2024. Available at: https://doi.org/10.1016/j.measurement.2024.114222. Accessed on: 07 may 2024.

QI, Jilin; CUI, Wenyu; WANG, Dongyong. Applicability of the principle of effective stress in cold regions geotechnical engineering. **Cold Regions Science and Technology**, [*s. l.*], v. 219, p. 1-8, mar. 2024. Available at: https://doi.org/10.1016/j.coldregions.2024.104129. Accessed on: 08 may 2024.

QIU, Liangsheng; DONG, Sufen; YU, Xun; HAN, Baoguo. Self-sensing ultra-high performance concrete for in-situ monitoring. **Sensors and Actuators A: Physical**, [*s. l.*], v. 331, p. 1-11, nov. 2021. Available at: https://doi.org/10.1016/j.sna.2021.113049. Accessed on: 24 feb. 2024.

QUERAL-BELTRAN, Aina; MARÍN-GARCÍA, Marc; LACORTE, Silvia; TAULER, Romà. UV-Vis absorption spectrophotometry and LC-DAD-MS-ESI(+)-ESI(−) coupled to chemometrics analysis of the monitoring of sulfamethoxazole degradation by chlorination, photodegradation, and chlorination/photodegradation. **Analytica Chimica Acta**, [*s. l.*], v. 1276, p. 1-14, oct. 2023. Available at: https://doi.org/10.1016/j.aca.2023.341563. Accessed on: 25 feb. 2024.

RAFAEL, N. F. **Chemical stabilization of soils using nanoparticles**. 2017. Master Thesis (Master's in chemical engineering) - Faculty of Sciences and Technology, University of Coimbra, Coimbra, 2017.

RAO, Rajani Kant; SASMAL, Saptarshi. Electromechanical impedance-based embeddable smart composite for condition-state monitoring. **Sensors and Actuators A: Physical**, [*s. l.*], v. 346, p. 1-17, oct. 2022. Available at: https://doi.org/10.1016/j.sna.2022.113856. Accessed on: 24 feb. 2024.

RAO, Rajani Kant; SASMAL, Saptarshi. Nanoengineered smart cement composite for electrical impedance-based monitoring of corrosion progression in structures. **Cement and Concrete Composites**, [*s. l.*], v. 126, p. 1-16, feb. 2022. Available at: https://doi.org/10.1016/j.cemconcomp.2021.104348. Accessed on: 11 jan. 2024.

RAO, Rajani Kant; SASMAL, Saptarshi. Smart nano-engineered cementitious composite sensors for vibration-based health monitoring of large structures. **Sensors and Actuators, A: Physical**, [*s. l.*], v. 311, p. 1-15, aug. 2020. Available at: https://doi.org/10.1016/j.sna.2020.112088. Accessed on: 12 feb. 2024.

RAO, Rajanikant; SINDU, B. S.; SASMAL, Saptarshi. Synthesis, design and piezo-resistive characteristics of cementitious smart nanocomposites with different types of functionalized MWCNTs under long cyclic loading. **Cement and Concrete Composites**, [*s. l.*], v. 108, p. 1-14, abr. 2020. Available at: https://doi.org/10.1016/j.cemconcomp.2020.103517. Accessed on: 7 may 2024

ROBERTS, Callum; AVENDAÑO-VALENCIA, Luis David; GARCÍA CAVA, David. Robust mitigation of EOVs using multivariate nonlinear regression within a vibration-based SHM methodology. **Mechanical Systems and Signal Processing**, [*s. l.*], v. 208, p. 1-17, feb. 2024. Available at: https://doi.org/10.1016/j.ymssp.2023.111028. Accessed on: 7 may 2024.

RODRÍGUEZ-TEMBLEQUE, L.; GARCÍA-SÁNCHEZ, F.; GARCÍA-MACÍAS, E.; BURONI, F. C.; SÁEZ, A. Crack-induced electrical resistivity changes in cracked CNT-reinforced composites. **Theoretical and Applied Fracture Mechanics**, [*s. l.*], v. 106, p. 1-15, apr. 2020. Available at: https://doi.org/10.1016/j.tafmec.2019.102470. Accessed on: 24 feb. 2024.

ROOPA, A. K.; HUNASHYAL, A. M. Evaluate the optimum dosage of nano materials on self-sensing properties of nano cement composites. *In:* GLOBAL CONFERENCE ON RECENT ADVANCES IN SUSTAINABLE MATERIALS, 2021, Mangalore. **Materials Today: Proceedings** [...]. [*S. l.*]: Elsevier Ltd, 2022. p. 2197–2204. Available at: https://doi.org/10.1016/j.matpr.2021.09.127. Accessed on: 28 apr. 2024.

SAIDUMOV M. S.; SALAMANOVA M. SH.; MURTAZAEVA T. S-A.; ALASKHANOV A.KH.; ISMAILOVA Z.KH. Water-reducing and plasticizing additives for highly mobile concrete mixtures. **Atlantis Highlights in Material Sciences and Technology**, [*s. l.*], v. 1, p. 491–495, aug. 2019. Available at: https://www.atlantis-press.com/proceedings/isees-19/125914229. Accessed on: 28 apr. 2024.

SAKR, Micheal; SADHU, Ayan. Visualization of structural health monitoring information using Internet-of-Things integrated with building information modeling. **Journal of Infrastructure Intelligence and Resilience**, [*s. l.*], v. 2, n. 3, p. 1-16, sep. 2023. Available at: https://doi.org/10.1016/j.iintel.2023.100053. Accessed on: 03 may 2024.

SALEHI, Hadi; GORODETSKY, Alex; SOLHMIRZAEI, Roya; JIAO, Pengcheng. High-dimensional data analytics in civil engineering: A review on matrix and tensor decomposition. **Engineering Applications of Artificial Intelligence**, [*s. l.*], v. 125, p. 1-16, oct. 2023. Available at: https://doi.org/10.1016/j.engappai.2023.106659. Accessed on: 23 apr. 2024.

SANCHES, Natália Beck; CASSU, Silvana Navarro; DE CÁSSIA LAZZARINI DUTRA, Rita. TG/FT-IR characterization of additives typically employed in EPDM formulations. **Polimeros**, [*s. l.*], v. 25, n. 3, p. 247–255, 2015. Available at: https://doi.org/10.1590/0104-1428.1819. Accessed on: 03 nov. 2023.

SARANYA, S.; RANJITHAM, M.; DINESH, A.; DIVYAPRIYA, S. Structural health monitoring using sensors with application of wavelet analysis. *In*: SUSTAINABLE MATERIALS AND SMART PRACTICES, 2021, [*s. l.*]. **Materials Research Proceedings** [...]. Washington: Association of American Publishers, 2022. p. 205–216. Available at: https://doi.org/10.21741/9781644901953-24. Accessed on: 22 apr. 2024.

SARMADI, Hassan; ENTEZAMI, Alireza; YUEN, Ka Veng; BEHKAMAL, Bahareh. Review on smartphone sensing technology for structural health monitoring. **Measurement: Journal of the International Measurement Confederation**, [*s. l.*], v. 223, p. 1-26, dez. 2023. Available at: https://doi.org/10.1016/j.measurement.2023.113716. Accessed on: 17 apr. 2024.

SENADHEERA, Harini; DEO, Ravin; AZOOR, Rukshan; BOUAZZA, Abdelmalek; KODIKARA, Jayantha. Electro-mechanical behaviour of graphene-based geotextiles for pavement health monitoring. **Geotextiles and Geomembranes**, [*s. l.*], v. 51, n. 2, p. 303–315, apr. 2023. Available at: https://doi.org/10.1016/j.geotexmem.2022.11.004. Accessed on: 23 apr. 2024.

SEO, Joonho; JANG, Daeik; YANG, Beomjoo; YOON, H. N.; JANG, Jeong Gook; PARK, Solmoi; LEE, H. K. Material characterization and piezoresistive sensing capability assessment of thin-walled CNT-embedded ultra-high performance concrete. **Cement and Concrete Composites**, [*s. l.*], v. 134, p. 1-17, nov. 2022. Available at: https://doi.org/10.1016/j.cemconcomp.2022.104808. Accessed on: 04 nov. 2023.

SEVIM, Ozer; JIANG, Zhangfan; OZBULUT, Osman E. Effects of graphene nanoplatelets type on self-sensing properties of cement mortar composites. **Construction and Building Materials**, [*s. l.*], v. 359, p. 1-13, dez. 2022. Available at: https://doi.org/10.1016/j.conbuildmat.2022.129488. Accessed on: 28 apr. 2024.

SHAH, S. P.; KONSTA-GDOUTOS, M. S.; METAXA, Z. S.; MONDAL, P. Nanoscale modification of cementitious materials. *In*: INTERNATIONAL SYMPOSIUM ON NANOTECHNOLOGY IN CONSTRUCTION, 3., 2009, Praga. **Nanotechnology in construction 3** […]. [*S. l.*]: Springer Berlin Heidelberg, 2009. p. 125–130. Available in: https://link.springer.com/chapter/10.1007/978-3-642-00980-8_16#citeas. Accessed on: 16 dez. 2023.

SHI, Cheng; LIN, Jinfeng; GE, Guanglong; HAO, Yali; SONG, Jiayue; WEI, Yongqi; YAO, Wu. Design and manufacture of lead-free eco-friendly cement-based piezoelectric composites achieving superior piezoelectric properties for concrete structure applications. **Composites Part B: Engineering**, [*s. l.*], v. 259, p. 1-13, jun. 2023. Available at: https://doi.org/10.1016/j.compositesb.2023.110750. Accessed on: 15 dez. 2023.

SIAHKOUHI, Mohammad; RAZAQPUR, Ghani; HOULT, N. A.; HAJMOHAMMADIAN BAGHBAN, Mohammad; JING, Guoqing. Utilization of carbon nanotubes (CNTs) in concrete for structural health monitoring (SHM) purposes: A review. **Construction and Building Materials**, [*s. l.*], v. 309, p. 1-14, nov. 2021. Available at: https://doi.org/10.1016/j.conbuildmat.2021.125137. Accessed on: 03 feb. 2024.

SIAHKOUHI, Mohammad; WANG, Junyi; HAN, Xiaodong; AELA, Peyman; NI, Yi Qing; JING, Guoqing. Railway ballast track hanging sleeper defect detection using a smart CNT self-sensing concrete railway sleeper. **Construction and Building Materials**, [*s. l.*], v. 399, p. 1-20, oct. 2023. Available at: https://doi.org/10.1016/j.conbuildmat.2023.132487. Accessed on: 01 may 2024.

SINGH, Moirangthem J.; CHOUDHARY, Sourabh; CHEN, Wen Bo; WU, Pei Chen; KUMAR GOYAL, Manish; RAJPUT, Abhishek; BORANA, Lalit. Applications of fibre Bragg grating sensors for monitoring geotechnical structures: A comprehensive review. **Measurement**, [*s. l.*], v. 218, p. 1-16, aug. 2023. Available at: https://doi.org/10.1016/j.measurement.2023.113171. Accessed on: 8 may 2024.

SIVASURIYAN, Arvindan; VIJAYAN, D. S. Prediction of displacement in reinforced concrete based on artificial neural networks using sensors. **Measurement: Sensors**, [*s. l.*], v.

27, p. 1-6, jun. 2023. Available at: https://doi.org/10.1016/j.measen.2023.100764. Accessed on: 28 feb. 2024.

SOLEYMANI, Atefeh; JAHANGIR, Hashem; NEHDI, Moncef L. Damage detection and monitoring in heritage masonry structures: Systematic review. **Construction and Building Materials**, [*s. l.*], v. 397, p. 1-24, set. 2023. Available at: https://doi.org/10.1016/j.conbuildmat.2023.132402. Accessed on: 02 feb. 2023.

SONG, Facheng; CHEN, Qing; ZHANG, Mingzhong; JIANG, Zhengwu; DING, Wenqi; YAN, Zhiguo; ZHU, Hehua. Exploring the piezoresistive sensing behaviour of ultra-high performance concrete: Strategies for multiphase and multiscale functional additives and influence of electrical percolation. **Composites Part B: Engineering**, [*s. l.*], v. 267, p. 1-15, dez. 2023. Available at: https://doi.org/10.1016/j.compositesb.2023.111042. Accessed on: 28 apr. 2024.

SRINIVASAN, S.; BARBHUIYA, S.A.; CHARAN, D.; PANDEY, S.P. Characterising cement–superplasticiser interaction using zeta potential measurements. **Construction and Building Materials**, [*s. l.*], v. 24, n. 12, p. 2517–2521, dez. 2010. Available at: https://doi.org/10.1016/j.conbuildmat.2010.06.005. Accessed on: 17 nov. 2023.

STECHER, J.; PLANK, J. Novel concrete superplasticizers based on phosphate esters. **Cement and Concrete Research**, [*s. l.*], v. 119, p. 36–43, may 2019. Available at: https://doi.org/10.1016/j.cemconres.2019.01.006. Accessed on: 18 nov. 2023.

SU, Linping; XIN, Xue; LIANG, Ming; WANG, Jianjiang; LUAN, Xuehao; WANG, Hao; JIAO, Yuepeng; ZHANG, Yunfeng; YAO, Zhanyong. Electric field–tunable self-sensing nanocomposites with aligned CNTs for in-situ pavement health monitoring: Electrodynamic alignment, sensor development, and performance validation. **Chemical Engineering Journal**, [*s. l.*], v. 481, p. 1-19, feb. 2024. Available at: https://doi.org/10.1016/j.cej.2023.148300. Accessed on: 25 feb. 2024.

SUH, Heongwon; CHO, Seongmin; IM, Sumin; MOON, Jaegeun; PARK, Jaeyeon; LIM, Jun; NEZHAD, Erfan Zal; SEOK, Seungwook; BAE, Baek-Il; BAE, Sungchul. Characterization of thermal resistance and mechanical strength recovery of carbon-nanotube-incorporated Portland cement composites subjected to heating and rehydration: Visualization of pore structural evolutions via synchrotron 3D X-ray nanoimaging. **Cement and Concrete Composites**, [*s. l.*], v. 146, n. 10, p. 1-16, feb. 2023. Available at: http://dx.doi.org/10.1016/j.cemconcomp.2023.105361. Accessed on: 25 nov. 2023.

SUN, Jiongfeng; QIAO, Guofu. Enhancement of the piezoresistive and mechanical properties of cement-based composites filled with CNTs/GO and nano-SiO2 sprayed steel fibers. **Construction and Building Materials**, [*s. l.*], v. 385, p. 1-13, jul. 2023. Available at: https://doi.org/10.1016/j.conbuildmat.2023.131463. Accessed on: 24 feb. 2024.

SUN, Junbo; WANG, Xiangyu; ZHANG, Junfei; XIAO, Fan; SUN, Yuantian; REN, Zhenhua; ZHANG, Genbao; LIU, Shukui; WANG, Yufei. Multi-objective optimisation of a graphite-slag conductive composite applying a BAS-SVR based model. **Journal of Building Engineering**, [*s. l.*], v. 44, p. 1-14, dez. 2021. Available at: https://doi.org/10.1016/j.jobe.2021.103223. Accessed on: 01 may 2024.

SUN, Ming-qing; LIEW, Richard J.Y.; ZHANG, Min-Hong; LI, Wei. Development of cement-based strain sensor for health monitoring of ultra high strength concrete. **Construction and Building Materials**, [*s. l.*], v. 65, p. 630–637, aug. 2014. Available at: https://doi.org/10.1016/j.conbuildmat.2014.04.105. Accessed on: 28 apr. 2024.

TAFESSE, Million; LEE, Nam Kon; ALEMU, Abel Shiferaw; LEE, Hyo Kyoung; KIM, Sung Wook; KIM, Hyeong Ki. Flowability and electrical properties of cement composites with mechanical dispersion of carbon nanotube. **Construction and Building Materials**, [*s. l.*], v. 293, p. 1-18, jul. 2021. Available at: https://doi.org/10.1016/j.conbuildmat.2021.123436. Accessed on: 11 may 2024.

TAHA, Mohd R.; ALSHAREF, Jamal M.A.; KHAN, Tanveer A.; AZIZ, Mubashir; GABER, Maryam. Compressive and tensile strength enhancement of soft soils using nanocarbons. **Geomechanics and Engineering**, [*s. l.*], v. 16, n. 5, p. 559–567, dez. 2018. Available at: https://doi.org/10.12989/gae.2018.16.5.559. Accessed on: 23 sep. 2024.

TAHERI, Shima. A review on five key sensors for monitoring of concrete structures. **Construction and Building Materials**, [*s. l.*], v. 204, p. 492–509, apr. 2019. Available at: https://doi.org/10.1016/j.conbuildmat.2019.01.172. Accessed on: 27 apr. 2024.

TAN, Xiao; ABU-OBEIDAH, Adi; BAO, Yi; NASSIF, Hani; NASREDDINE, Wassim. Measurement and visualization of strains and cracks in CFRP post-tensioned fiber reinforced concrete beams using distributed fiber optic sensors. **Automation in Construction**, [*s. l.*], v. 124, p. 1-13, apr. 2021. Available at: https://doi.org/10.1016/j.autcon.2021.103604. Accessed on: 28 apr. 2024.

TIAN, Hongwei; KONG, Xiangming; SU, Tong; WANG, Dongmin. Comparative study of two PCE superplasticizers with varied charge density in Portland cement and sulfoaluminate cement systems. **Cement and Concrete Research**, [*s. l.*], v. 115, p. 43–58, jan. 2019. Available at: https://doi.org/10.1016/j.cemconres.2018.10.003. Accessed on: 30 nov. 2023.

TORABIAN ISFAHANI, Forood; LI, Weiwen; REDAELLI, Elena. Dispersion of multi-walled carbon nanotubes and its effects on the properties of cement composites. **Cement and Concrete Composites**, [*s. l.*], v. 74, p. 154–163, nov. 2016. Available at: https://doi.org/10.1016/j.cemconcomp.2016.09.007. Accessed on: 27 nov. 2023.

UBERTINI, Filippo; MATERAZZI, Annibale Luigi; D'ALESSANDRO, Antonella; LAFLAMME, Simon. Natural frequencies identification of a reinforced concrete beam using carbon nanotube cement-based sensors. **Engineering Structures**, [*s. l.*], v. 60, p. 265–275, feb. 2014. Available at: https://doi.org/10.1016/j.engstruct.2013.12.036. Accessed on: 22 feb. 2024.

VAKHITOVA, Roza Il; SARACHEVA, Diana A.; KIYAMOV, Ilgam K.; SABITOV, Linar S.; OLEINIK, Vasily Iv. Investigating the influence of carbon nanotube-based additives on the phase composition of cement mortar during well cementation. **Nanotechnologies in Construction**, [*s. l.*], v. 15, n. 5, p. 418–423, 2023. Available at: https://doi.org/10.15828/2075-8545-2023-15-5-418-423. Accessed on: 03 feb. 2024.

WANG, Jialiang; WANG, Xinyue; DING, Siqi; ASHOUR, Ashraf; YU, Feng; LV, Xingjun; HAN, Baoguo. Micro-nano scale pore structure and fractal dimension of ultra-high

performance cementitious composites modified with nanofillers. **Cement and Concrete Composites**, [*s. l.*], v. 141, p. 1-12, aug. 2023. Available at: https://doi.org/10.1016/j.cemconcomp.2023.105129. Accessed on: 17 feb. 2023.

WANG, Yanlei; WANG, Yongshuai; WAN, Baolin; HAN, Baoguo; CAI, Gaochuang; LI, Zhizheng. Properties and mechanisms of self-sensing carbon nanofibers/epoxy composites for structural health monitoring. **Composite Structures**, [*s. l.*], v. 200, p. 669–678, sep. 2018. Available at: https://doi.org/10.1016/j.compstruct.2018.05.151. Accessed on: 24 feb. 2024.

WANG, Yunyang; ZHANG, Liqing. Development of self-sensing cementitious composite incorporating hybrid graphene nanoplates and carbon nanotubes for structural health monitoring. **Sensors and Actuators A: Physical**, [*s. l.*], v. 336, p. 1-11, apr. 2022. Available at: https://doi.org/10.1016/j.sna.2022.113367. Accessed on: 28 apr. 2024.

WANG, Zhongkun; YU, Jing; LI, Gengying; ZHANG, Min; LEUNG, Christopher K.Y. Corrosion behavior of steel rebar embedded in hybrid CNTs-OH/polyvinyl alcohol modified concrete under accelerated chloride attack. **Cement and Concrete Composites**, [*s. l.*], v. 100, p. 120–129, jul. 2019. Available at: https://doi.org/10.1016/j.cemconcomp.2019.02.013. Accessed on: 02 may 2024.

WU, Stephen; OTAKE, Yu; HIGO, Yosuke; YOSHIDA, Ikumasa. Pathway to a fully data-driven geotechnics: Lessons from materials informatics. **Soils and Foundations**, [*s. l.*], v. 64, n. 3, p. 1-14, jun. 2024. Available at: https://doi.org/10.1016/J.SANDF.2024.101471. Accessed on: 8 may 2024.

WYJADŁOWSKI, Marek; KUJAWA, Paulina; MUSZYŃSKI, Zbigniew; RYBAK, Jarosław; DRUSA, Marian. Application of photogrammetry for 3D roughness measurement of failure surface in cemented soils. **Construction and Building Materials**, [*s. l.*], v. 430, p. 1-14, jun. 2024. Available at: https://doi.org/10.1016/j.conbuildmat.2024.136431. Accessed on: 8 may 2024.

XIANG, Shuncheng; GAO, Yingli; SHI, Caijun. Progresses in synthesis of polycarboxylate superplasticizer. **Advances in Civil Engineering**, [*s. l.*], v. 2020, n. 1, p. 1-14, jul 2020. Available at: https://doi.org/10.1155/2020/8810443. Accessed on: 17 nov. 2023.

XU, Donghui; XU, Xiang; FORDE, Michael C.; CABALLERO, Antonio. Concrete and steel bridge structural health monitoring—Insight into choices for machine learning applications. **Construction and Building Materials**, [*s. l.*], v. 402, p. 1-16, oct. 2023. Available at: https://doi.org/10.1016/j.conbuildmat.2023.132596. Accessed on: 29 jan. 2024.

YANG, C. Q.; WANG, X. L.; JIAO, Y. J.; DING, Y. L.; ZHANG, Y. F.; WU, Z. S. Linear strain sensing performance of continuous high strength carbon fibre reinforced polymer composites. **Composites Part B: Engineering**, [*s. l.*], v. 102, p. 86–93, oct. 2016. Available at: https://doi.org/10.1016/j.compositesb.2016.07.013. Accessed on: 15 apr. 2024.

YANG, Yanping; ZHU, Zuo; AU, Siu Kui. Bayesian dynamic programming approach for tracking time-varying model properties in SHM. **Mechanical Systems and Signal Processing**, [*s. l.*], v. 185, p. 1-22, feb. 2023. Available at: https://doi.org/10.1016/j.ymssp.2022.109735. Accessed on: 15 mar. 2024.

YANG, Ziqian; GAO, Weihang; LI, Menglei; CHEN, Qingjun; KONG, Qingzhao. Monitoring and modeling the hydration of steel fibre-reinforced cement-based material in very early age. **Composite Structures**, [*s. l.*], v. 311, p. 1-14, may 2023. Available at: https://doi.org/10.1016/j.compstruct.2023.116780. Accessed on: 24 feb. 2024.

YIN, Jie; LIU, Rong gui; HUANG, Jun jie; LIANG, Ge; LIU, Dan; XIE, Gui Hua. Comparative study on piezoresistive properties of CFRP tendons prepared by two different methods. **Composites Part B: Engineering**, [*s. l.*], v. 129, p. 124–132, nov. 2017. Available at: https://doi.org/10.1016/j.compositesb.2017.07.064. Accessed on: 15 apr. 2024.

YIN, Tianjiao; XU, Jinxia; WANG, Yang; LIU, Liyuan. Increasing self-sensing capability of carbon nanotubes cement-based materials by simultaneous addition of Ni nanofibers with low content. **Construction and Building Materials**, [*s. l.*], v. 254, p. 1-8, set. 2020. Available at: https://doi.org/10.1016/j.conbuildmat.2020.119306. Accessed on: 22 apr. 2024.

YOO, Doo Yeol; OH, Taekgeun; BANTHIA, Nemkumar. Nanomaterials in ultra-high-performance concrete (UHPC) – A review. **Cement and Concrete Composites**, [*s. l.*], v. 134, p. 1-28, nov. 2022. Available at: https://doi.org/10.1016/j.cemconcomp.2022.104730. Accessed on: 30 jan. 2024.

YOU, Ilhwan; YOO, Doo Yeol; KIM, Sooho; KIM, Min Jae; ZI, Goangseup. Electrical and self-sensing properties of ultra-high-performance fiber-reinforced concrete with carbon nanotubes. **Sensors (Switzerland)**, [*s. l.*], v. 17, n. 11, p. 1-19, nov. 2017. Available at: https://doi.org/10.3390/s17112481. Accessed on: 11 nov. 2023.

YU, Hua; JOSHI, Priyanka; LAU, Chooikim; NG, Kam. Novel application of sustainable coal-derived char in cement soil stabilization. **Construction and Building Materials**, [*s. l.*], v. 414, p. 1-12, feb. 2024. Available at: https://doi.org/10.1016/j.conbuildmat.2024.134960. Accessed on: 23 feb. 2024.

YU, Xiao; FU, Yuguang; LI, Jian; MAO, Jianxiao; HOANG, Tu; WANG, Hao. Recent advances in wireless sensor networks for structural health monitoring of civil infrastructure. **Journal of Infrastructure Intelligence and Resilience**, [*s. l.*], v. 23, p. 1-18, nov. 2023. Available at: http://dx.doi.org/10.1016/j.iintel.2023.100066. Accessed on: 03 may 2024.

ZHANG, Jiawen; HAN, Shuai; LI, Mingchao; LI, Heng; ZHAO, Wenchao; WANG, Jia; LIANG, Hui. CasMDN: A deep learning-based multivariate distribution modelling approach and its application in geotechnical engineering. **Computers and Geotechnics**, [*s. l.*], v. 168, p. 1-15, apr. 2024. Available at: https://doi.org/10.1016/j.compgeo.2024.106164. Accessed on: 8 may 2024.

ZHANG, Ru; DUAN, Yuanfeng; XING, Li; ZHAO, Yang; WEI, Wei; HU, Xiaoyang. Elasto-magneto-electric (EME) sensors for force monitoring of prestressing tendons. **Advances in Bridge Engineering**, [*s. l.*], v. 4, n. 1, p. 1–13, dez. 2023. Available at: https://link.springer.com/articles/10.1186/s43251-023-00086-1. Accessed on: 15 apr. 2024.

ZHANG, Wei Heng; QIN, Jianjun; LU, Da Gang; LIU, Min; FABER, Michael Havbro. Optimizing utilization strategy of real-time SHM information for structural integrity management based on preposterior decision analysis. **Ocean Engineering**, [*s. l.*], v. 297, p. 1-

14, apr. 2024. Available at: https://doi.org/10.1016/j.oceaneng.2024.117044. Accessed on: 7 may 2024.

ZHANG, Wengang; HUANG, Ruijie; XIANG, Jiaying; ZHANG, Ningning. Recent advances in bio-inspired geotechnics: From burrowing strategy to underground structures. **Gondwana Research**, [*s. l.*], v. 130, p. 1–17, jun. 2024. Available at: https://doi.org/10.1016/j.gr.2023.12.018. Accessed on: 8 may 2024.

ZHAO, J. H.; RIVERA, E.; MUFTI, A.; STEPHENSON, Doug; THOMSON, D. J. Evaluation of dielectric based and other methods for moisture content measurement in building stones. **Journal of Civil Structural Health Monitoring**, [*s. l.*], v. 2, n. 3/4, p. 137–148, dez. 2012. Available at: https://link.springer.com/article/10.1007/s13349-012-0024-1. Accessed on: 22 apr. 2024.

ZHOU, Jian; YU, Sheng; LI, Hongwei; WANG, Ying; OU, Jinping. Automated operational modal analysis for civil engineering structures with compressed measurements. **Measurement: Journal of the International Measurement Confederation**, [*s. l.*], v. 223, p. 1-12, dez. 2023. Available at: https://doi.org/10.1016/j.measurement.2023.113772. Accessed on: 03 may 2024.

ZHOU, Zhiliang; XIE, Ning; CHENG, Xin; FENG, Lichao; HOU, Pengkun; HUANG, Shifeng; ZHOU, Zonghui. Electrical properties of low dosage carbon nanofiber/cement composite: Percolation behavior and polarization effect. **Cement and Concrete Composites**, [*s. l.*], v. 109, p. 1-9, may 2020. Available at: https://doi.org/10.1016/j.cemconcomp.2020.103539. Accessed on: 13 dez. 2023.

ZOU, Fubing; TAN, Hongbo; GUO, Yulin; MA, Baoguo; HE, Xingyang; ZHOU, Yang. Effect of sodium gluconate on dispersion of polycarboxylate superplasticizer with different grafting density in side chain. **Journal of Industrial and Engineering Chemistry**, [*s. l.*], v. 55, p. 91–100, nov. 2017. Available at: https://doi.org/10.1016/j.jiec.2017.06.032. Accessed on: 14 dez. 2023.